ACTA
PROTOZOOLOGICA

ACTA
PROTOZOOLOGICA

Amphisiella annulata (Kahl, 1928) Borror, 1972 (Ciliophora: Hypotricha): Morphology, Notes on Morphogenesis, Review of Literature, and Neotypification

Helmut BERGER

Consulting Engineering Office for Ecology, Salzburg, Austria

Summary. The morphology and some morphogenetic details of the marine hypotrich *Amphisiella annulata* (Kahl, 1928) were investigated using live observation and protargol impregnation. The population from the Adriatic Sea matches almost perfectly the authoritative redescription by Kahl (1932). Characteristic features of *A. annulata* are (i) several ring-shaped structures (lithosomes?) 4-8 μm across scattered throughout the cytoplasm; (ii) the very narrowly spaced and rather wide cirri of the amphisiellid median cirral row; and (iii) the formation of an additional cirral anlage between the ordinary anlagen IV and V. This additional anlage produces only a transverse cirrus so that *A. annulata* has six transverse cirri. In addition, the oral primordium is formed from several roundish anlagen pits which originate left of the middle and rear portion of the amphisiellid median cirral row, resembling the situation in *A. marioni*, type of the genus. The literature on *A. annulata* is reviewed, showing that this conspicuous and thus easy to identify species has been recorded only about 11 times since its discovery before 75 years. The population from the Italian coast of the northern Adriatic Sea is designated as neotype because (i) no preparations are available of the original type population from saltwater in North Germany; (ii) synonymy with an older species was proposed in the revision by Hemberger (1982); and (iii) the descriptions available so far do not agree very well.

Key words: Adriatic Sea, cell division, Italy, marine ciliate, reorganization.

INTRODUCTION

The original description of *Holosticha annulata* is very brief (Kahl 1928b). Kahl (1932) reinvestigated this salt water hypotrich and provided more data and a much better illustration. The cirral pattern resembles that of *Amphisiella marioni*, type of *Amphisiella*. Consequently Kahl classified the present species in the subgenus *Holosticha (Amphisiella)*. The redescriptions by Borror (1963) and Aladro Lubel (1985) are based on live observations only and therfore did not increase the knowledge about this species significantly. Recently, Alekperov and Asadullayeva (1999) found *A. annulata* in the Caspian Sea. Their silver preparations basically confirmed Kahl's (1932) data.

In spring 2002, I found this hypotrichous ciliate in the northern Adriatic Sea. Live and protargol preparations showed that Kahl (1932) recognized the cirral pattern more or less perfectly. In addition, the present study revealed some interesting morphogenetic features in *Amphisiella annulata*.

Address for correspondence: Helmut Berger, Consulting Engineering Office for Ecology, Radetzkystrasse 10, 5020 Salzburg, Austria; Fax: +43 (0)662 443139; E-mail: office@protozoology.com

MATERIALS AND METHODS

Sampling and culture. *Amphisiella annulata* was found in a sample which I collected at the sandy beach of the northern Adriatic Sea ahead the campground Pra' delle Torri (45°34'N 12°49'E) near the Italian village of Duna Verde on 25.05.2002. The sample contained mainly seagrass run ashore and sand. It was transported to Salzburg (Austria) in a 1-litre bottle. In the laboratory raw cultures were established using Petri dishes 15 cm across filled with sea water from the sample site. Some squashed wheat grains were added to support microbial growth.

Morphological methods. Cells were studied in life using, inter alia, a high-power oil immersion objective and differential interference contrast optics. Live measurements were made at magnifications of 125-1250×. Although live values are more or less rough estimates, it is worth giving such data as specimens usually contract during fixation or shrink in preparations. The infraciliature was revealed with the protargol method according to protocol A in Foissner *et al.* (1999). Counts and measurements on prepared specimens were performed at a magnification of 1250×. Illustrations of live specimens are based on freehand sketches, while those of prepared cells were made with a camera lucida. Five neotype slides of protargol preparations are deposited in the Oberösterreichische Landesmuseum in Linz (LI), Austria (accession numbers 2003/146-150). The specimens illustrated and some used for morphometric analysis are marked.

The morphometric data shown in Table 1 are repeated in the description only as needed for clarity. All observations are from raw cultures, that is, not from clones. Consequently, it cannot be excluded that similar species are mixed, although this is very unlikely because specimens which deviate in at least one important character are excluded. Certainly, this can generate some bias in the data, if applied to uncritically. However, I usually excluded only such individuals which have, for example, a different nuclear structure (very likely often postconjugates), a distinctly deviating cirral pattern (very likely often injured, regenerating, or malformed specimens), or an unusually small size (very likely often degenerating or just divided specimens). The inclusion of such specimens would artificially increase variability.

Nomenclature and terminology. For authorship and date of scientific names, see Berger (2001). Terminology is basically according to Eigner and Foissner (1994) and Berger (1999). For the designation of the frontal-ventral-transverse cirri anlagen and cirri, the numbering system by Wallengren (1900) is used.

RESULTS AND DISCUSSION

Amphisiella annulata (Kahl, 1928) Borror, 1972 (Figs 1-23, Table 1)

1928 *Holosticha annulata* - Kahl, *Arch. Hydrobiol.*, **19:** 212, Fig. 44f (Fig. 17; original description; no type material available).

1932 *Amphisiella* (*Holosticha*) *annulata* Kahl, 1928 - Kahl, *Tierwelt Dtl.*, **25:** 590, Fig. 112 *1* (Fig. 18; authoritative redescription and revision; see nomenclature for correct name).

1933 *Amphisiella annulata* Kahl 1928 - Kahl, *Tierwelt N.- u. Ostsee*, **23:** 112, Fig. 17.21 (Fig. 19; guide to marine ciliates; see nomenclature for correct name).

1963 *Holosticha annulata* Kahl, 1928 - Borror, *Arch. Protistenk.*, **106:** 511, Fig. 118 (Fig. 20; redescription).

1972 *Amphisiella annulata* (Kahl, 1928) Kahl, 1932 - Borror, *J. Protozool.*, **19:** 9 (combining author, see nomenclature; revision of hypotrichs).

1985 *Amphisiella annulata* (Kahl, 1928) - Aladro Lubel, *An. Inst. Biol. Univ. Méx.*, **55:** 25, Lámina 12, Fig. 4 (Fig. 21; illustrated record).

1990 *Amphisiella annulata* (Kahl, 1928) - Aladro Lubel, Martínez Murillo and Mayén Estrada, Manual de Ciliados, p. 125, Figure on p. 125 (Fig. 22; review).

1992 *Amphisiella annulata* (Kahl, 1928) Kahl, 1930-5 - Carey, Marine Interstitial Ciliates, p. 179, Fig. 701 (guide; the illustration is a redrawing of Fig. 17).

1999 *Amphisiella annulata* (Kahl, 1928) - Alekperov and Asadullayeva, *Turkish J. Zool.*, **23:** 219, Fig. 8 (Fig. 23; redescription).

Nomenclature. No derivation of the name is given in the original description. The species-group name *annulát·us, -a, -um* (Latin adjective [m, f, n]; ringed, having a small ring; Hentschel and Wagner 1996) obviously alludes to the ring-shaped structures in the cytoplasm. Kahl (1932, 1933) classified *Amphisiella* as subgenus of *Holosticha*. Thus, the correct name in his reviews is *Holosticha* (*Amphisiella*) *annulata* Kahl, 1928. This was obviously overlooked by Borror (1972) and Carey (1992), who assumed that Kahl (1932) has transferred it from the genus *Holosticha* to the genus *Amphisiella* (see list of synonyms). For the sake of simplicity I suggest to fix Borror (1972) as combining author, although he did not formally transfer it to *Amphisiella*.

Improved diagnosis. Body size about 130×33 µm in life. Body outline elongate elliptical to oval. Two macronuclear nodules. Cortical granules colourless, arranged mainly along dorsal kineties. Amphisiellid median cirral row extends sigmoidally from near right frontal cirrus to near transverse cirri, consists of about 44 narrowly spaced cirri which are conspicuously wide (4-5 µm!) in middle portion of row. On average 47 adoral membranelles and each 34 cirri in left and right marginal row. More or less invariably 1 buccal cirrus, 1 cirrus behind right frontal cirrus, 3 cirri left of anterior portion of median cirral row, 2 pretransverse ventral cirri, 6 transverse cirri, and 6-7 dorsal kineties. Oral primordium originates from several anlagen pits. Fourth transverse cirrus from left is formed from additional anlage which produces no other cirri.

**Table 1.** Morphometric data on *Amphisiella annulata* [a].

Characteristics	x	M	SD	SE	CV	Min	Max	n
Body, length	96.4	97.0	12.3	2.3	12.8	68.0	121.0	30
Body, width	37.4	36.0	7.7	1.4	20.5	23.0	55.0	29
Body length : width, ratio	2.6	2.5	0.4	0.1	15.9	2.0	3.6	29
Adoral zone of membranelles, length [b]	40.6	40.0	5.1	0.9	12.5	26.0	50.0	29
Adoral zone, relative length (%)	42.3	42.9	4.0	0.7	9.4	33.3	49.5	29
Anterior body end to distal end of adoral zone, distance	11.3	11.5	3.5	0.7	31.0	4.0	19.0	28
Anterior body end to paroral, distance	11.3	12.0	3.1	0.6	27.3	5.0	17.0	28
Paroral, length	17.9	18.0	2.1	0.4	11.9	12.0	22.0	27
Anterior body end to buccal cirrus, distance	9.4	9.0	3.0	0.6	31.9	4.0	18.0	29
Anterior body end to cirrus III/2, distance	12.7	12.0	3.7	0.7	29.0	7.0	22.0	28
Anterior body end to anlagen IV cirri [c], distance	15.9	16.0	3.6	0.7	22.5	9.0	25.0	30
Anterior body end to amphisiellid median cirral row, distance	12.4	12.0	3.6	0.7	28.9	4.0	21.0	28
Anterior body end to left marginal row, distance	20.3	21.0	4.4	0.8	21.7	10.0	30.0	30
Posterior body end to left marginal row, distance	7.0	7.0	2.0	0.4	28.8	4.0	12.0	28
Anterior body end to right marginal row, distance	24.2	24.0	4.6	0.9	18.9	16.0	36.0	30
Posterior body end to right marginal row, distance	6.2	6.0	1.6	0.3	25.7	4.0	11.0	27
Rearmost transverse cirrus to rear body end, distance	4.5	4.0	1.6	0.3	35.4	2.0	8.0	30
Anterior macronuclear nodule, length	19.2	18.0	3.6	0.7	18.6	14.0	29.0	30
Anterior macronuclear nodule, width	6.9	7.0	1.2	0.2	17.0	4.0	9.0	30
Macronuclear nodules, distance in between	5.2	4.5	3.0	0.5	57.8	1.0	12.0	30
Posterior macronuclear nodule, length	18.1	18.0	3.1	0.6	17.2	13.0	27.0	30
Posterior macronuclear nodule, width	7.7	8.0	1.3	0.2	16.8	5.0	10.0	30
Anteriormost micronucleus, length	3.4	3.0	0.8	0.1	22.7	2.0	5.0	30
Anteriormost micronucleus, width	1.7	1.6	0.3	0.1	17.8	1.5	2.5	30
Macronuclear nodules, number	2.0	2.0	0.0	0.0	0.0	2.0	2.0	30
Micronuclei near anterior macronuclear nodule, number	2.6	2.5	1.0	0.2	39.2	1.0	5.0	30
Micronuclei near posterior macronuclear nodule, number	3.0	2.5	1.3	0.2	42.9	1.0	6.0	30
Micronuclei, total number	5.6	6.0	1.3	0.2	23.5	3.0	8.0	30
Adoral membranelles, number	47.2	48.0	5.9	1.1	12.4	31.0	57.0	28
Frontal cirri, number	3.0	3.0	0.2	0.0	6.0	3.0	4.0	30
Buccal cirri, number	1.0	1.0	0.0	0.0	0.0	1.0	1.0	30
Cirri behind right frontal cirrus, number	1.0	1.0	0.0	0.0	0.0	1.0	1.0	30
Anlagen IV cirri [c], number	3.1	3.0	0.3	0.0	8.3	3.0	4.0	30
Amphisiellid median cirral row, number of cirri	44.5	45.0	5.7	1.2	12.9	25.0	54.0	24
Pretransverse ventral cirri, number	2.0	2.0	0.0	0.0	0.0	2.0	2.0	28
Transverse cirri, number	6.0	6.0	0.2	0.0	3.1	5.0	6.0	29
Left marginal cirri, number	34.6	34.0	3.5	0.6	10.0	25.0	41.0	29
Right marginal cirri, number	34.1	34.0	3.2	0.6	9.3	28.0	41.0	27
Dorsal kineties, number	6.4	6.0	0.6	0.1	9.2	6.0	8.0	23

[a] Measurements in µm. Data based on mounted and protargol-impregnated specimens (only specimens in which most characteristics were measurable, respectively, countable have been used). CV - coefficient of variation in %, M - median, Max - maximum, Min - minimum, n - number of specimens investigated, SD - standard deviation, SE - standard error of arithmetic mean, x - arithmetic mean. [b] Distance between anterior body end and proximal end of adoral zone of membranelles. [c] This is the short cirral row left of the anterior portion of the amphisiellid median cirral row.

Morphology (Figs 1-10, 17-23, Table 1). The improved diagnosis above is solely based on data from the Adriatic neotype population. However, it covers Kahl's data rather well. The ring-shaped structures (lithosomes?), although very conspicuous, have been omitted from the diagnosis because they can be absent (Kahl 1932; see below). The present chapter contains original observations and data from the populations studied by Kahl (1928b, 1932, 1933) and the other workers (Borror 1963, Aladro Lubel 1985, Aladro Lubel *et al.* 1990, Alekperov and Asadullayeva 1999). However, the data are kept separate.

Description of Adriatic population (Figs 1-10, Table 1): Size in life about 100-160 × 30-40 µm (I made only one live measurement, namely 160 × 40 µm; the range is derived from the morphometric data shown in
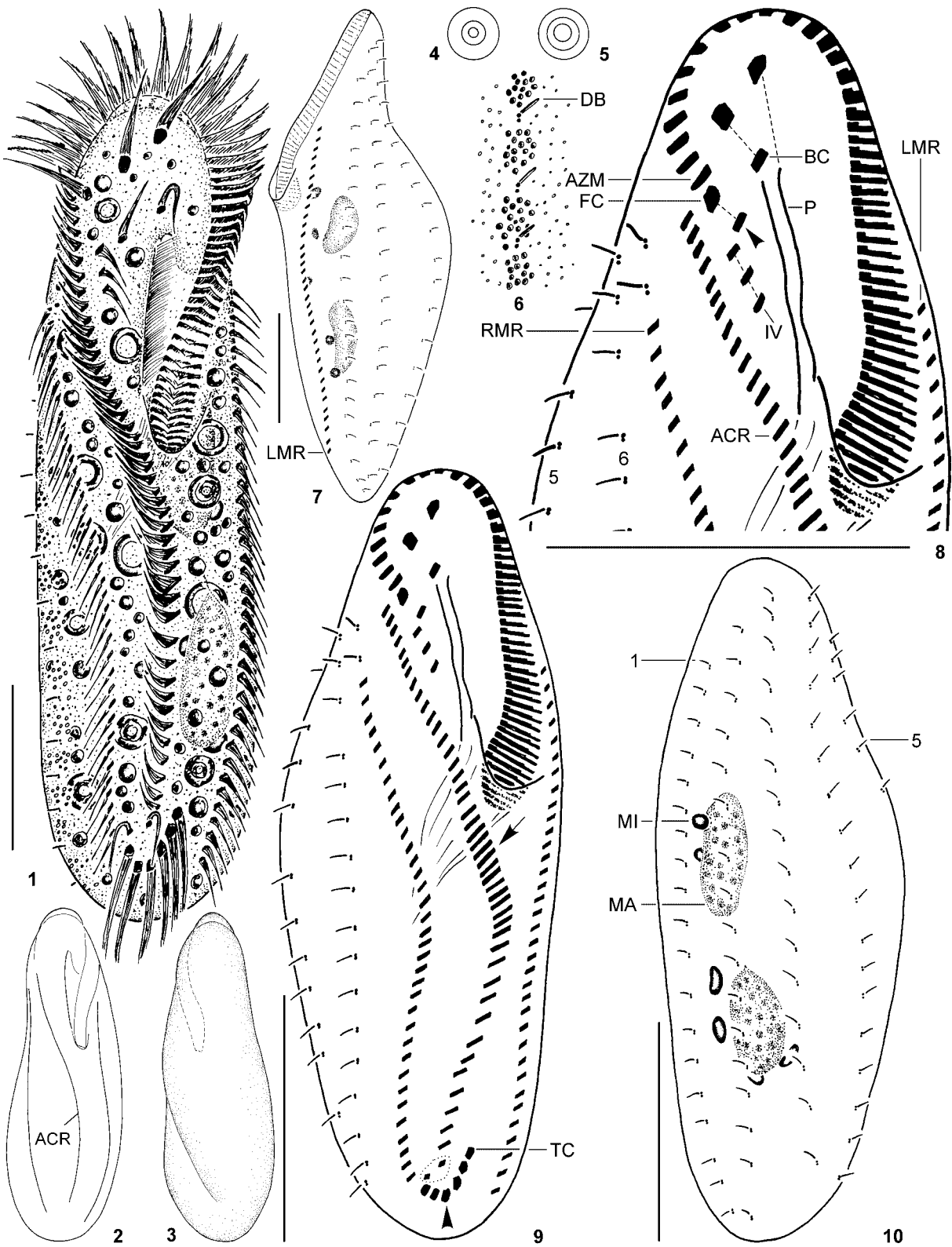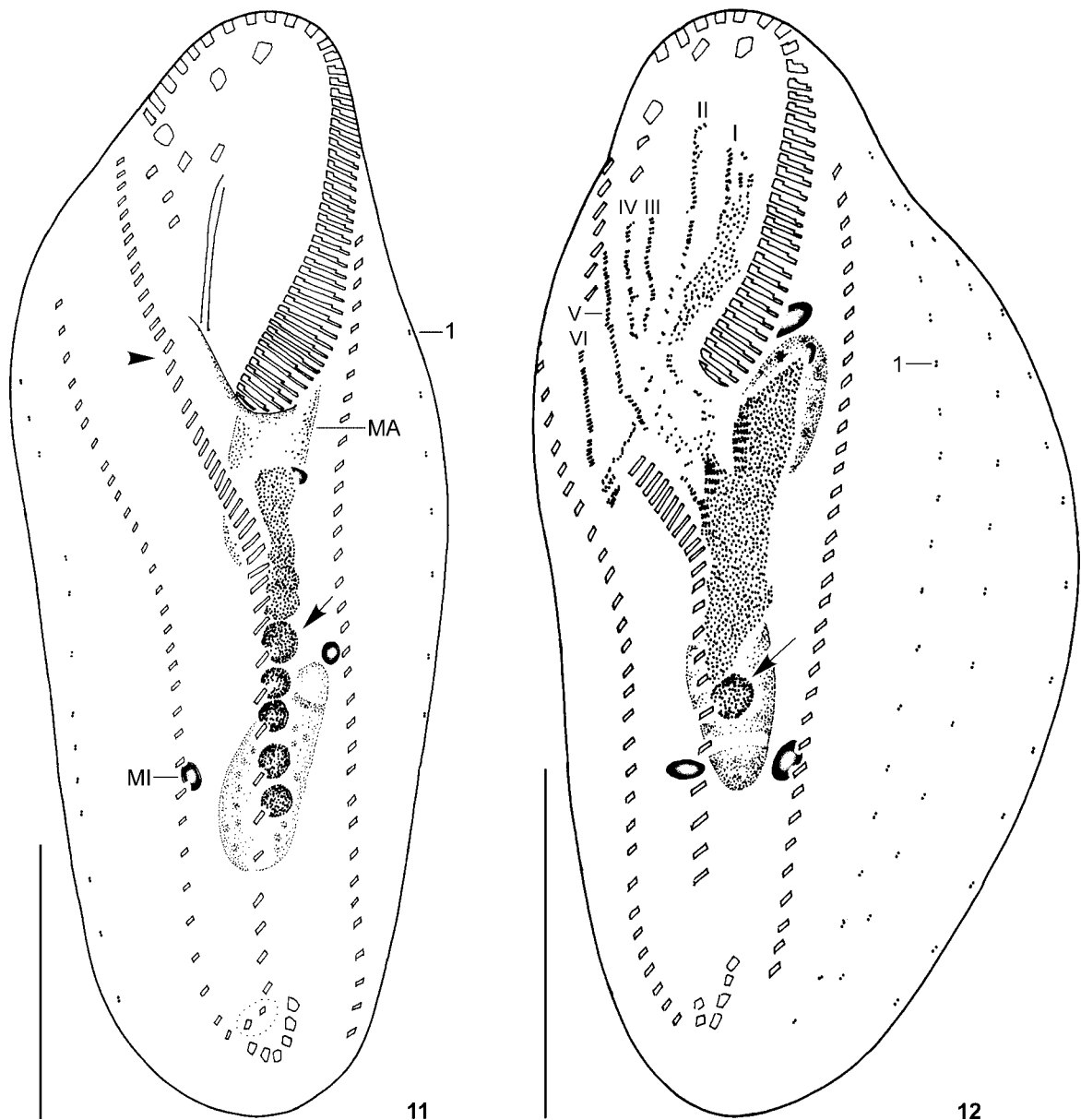
Figs 11, 12. *Amphisiella annulata* after protargol impregnation (parental structures white, new black). Neotype populat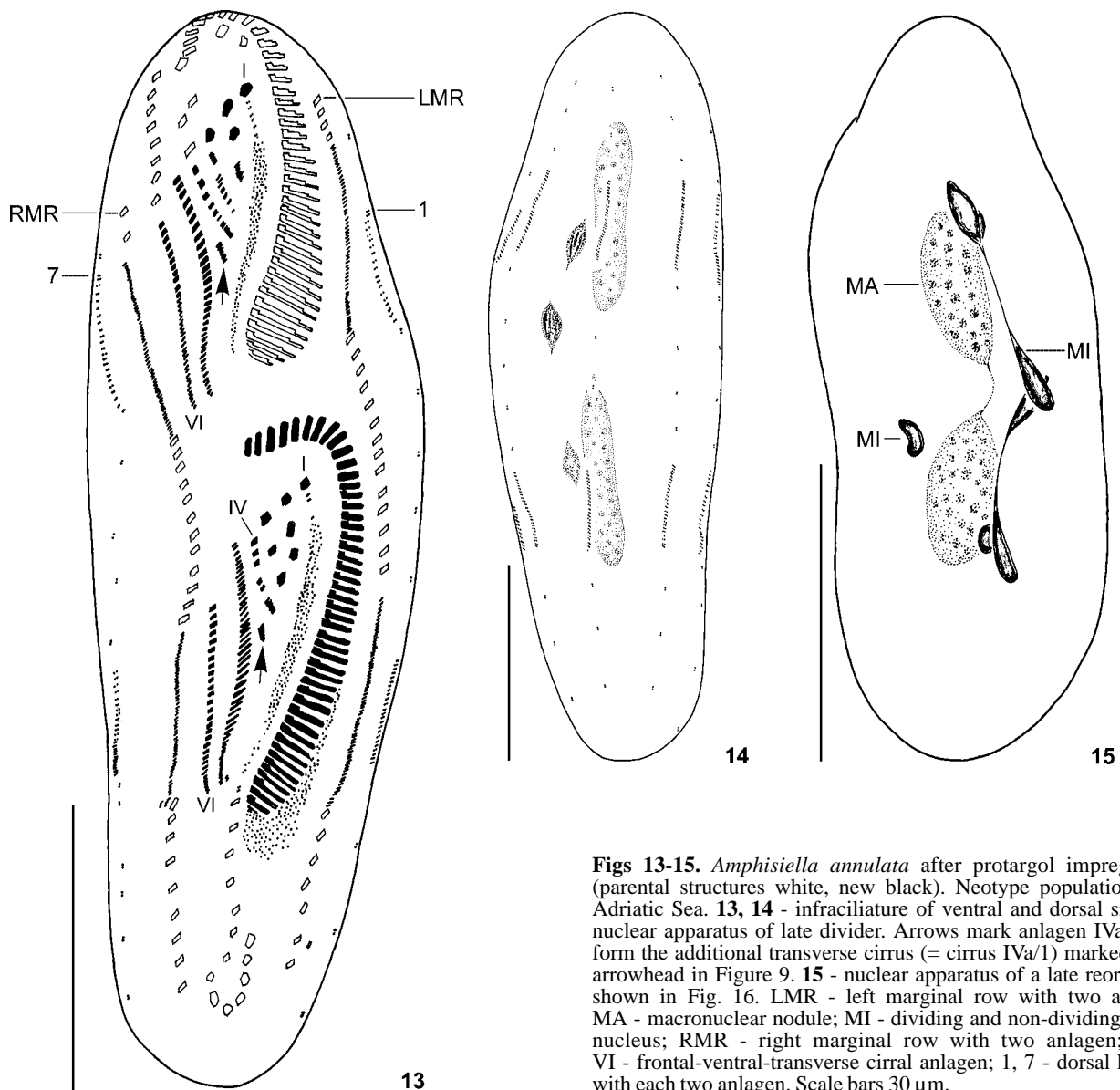ion from Adriatic Sea. **11** - infraciliature of ventral side and nuclear apparatus of early divider. Arrow marks an anlagen pit. Arrowhead denotes discontinuity in amphisiellid median cirral row (site where the 2 portions of the row join). Pretransverse ventral cirri encircled by dotted line; **12** - infraciliature of ventral side and nuclear apparatus of an early to middle reorganizer. Arrow marks an anlagen pit. I assume that this is a reorganizer because in dividers of such a stage the anlagen for both the proter and the opisthe would be recognizable. Note that the additional anlage IVa is not yet clearly recognizable. Area ahead transverse cirri not recognizable because covered by debris. MA - macronuclear nodule; MI - micronucleus; I-VI - cirral anlagen; 1 - dorsal kinety 1 (= leftmost kinety). Scale bars 30 μm.

Figs 1-10. *Amphisiella annulata* from life (1-6) and after protargol impregnation (7–10). Neotype population from Adriatic Sea. **1** - ventral view of a representative specimen. Note ring-shaped structures (hollow globules?); **2, 3** - body outline of posteriorly widened specimens in ventral and dorsal view showing, inter alia, marginal cirral rows, amphisiellid median cirral row, and a dorsal furrow; **4, 5** - ring-shaped structures (hollow globules?) about 4-8 μm across (fine structure not completely discerned); **6** - two size classes of cortical granules are present: (i) 0.8-1.0 μm sized, colourless globules which form patches between dorsal bristles; (ii) tiny (about 0.3-0.5 μm across) colourless globules scattered throughout cortex; **7** - infraciliature of left side. Note strong vaulting of dorsal side, that is, specimens almost not flattened dorsoventrally; **8-10** - infraciliature of ventral and dorsal side and nuclear apparatus of neotype specimen. Arrowhead in (8) denotes cirrus III/2, arrowhead in (9) marks the "additional" transverse cirrus IVa/1 (see Figs 13, 16). Note that the middle portion of the median cirral row is composed of rather wide and narrowly spaced cirri (arrow in 9). Pretransverse ventral cirri encircled by dotted line. Cirri which originate from same frontal-ventral-transverse cirral anlage are connected by broken lines (only shown for anlagen I-IV). ACR - amphisiellid median cirral row; AZM - distal end of adoral zone of membranelles; BC - buccal cirrus (= cirrus II/2); DB - dorsal bristle; FC - right frontal cirrus (= cirrus III/3); LMR - left marginal row; MA - macronuclear nodule; MI - micronucleus; P - paroral; RMR - right marginal row; TC - leftmost transverse cirrus (= cirrus II/1); IV - short row of three cirri left of anterior portion of median cirral row formed by anlage IV; 1, 5, 6 - dorsal kineties. Scale bars 30 μm.

Figs 13-15. *Amphisiella annulata* after protargol impregnation (parental structures white, new black). Neotype population from Adriatic Sea. **13, 14** - infraciliature of ventral and dorsal side and nuclear apparatus of late divider. Arrows mark anlagen IVa which form the additional transverse cirrus (= cirrus IVa/1) marked by an arrowhead in Figure 9. **15** - nuclear apparatus of a late reorganizer shown in Fig. 16. LMR - left marginal row with two anlagen; MA - macronuclear nodule; MI - dividing and non-dividing micronucleus; RMR - right marginal row with two anlagen; I, IV, VI - frontal-ventral-transverse cirral anlagen; 1, 7 - dorsal kineties with each two anlagen. Scale bars 30 μm.

Table 1 assuming a shrinkage of up to 30% due to the preparation procedure; Berger *et al.* 1983); body length : width ratio of live specimens ranging from 3-4 : 1; prepared specimens only 68-121 μm long, length : width ratio on average 2.6 : 1 (Table 1). Body outline elongate elliptical (Fig. 1) to slightly oval (Figs 2, 3), that is, posterior portion wider than anterior; both ends rounded. Body very flexible and often slightly twisted about main body axis, not distinctly contractile, rather resistant against cover glass pressure; ventral side flat, dorsal side often distinctly vaulted so that many specimens are arranged with dorsal or lateral surface above in protargol preparations (Fig. 7). Invariably two macronuclear nodules

slightly left of midline; individual nodules ellipsoidal, in life up to about 28 × 12 μm, with many nucleoli of ordinary size; nodules usually connected by fine strand; length : width ratio of anterior nodule ranging from 1.8-4.8 : 1 (average 2.1 : 1), posterior nodule 1.4-3.4 : 1 (average 2.4 : 1; Table 1). Micronuclei ellipsoidal, arranged close to macronuclear nodules. No contractile vacuole recognizable. Two size-classes of colourless cortical granules; larger globules about 0.8-1.0 μm across, form distinct patches between individual bristles of a dorsal kinety; smaller granules about 0.3-0.5 μm across, more or less densely distributed in whole cortex (Figs 1, 6); stainability with methyl-green pyronin not checked; sometimes
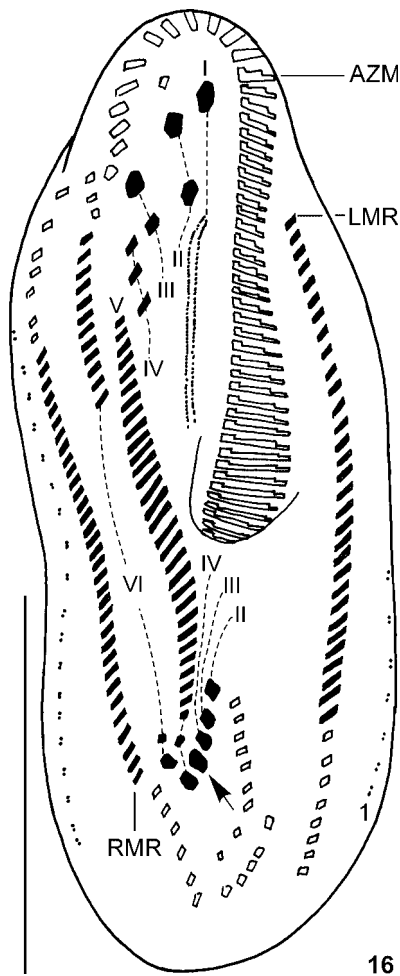
Fig. 16. *Amphisiella annulata* after protargol impregnation (old structures white, new black). Neotype population from Adriatic Sea. Infraciliature of ventral side of a late reorganizer (nuclear apparatus shown in Fig. 15). Cirri originating from same anlage connected by broken line. Arrow marks the additional transverse cirrus originating from the anlage IVa which is formed between anlagen IV and V (see Fig. 13). AZM - adoral zone of membranelles (possibly partially reorganized); LMR - anterior end of new left marginal row; I-VI - frontal-ventral-transverse cirral anlagen; RMR - posterior end of new right marginal row; 1 - dorsal kinety 1 (= leftmost kinety). Scale bar 30 µm.

cortical granules impregnate with protargol. Cells appear steel-grey; cytoplasm colourless, contains many fatty-shining globules 2-5 µm across and several (up to about 20) fatty-shining, ring-shaped structures ("hollow" spheres; lithosomes?) about 4-8 µm in diameter (Figs 1, 4, 5); rings not clearly recognizable in protargol preparations. Movement fast gliding showing great flexibility.

Adoral zone occupies 42% of body length, composed of 47 membranelles on average, individual membranelles of ordinary fine structure (Figs 1-3, 7-9). Distal end of adoral zone extends on average to 12% of body length on right body margin, proximal portion usually slightly spoon-shaped widened. Buccal field inconspicuous, that is, narrow to ordinary wide. Buccal lip inconspicuous because it does not cover proximal portion of adoral zone distinctly. Undulating membranes more or less straight and in parallel; fine structure of membranes not clearly recognizable. Cytopharynx inconspicuous in life and protargol preparations.

Cirral pattern and number of cirri of usual variability (Figs 7-10, Table 1). Three distinctly enlarged frontal cirri in ordinary arrangement, that is, in oblique row along anterior body margin with right cirrus (= cirrus III/3) close behind distal end of adoral zone. Invariably one slightly enlarged buccal cirrus (= cirrus II/2) closely ahead anterior end of paroral, and one cirrus (= cirrus III/2; Fig. 8, arrowhead) left behind right frontal cirrus. A short row composed of three, occasionally of four cirri left of anterior portion of amphisiellid median cirral row; very rarely a second such row present. Amphisiellid median cirral row commences right of right frontal cirrus, extends slightly to distinctly sigmoidally close to transverse cirri, composed of 44 cirri on average (Figs 1, 8, 9, Table 1); median cirral row usually without distinct break although composed of two portions (see morphogenesis); cirri narrowly spaced, especially behind buccal vertex where they are also rather wide, that is, up to 4-5 µm! Invariably two pretransverse ventral cirri, one ahead right transverse cirrus, the other roughly in line with amphisiellid median cirral row. Usually six, rarely (1 out of 29 specimens) only five transverse cirri arranged in J-shaped, slightly subterminal row; cirri about 20 µm long in life and thus distinctly (right) to almost not (left) projecting beyond rear body end. Marginal cirri and cirri of amphisiellid median row only 8-10 µm long in life; marginal cirri relatively narrowly spaced. Left marginal row commences distinctly ahead level of buccal vertex, ends subterminally. Right marginal row begins on average at 25% of body length, often more or less distinctly sigmoidal, terminates near right transverse cirrus; usually two ciliated basal body pairs ahead right marginal row (Figs 7-10).

Dorsal cilia 2-3 µm long; about 2/3 of specimens with six and 1/3 with seven more or less bipolar kineties (Figs 7-10); rarely (1 out of 23 specimens analyzed morphometrically) eight kineties. Caudal cirri lacking.

Beside the very brief original description by Kahl (1928b, Fig. 17), four redescriptions are available, namely by Kahl (1932, 1933; Figs 18, 19), Borror (1963, Fig. 20), Aladro Lubel (1985; including a review by Aladro Lubel
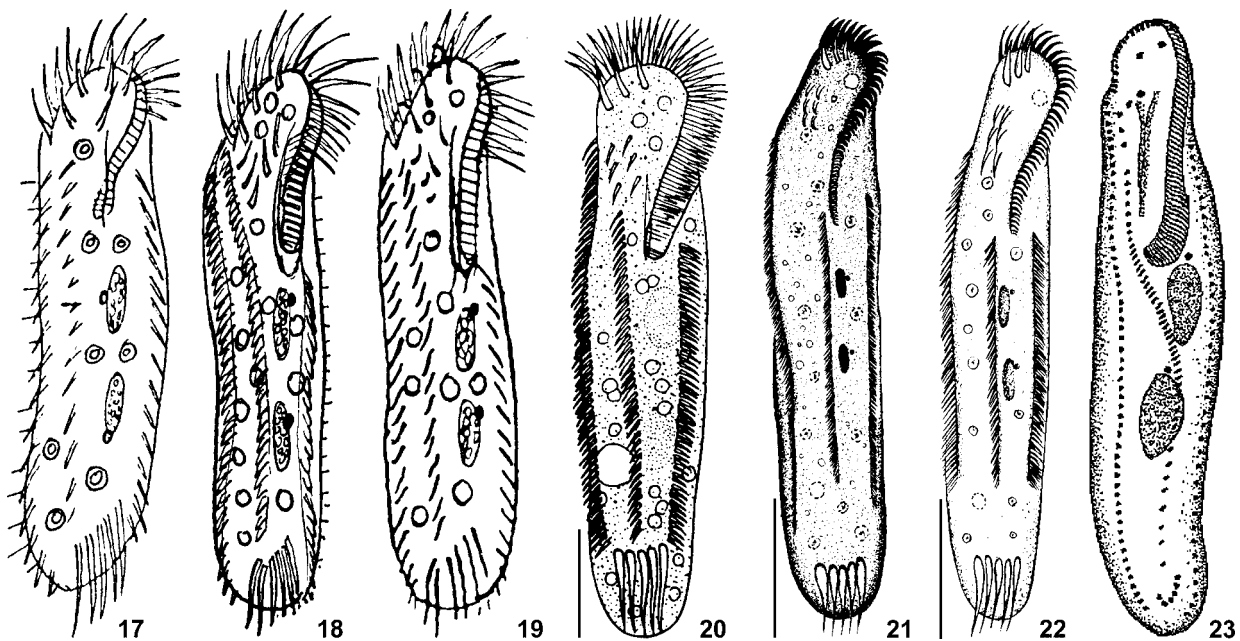
Figs 17-23. *Amphisiella annulata* from life (17-19, from Kahl 1928b, 1932, 1933; 20, from Borror 1963; 21, from Aladro Lubel 1985; 22, from Aladro Lubel *et al.* 1990) and silver preparations (23, from Alekperov and Asadullayeva 1999). Ventral views showing, inter alia, basic cirral pattern, nuclear apparatus, and ring-shaped structures. Note that the cirral pattern illustrated by Kahl (1932) matches almost perfectly the pattern of the neotype (Fig. 9). Borror illustrated a large vacuole in the posterior body portion near the right body margin; it must not be misinterpreted as contractile vacuole because Borror did not mention such an organelle; interestingly enough, in Figures 21, 22 a somewhat smaller vacuole (inclusion?) is shown in a very similar position. Scale bars 30 µm for Figs 17-19, 23; individual sizes not indicated; see text for size ranges.

et al. 1990; Figs 21, 22), and Alekperov and Asadullayeva (1999; Fig. 23). To complete the picture of *A. annulata*, I provide the original data of these populations separately; see also corresponding illustrations for some features, for example, body outline, cirral pattern. For a detailed comparison of the populations, see below. The review by Carey (1992) is not considered further because it contains only a redrawing of Figure 17 and lacks original data.

Population described by Kahl (1928b; Fig. 17): body length 120-150 µm in life; five frontal cirri and five long transverse cirri; single ventral row; scattered ring-shaped "reserve bodies"; lively, metabolic, slightly contractile; two elongated macronuclear nodules.

Population described by Kahl (1932, 1933; Figs 18, 19): body length 150-200 µm in life; body slenderly ellipsoidal, soft, flexible, metabolic, slightly contractile, usually greyish granulated, with a variable number (zero to numerous, but never two, that is, never each one in anterior and posterior body portion) of ring-shaped (probably hollow-spherical) reserve bodies; ectoplasm colourless; two elongated macronuclear nodules, each with a single (?) micronucleus; 6-7 transverse cirri

(specimen illustrated has 6 cirri) which project slightly beyond rear body end; frontal cirri likely as in *Oxytricha* (3 + 2 + 3; homologisation not quite correct, see last chapter); cirri of marginal rows and ventral row very short, wide, and narrowly spaced; for cirral pattern, see the excellent illustration (Fig. 18); posterior portion of adoral zone of membranelles longitudinally arranged.

Population described by Borror (1963; Fig. 20): body size 160×30-36 µm in life; body evenly rounded at ends, slightly flat ventrally. Two oval macronuclear nodules, each 18 µm long; cytoplasm with many spherical granules 4 µm across. Adoral zone of membranelles 55 µm long, composed of 60-65 membranelles. Nine frontal cirri, the anterior three larger; ventral row composed of about 40 narrowly spaced cirri; five transverse cirri 24 µm long, extending just beyond rear body end; about 50 left and 60 right marginal cirri, very closely set; six dorsal kineties.

Population described by Aladro Lubel (1985; Fig. 21): body size 123×21 µm; body outline elongated; two oval-shaped macronuclear nodules, each with a spherical micronucleus; contractile vacuole in posterior body third (side not mentioned and vacuole likely not illustrated);
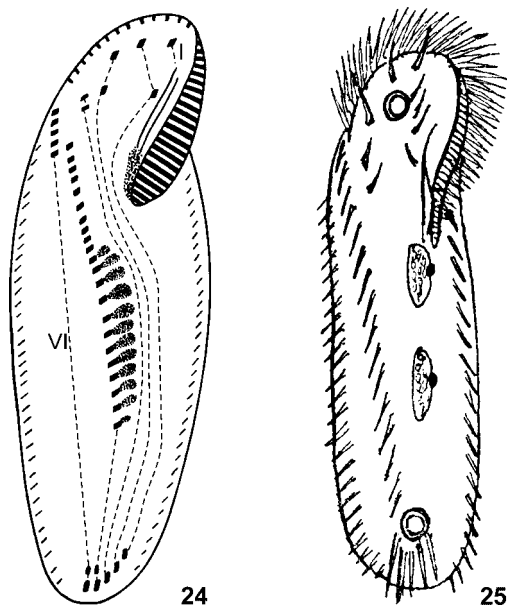
Figs 24, 25. Marine *Amphisiella* species (24, from Wicklow 1982; 25, from Kahl 1932). **24** - *Amphisiella marioni* after protargol impregnation, infraciliature of ventral side of a very early divider, individual size not indicated (size range 75-125 μm in life?). Frontal-ventral-transverse cirri originating from same anlage connected by broken line. **25** - *Amphisiella milnei* from life, ventral view showing cirral pattern, nuclear apparatus, and each one ring-shaped structure in the anterior and posterior body portion, individual size not indicated (size range 100-140 μm in life). I, VI - frontal-ventral-transverse cirral anlagen I and VI.

several food vacuoles and cytoplasmic granules; adoral zone about 1/3 of body length; one left and one right marginal row and one ventral cirral row; cirri narrowly spaced in all rows; nine frontal cirri, three anteriormost larger; five transverse cirri which slightly protrude beyond rear body end.

Population described by Alekperov and Asadullayeva (1999; Fig. 23): body length 130-180 μm in life, 110-145 μm in silver preparations. Body elongated, strongly flattened dorsoventrally. Two macronuclear nodules, 2 micronuclei. Contractile vacuole near proximal end of adoral zone. Cytoplasm transparent, without inclusions. Adoral zone composed of 65-70 membranelles. Two frontal cirri near anterior end, 5 further frontal cirri at level of anterior portion of undulating membranes. Amphisiellid median cirral row composed of 48 cirri, extends from rear frontal cirri to near the 6 transverse cirri. 55 right and 40 left marginal cirri. Four dorsal kineties (3 bipolar, 1 shortened). Caudal cirri absent.

Notes on morphogenesis and reorganization. Only few dividers and reorganizers have been found. However, they allow to elucidate some highly interesting morphogenetic features (Figs 11-16). Some early and middle stages of division are lacking so that the origin of the frontal-ventral-transverse cirral anlagen remains basically unknown.

Cell division commences with the formation of some anlagen pits left of the third quarter of the median cirral row (Fig. 11). The pits are roundish and up to 5 μm deep. Very likely the cirri of the median cirral row beside the pits are not altered at this stage. Ahead the five pits of the divider shown is a large field of basal bodies which likely originated by the fusion of some further pits.

Figure 12 shows an early to middle reorganizer in which the anlagen I-VI are clearly recognizable. The additional anlage IVa, which produces the fourth transverse cirrus from left, is not yet clearly recognizable.

A middle to late divider shows the differentiation of the frontal-ventral-transverse cirri which originate from basically six anlagen (I-VI; Fig. 13). A curiosity is the formation of a small basal body field between anlagen IV and V (Fig. 13, arrows). This small basal body field only forms a transverse cirrus, namely the fourth from left. Consequently, the cirral anlagen produce the following structures: anlage I → undulating membranes (paroral, endoral) and left frontal cirrus (= cirrus I/1); anlage II → leftmost transverse cirrus (= cirrus II/1), buccal cirrus (= cirrus II/2), and middle frontal cirrus (= cirrus II/3); anlage III → second transverse cirrus from left (= cirrus III/1), cirrus left behind right frontal cirrus (= cirrus III/2), and right frontal cirrus (= cirrus III/3); anlage IV → third transverse cirrus from left (= cirrus IV/1) and three cirri left of anterior portion of amphisiellid median cirral row; anlage IVa (Fig. 13, arrows; see below, for explanation) → only fourth transverse cirrus from left (= cirrus IVa/1; Fig. 9, arrowhead; Fig. 16, arrow); anlage V → fifth transverse cirrus from left (= cirrus V/1), left pretransverse ventral cirrus (= cirrus V/2), and posterior portion (around 31 cirri) of amphisiellid median cirral row; anlage VI → sixth transverse cirrus from left (= cirrus VI/1), right pretransverse ventral cirrus (= cirrus VI/2), and anterior portion (about 13 cirri) of amphisiellid median cirral row. The parental adoral zone of membranelles remains obviously more or less unchanged whereas the parental undulating membranes are reorganized (Fig. 13).

A late reorganizer shows that the amphisiellid median cirral row of *A. annulata* is formed by cirri of the two rightmost anlagen (Fig. 16). Anlage V produces the posterior portion which commences slightly ahead the level of the buccal vertex in interphasic specimens. The front portion is formed by the anteriorly migrating cirri

(except the right pretransverse ventral cirrus and the right transverse cirrus) of anlage VI. This conspicuous migration enforces the homologisation of the anterior portion with the frontoterminal cirri of the oxytrichids and urostylids. In interphasic specimens the two portions form a continuous row (Fig. 9); only very rarely a discontinuity is recognizable (Fig. 11, arrowhead).

The development of the marginal rows and dorsal kineties does not show a peculiarity. Two primordia each occur within the parental cirral and bristle rows. No caudal cirri are formed (Figs 13, 14). The division of the nuclear apparatus proceeds in ordinary manner, that is, the two macronuclear nodules fuse to a single mass which subsequently divides. The micronuclei behave like those of other hypotrichs (Figs 11, 14).

The morphogenetic pattern of *A. annulata* largely agrees with that of *A. marioni* (Wicklow 1982). Of course there are also several agreements with many other hypotrichs, for example, that the left frontal cirrus originates from the undulating membrane anlage or that the buccal cirrus is the middle cirrus of anlage II. However, these are rather old symplesiomorphies and are therefore not considered further.

A very interesting morphogenetic feature of *A. annulata* is the formation of roundish anlagen pits left of the middle and posterior portion of the median cirral row (Fig. 11). Wicklow (1982) illustrated an early divider of *A. marioni* which shows several roundish patches of basal bodies, strongly resembling the pits of *A. annulata* (Fig. 24). However, Wicklow mentioned no details about this stage so that it is unknown whether these patches are invaginated or flat. Thus, reinvestigation of the morphogenesis of the type species is needed. In most hypotrichs the oral anlage develops on the cell surface (for review, see Foissner 1996). In euplotids, strombidiids, strobilidiids, and few non-euplotid hypotrichs, e.g., *Psilotricha succisa* (Foissner 1983), the anlage originates in a more or less distinct subsurface pouch (= hypoapokinetal stomatogenesis). In *Pseudo-amphisiella lacazei* morphogenesis commences with the proliferation of loosely arranged basal bodies below the cortex and therefore parental cirri and fibres remain intact (Song *et al.* 1997). According to molecular data, the oligotrichs/choreotrichs and the euplotids are the next relatives of the remaining hypotrichs (e.g., Bernhard *et al.* 2001, Modeo *et al.* 2003). This indicates that the hypoapokinetal stomatogenesis is a plesiomorphy for the non-euplotid hypotrichs. Unfortunately, we do not know whether or not the roundish pits of *A. annulata* are homologous with the subsurface pouches of the groups

mentioned above or with the subcortical formation of the anlagen field in *Pseudoamphisiella lacazei*. If they are not homologous then the anlagen pits can be interpreted as apomorphy of *Amphisiella*.

A further interesting morphogenetic feature of *A. annulata* is the formation of an additional cirral anlage between the ordinary anlagen IV and V. Since all anlagen of *A. annulata* - except this additional one - can be unequivocally homologized with the anlagen of *A. marioni*, I keep the ordinary numbering (I-VI) and designate the additional anlage, more or less arbitrarily, as anlage IVa. This anlage produces only a transverse cirrus so that *A. annulata* has six transverse cirri (Table 1). In contrast, *Amphisiella marioni* lacks such an additional anlage and therfore has the ordinary number of five transverse cirri (see Figs 45a-h in Wicklow 1982). *Amphisiella turanica*, described by Alekperov and Asadullayeva (1999), also has 6 transverse cirri indicating that it forms, like *A. annulata*, an additional anlage.

Occurrence and ecology. *Amphisiella annulata* is a salt water species. Kahl (1928b) discovered it in the Brennermoor, a saline (25‰), silt peat bog near the north German village Bad Oldesloe (Kahl 1928a). Later, he found it in the harbour of the German city of Kiel, Baltic Sea (Kahl 1932). Alekperov and Asadullayeva (1999) isolated their population from the periphyton of the South Apsheron coast of the Caspian Sea. I found *A. annulata* in the littoral of the northern Adriatic Sea at a water temperature of about 20°C (further details on the sample site, see materials and methods). It occurred together with *Uroleptopsis citrina*, *Pseudoamphisiella* sp., and some euplotids. In the cultures the abundance of *A. annulata* was rather low, while *U. citrina* grew very well.

Records from the Gulf of Mexico: rare in diatom detritus from the mouth of a saltmarsh near the Florida State University Marine Laboratory at Alligator Harbor, USA (Borror 1962, 1963); interstitial of Enmedio Island and Laguna de Mandinga, Veracruz, Mexico (Aladro Lubel 1985; Aladro Lubel *et al.* 1988, 1990).

Records not substantiated by morphological data: during summer and winter in the sublittoral (Stoller Grund, Großer Belt) of the Bay of Kiel, Baltic Sea (Bock 1952); Schlei, a polluted, brackish fjord in the western Baltic (Bock 1960, Jaeckel 1962); with a frequency of 2.7% at 21-22°C and 17-18‰ salinity at the Bulgarian coast of the Black Sea (Detcheva 1982, 1983); sediment of Loch Eil on the west coast of Scotland (Wyatt and Pearson 1982).

Amphisiella annulata feeds on small diatoms (Kahl 1932, Borror 1963; for review, see Fenchel 1968). In cultures, it ingests also wheat stark (own observations).

Comparison of *Amphisiella annulata* populations. The original description of *A. annulata* is very brief but contains most diagnostic features (Kahl 1928b). Accordingly, the present species has each five frontal and transverse cirri (Fig. 17). As concerns the frontal cirri, Kahl (1928b) very likely included only the three enlarged frontal cirri, the buccal cirrus, and cirrus III/2. The short row composed of three cirri left of the anterior portion of the median cirral row is less distinct than the other five "frontal cirri" and thus easily overlooked or misinterpreted as anterior end of the median cirral row. Somewhat more difficult is the interpretation of the five transverse cirri because this number was not mentioned by Kahl (1932) and Alekperov and Asadullayeva (1999) and occurred only very rarely in the Adriatic population (Table 1). The following possibilities exist: (i) Kahl (1928b) observed and illustrated a rare specimen which had indeed only five transverse cirri; (ii) Kahl (1928b) did not count correctly. On page 211, Kahl (1928b) wrote that he would like to investigate the species again, indicating that his observations are not very detailed and precise; (iii) the populations studied by Kahl (1928b) and Kahl (1932) are not conspecific. I prefer possibilities (i) and (ii) because it is unlikely that Kahl (1932) did not recognize his own species, inasmuch as it has a conspicuous feature, namely the large, ring-shaped structures. To avoid this permanent uncertainty it seems wise to designate a neotype (see last chapter).

My data match almost perfectly the redescription and illustrations by Kahl (1932, 1933) so that the identification is beyond reasonable doubt. Very likely all identifications listed in the synonymy and the occurrence and ecology section have been done after Kahl (1932), and not after the original description (Kahl 1928b). Consequently, the 1932 review was *de facto* the authoritative redescription. There are only few differences between Kahl's (1932) data and my observations which, however, can be explained: (i) body length is 150-200 µm against 100-160 µm. My sole live measurement, which I made some days before the fixation of the material, was 160 x 40 µm which fits into the range provided by Kahl. Obviously the Adriatic specimens became slightly smaller in cultures as indicated by the morphometric analysis (Table 1). Further, the specimens of Kahl's (1928b) population were also only 120-150 µm long. (ii) Kahl did not mention the cortical granules which are present in the population from the Adriatic Sea. However, the

granules are colourless and rather small (0.3-1.0 µm) and thus easily overlooked especially with bright field illumination. Kahl (1932) wrote " ..., usually grey granulated and in between with numerous ring-shaped reserve bodies"; this indicates that the term grey granulated refers to the cytoplasm and not to a cortical granulation. Indeed, the specimens of my population were also steel-grey; however, I do not know whether this impression is mainly due to the cytoplasm or the colourless cortical granulation. (iii) The Adriatic population has two pretransverse ventral cirri which are neither mentioned nor illustrated by Kahl (1932, 1933). However, they are rather small and at least the left cirrus is almost not set off from the rear end of the median cirral row indicating that Kahl has not distinguished this small cirral group from the median cirral row. But more important than these few differences is the exact agreement in the remaining cirral pattern which is not very difficult to recognize in life. Kahl (1932) emphasized the short, wide, and narrowly spaced cirri in the marginal and median rows, a feature which is indeed very conspicuous (Figs 1, 9, 18).

The redescriptions by Borror (1963, Fig. 20) and Aladro Lubel (1985, Fig. 21) are less detailed than Kahl's (1932, Fig. 18) data. Especially the cirral patterns do not correspond very well with those described by Kahl (1932) and in the present paper (Fig. 9). The following differences are the most conspicuous ones: (i) the median cirral row is distinctly shortened against unshortened; (ii) only five transverse cirri present (Figs 20-22) against six (Fig. 18). Admittedly, five fits exactly the original description by Kahl (1928b), but as discussed above this is obviously not the ordinary number for *A. annulata*. (iii) Borror and Aladro Lubel did not mention the conspicuous ring-shaped structures, although some globules are illustrated which can be also interpreted as rings (Figs 20-22). They write about digestive vacuoles and cytoplasmic granules (Aladro Lubel 1985) and many endoplasmic spherical granules 4 µm in diameter (Borror 1963). The non-mention of these large, conspicuous ring-shaped structures indicates that they were not present in the American populations which is, however, not a proof for a misidentification because Kahl (1932) also mentioned that the rings, which could be lithosomes (for review, see Hausmann and Hülsmann 1996), can be absent. It is noticeable that the illustrations provided by Borror (1963; Fig. 20) on the one hand and by Aladro Lubel (1985, Fig. 21) and Aladro Lubel *et al.* (1990, Fig. 22) on the other hand are very similar, especially as concerns the anterior shortage of the

median cirral row, the five strong transverse cirri, and the six paired cirri ahead the median cirral row. The Caspian Sea population (Fig. 23) differs from the Adriatic population mainly by the lack of the ring-shaped structures (*vs*. present), in the higher number of adoral membranelles (65-70 *vs*. 31-57), the lack of pretransverse ventral cirri (*vs*. 2 such cirri present), and the lower number of dorsal kineties (4 *vs*. usually 6).

Generic classification and comparison with related species. The classification of the present species in the subgenus/genus *Amphisiella* by Kahl (1932), respectively, Borror (1972) seems correct because the cirral pattern matches very well that of *A. marioni*, type of the genus. Further, the morphogenesis proceeds largely identical in these two species (see above) also indicating that the assignment to *Amphisiella* - as defined recently by Voss (1992), Eigner and Foissner (1994), and Petz and Foissner (1996) - is correct.

More than 20 species have been originally described in *Amphisiella* and many species have been transferred to and excluded from this group (Berger 2001, Foissner *et al*. 2002). However, many of them are confined to terrestrial habitats. Thus, the comparison is restricted to similar marine congeners. According to Hemberger (1982), *Amphisiella marioni*, *A. annulata*, and *A. milnei* are junior synonyms of *A. capitata*. Indeed, synonymy of *A. capitata* and *A. marioni* could be possibly. However, this problem is beyond the scope of the present paper and therefore not considered further.

Amphisiella marioni, which is reliably redescribed by Wicklow (1982), has (i) only two cirri in the short row left of the anterior portion of the median cirral row (Fig. 24; against three in *A. annulata*, Figs 8, 9, 18); (ii) a shorter and distinctly interrupted median cirral row (terminates distinctly ahead transverse cirri *vs*. very near transverse cirri and usually continuous) which is composed of about 26-29 ordinary sized and spaced cirri (against 25-54, on average 44 rather wide cirri which are narrowly spaced); (iii) 4-5 transverse cirri (against usually 6). *Amphisiella marioni* and *A. annulata* agree, inter alia, in the marine habitat, the number of dorsal kineties (6, respectively, 6.4 on average), the arrangement of the undulating membranes (straight and in parallel), and the presence of invariably two pretransverse ventral cirri (termed accessory transverse cirri by Wicklow 1982) ahead the two rightmost transverse cirri. Further, morphogenesis obviously proceeds very similar (see above) so that a close relationship of these two species is very likely.

Amphisiella milnei (Kahl 1932; Fig. 25) has, inter alia, yellowish cortical granules (*vs*. colourless in *A. annulata*), five transverse cirri (*vs*. 6), possibly a different cirral pattern in the frontal area (cf. Fig. 25 with Fig. 18), and each one ring-shaped structure in the anterior and posterior body portion (rear one sometimes lacking *vs*. usually several rings scattered throughout cytoplasm). Further, the cirri of the marginal rows and the median row are of ordinary size and arrangement in *A. milnei* whereas they are rather wide and narrowly spaced in *A. annulata*.

Amphisiella turanica from the Caspian Sea is somewhat larger (170-210 µm long in life) than *A. annulata*, has 70-85 adoral membranelles, 4 dorsal kineties, and, most importantly, 4 macronuclear nodules (Alekperov and Asadullayeva 1999).

According to Kahl (1932), the frontal cirri of *A. annulata* are arranged "as in *Oxytricha* (3 + 2 + 3)". This is only correct for the first two parts (3 + 2), that is, the three enlarged frontal cirri (cirri I/1, II/3, III/3), the buccal cirrus (cirrus II/2), and cirrus III/2 which is behind the right frontal cirrus. The last three cirri of the (3 + 2 + 3) pattern are formed by the anlage IV in *A. annulata* whereas they are produced from two different anlagen in the 18-cirri oxytrichids, namely the anterior two cirri (cirri VI/3, VI/4 = frontoterminal cirri) from anlage VI and the rearmost cirrus from anlage IV (cirrus IV/3; for review on oxytrichids, see Berger 1999).

Kahl (1932, p. 582, 583) wrote that he had confused *A. annulata* with his *Holosticha setifera* earlier, likely because both species have large, ring-shaped structures. *Holosticha setifera*, which occurred like *A. annulata* in saltwater habitats near Bad Oldesloe (Germany), has a distinct midventral pattern, a single micronucleus between the two macronuclear nodules, and distinct caudal cirri (Kahl 1932, his Fig. 106 *9*) and therefore differs clearly from *A. annulata*. *Holosticha obliqua* sensu Kahl (1932, his Fig. 106 *26*) has also only one micronucleus between the two macronuclear nodules and five transverse cirri (against several micronuclei and six transverse cirri in *A. annulata*). Possibly, this illustration contains features of *H. setifera* and *A. annulata*, as supposed by Kahl (1932) himself.

In life, *Amphisiella annulata* is rather conspicuous mainly because of the wide and narrowly spaced cirri of the median cirral row. This feature and the conspicuous ring-shaped structures enable a very simple identification of this salt water species. Since the cell is rather

large and resistant against cover glass pressure, the cirral pattern can be studied very detailed even in life (own observations), as impressively demonstrated by Kahl more than 70 years ago!

Neotypification. No type or voucher slides are available from the *A. annulata* populations described by Kahl (1928b, 1932), Borror (1963), and Aladro Lubel (1985). Voucher slides of the Caspian Sea population studied by Alekperov and Asadullayeva (1999) are likely deposited in the Protistological Laboratory of the Institute of Zoology of the Academy of Sciences of Azerbaijan in Baku.

As mentioned above there are some discrepancies between the original description (Kahl 1928b) and the authoritative redescription by Kahl (1932). In addition, the redescriptions provided by Borror (1963) and Aladro Lubel (1985) do not fit very well the authoritative redescription and also not the original description. Further, Hemberger (1982) put *A. annulata* into the synonymy of *A. capitata*. Thus, it seems wise to define *A. annulata* objectively by the designation of a neotype (ICZN 1999, Foissner 2002). According to Article 75.3 of the ICZN (1999), the designation has to be accompanied by the publication of some particulars:

(i) the taxonomic status of the present species is somewhat unclear because the original description, the authoritative redescription, and two redescriptions do not agree in some important features (see above for details).

(ii) for a differentiation of *A. annulata* from related taxa, see above.

(iii) the neotype specimen (Figs 9, 10), respectively, neotype population from the Adriatic Sea is described in detail (see above); thus, recognition of the neotype designated is ensured.

(iv) it is generally known that no type material is available from species described by Kahl. Further, there is no indication that Borror (1963) or Aladro Lubel (1985) made permanent preparations of the present species. Alekperov and Asadullayeva (1999) did not designate a neotype.

(v) there is strong evidence that the neotype is consistent with *A. annulata* as originally described by Kahl (1928b). For a detailed comparison, see above. In addition, there is no reasonable doubt that the neotype population is conspecific with the population described by Kahl (1932). This 1932 revision, and certainly not the original description, was very likely used by most (all?) subsequent workers for the identification of *A. annulata*.

(vi) unfortunately, the neotype does not come from very near the original type locality (northern Adriatic Sea *vs*. saline waters in North Germany; distance about 1000 km). However, both sites are salt water habitats from the holarctic region, and many ciliates - especially marine ones, which live in a comparatively homogenous medium - are cosmopolitans (Patterson *et al.* 1989) so that this point should not be over-interpreted (for a thorough discussion of this problem, see Foissner *et al.* 2002, p. 44 and Foissner 2002). A detailed description of the new type locality, that is, the sample site of the neotype population, is given in the materials and methods section.

(vii) the slide containing the neotype specimen and four slides containing some further specimens (including those depicted in the present paper) of the neotype population are deposited in the Biologiezentrum des Oberösterreichischen Landesmuseums in Linz (LI), Austria.

REFERENCES

Aladro Lubel M. A. (1985) Algunos ciliados intersticiales de Isla de Enmedio, Veracruz, México. *An. Inst. Biol. Univ. Méx., Ser. Zoología* (1) **55:** 1-59

Aladro Lubel M. A., Martínez Murillo M. E., Mayén Estrada R. (1988) Lista de los ciliados bentonicos salobres y marinos registrados en Mexico. *An. Inst. Biol. Univ. Méx., Ser. Zoología* (1) **58:** 403-447

Aladro Lubel M. A., Martínez Murillo M. E., Mayén Estrada R. (1990) Manual de ciliados psamofilos marinos y salobres de Mexico. Cuadernos del Instituto de Biologia 9. Universida Nacional Autonoma de Mexico

Alekperov I. K., Asadullayeva E. S. (1999) New, little-known and characteristic ciliate species from the Apsheron coast of the Caspian Sea. *Turkish J. Zool.* **23:** 215-225

Berger H. (1999) Monograph of the Oxytrichidae (Ciliophora, Hypotrichia). *Monographiae biol.* **78:** i-xii, 1-1080

Berger H. (2001) Catalogue of Ciliate Names 1. Hypotrichs. Verlag Helmut Berger, Salzburg

Berger H., Foissner W., Adam H. (1983) Morphology and morphogenesis of *Fuscheria terricola* n. sp. and *Spathidium muscorum* (Ciliophora: Kinetofragminophora). *J. Protozool.* **30:** 529-535

Bernhard D., Stechmann A., Foissner W., Ammermann D., Hehn M., Schlegel M. (2001) Phylogenetic relationships within the class Spirotrichea (Ciliophora) inferred from small subunit rRNA gene sequences. *Molec. Phyl. Evol.* **21:** 86-92

Bock K. J. (1952) Zur Ökologie der Ciliaten des marinen Sandgrundes der Kieler Bucht I. *Kieler Meeresforsch.* **9:** 77-89

Bock K. J. (1960) Biologische Untersuchungen, insbesondere der Ciliatenfauna, in der durch Abwässer belasteten Schlei (westliche Ostsee). *Kieler Meeresforsch.* **16:** 57-68

Borror A. C. (1962) Ciliate protozoa of the Gulf of Mexico. *Bull. mar. Sci. Gulf. Caribb.* **12:** 333-349

Borror A. C. (1963) Morphology and ecology of the benthic ciliated protozoa of Alligator Harbor, Florida. *Arch. Protistenk.* **106:** 465-534

Borror A. C. (1972) Revision of the order Hypotrichida (Ciliophora, Protozoa). *J. Protozool.* **19:** 1-23

Carey P. G. (1992) Marine Interstitial Ciliates. An Illustrated Key. Chapman and Hall, London, New York, Tokyo, Melbourne, Madras

Detcheva R. B. (1982) Recherches, en Bulgarie, sur les cilies de certaines plages de la Mer Noire et des rivieres y aboutissant. *Annls. Stn limnol. Besse* **15** (1981/1982)**:** 231-253

Detcheva R. B. (1983) Contribution sur la faune des ciliés mesopsammiques de quelques plages bulgares et celles des rivières qui se jettent dans la mer. *Hydrobiology* **18:** 64-76

Eigner P., Foissner W. (1994) Divisional morphogenesis in *Amphisiellides illuvialis* n. sp., *Paramphisiella caudata* (Hemberger) and *Hemiamphisiella terricola* Foissner, and redefinition of the Amphisiellidae (Ciliophora, Hypotrichida). *J. Euk. Microbiol.* **41:** 243-261

Fenchel T. (1968) The ecology of marine microbenthos II. The food of marine benthic ciliates. *Ophelia* **5:** 73-121

Foissner W. (1983) Morphologie und Morphogenese von *Psilotricha succisa* (O. F. Müller, 1786) nov. comb. (Ciliophora, Hypotrichida). *Protistologica* **19:** 479-493

Foissner W. (1996) Ontogenesis in ciliated protozoa, with emphasis on stomatogenesis. In: Ciliates. Cells as Organisms (Eds K. Hausmann, P. C. Bradbury). Fischer, Stuttgart, Jena, Lübeck, Ulm, 95-177

Foissner W. (2002) Neotypification of protists, especially ciliates (Protozoa, Ciliophora). *Bull. zool. Nom.* **59:** 165-169

Foissner W., Berger H., Kohmann F. (1999) Identification and ecology of limnetic plankton ciliates. *Informationsberichte des Bayer. Landesamtes Wasswirt.* **3/99:** 1-793

Foissner W., Agatha S., Berger H. (2002) Soil ciliates (Protozoa, Ciliophora) from Namibia (Southwest Africa), with emphasis on two contrasting environments, the Etosha region and the Namib desert. Part I: Text and line drawings. Part II: Photographs. *Denisia* **5:** 1-1459

Hausmann K., Hülsmann N. (1996) Protozoology. 2 nd. Thieme, Stuttgart, New York

Hemberger H. (1982) Revision der Ordnung Hypotrichida Stein (Ciliophora, Protozoa) an Hand von Protargolpräparaten und Morphogenesedarstellungen. Dissertation Universität Bonn

Hentschel E. J., Wagner G. H. (1996) Zoologisches Wörterbuch. Tiernamen, allgemeinbiologische, anatomische, physiologische Termini und Kurzbiographien. Gustav Fischer Verlag, Jena

ICZN (The International Commission on Zoological Nomenclature) (1999) International Code of zoological nomenclature. International Trust for Zoological Nomenclature, London

Jaeckel S. G. A. (1962) Die Tierwelt der Schlei. Übersicht einer Brackwasserfauna. *Schr. naturw. Ver. Schlesw.-Holst.* **33:** 11-32

Kahl A. (1928a) Die Infusorien (Ciliata) der Oldesloer Salzwasserstellen. *Arch. Hydrobiol.* **19:** 50-123

Kahl A. (1928b) Die Infusorien (Ciliata) der Oldesloer Salzwasserstellen. *Arch. Hydrobiol.* **19:** 189-246

Kahl A. (1932) Urtiere oder Protozoa I: Wimpertiere oder Ciliata (Infusoria) 3. Spirotricha. *Tierwelt Dtl.* **25:** 399-650

Kahl A. (1933) Ciliata libera et ectocommensalia. *Tierwelt N.-u. Ostsee Lieferung* **23 (Teil II. c₂):** 29-146

Modeo L., Petroni G., Rosati G., Montagnes D. J. S. (2003) A multidisciplinary approach to describe protists: redescriptions of *Novistrombidium testaceum* Anigstein 1914 and *Strombidium inclinatum* Montagnes, Taylor, and Lynn 1990 (Ciliophora, Oligotrichia). *J. Euk. Microbiol.* **50:** 175-189

Patterson D. J., Larsen J., Corliss J. O. (1989) The ecology of heterotrophic flagellates and ciliates living in marine sediments. *Progr. Protistol.* **3:** 185-277

Petz W., Foissner W. (1996) Morphology and morphogenesis of *Lamtostyla edaphoni* Berger and Foissner and *Onychodromopsis flexilis* Stokes, two hypotrichs (Protozoa: Ciliophora) from Antarctic soils. *Acta Protozool.* **35:** 257-280

Song W., Warren A., Hu X. (1997) Morphology and morphogenesis of *Pseudoamphisiella lacazei* (Maupas, 1883) Song, 1996 with suggestion of establishment of a new family Pseudoamphisiellidae nov. fam. (Ciliophora, Hypotrichida). *Arch. Protistenk.* **147:** 265-276

Voss H.-J. (1992) Morphogenesis in *Amphisiella australis* Blatterer and Foissner, 1988 (Ciliophora, Hypotrichida). *Europ. J. Protistol.* **28:** 405-414

Wallengren H. (1900) Zur Kenntnis der vergleichenden Morphologie der hypotrichen Infusorien. *Bih. K. svenska Vetenska Akad. Handl.* **26:** 1-31

Wicklow B. J. (1982) The Discocephalina (n. subord.): ultrastructure, morphogenesis and evolutionary implications of a group of endemic marine interstitial hypotrichs (Ciliophora, Protozoa). *Protistologica* **18:** 299-330

Wyatt C. E., Pearson T. H. (1982) The Loch Eil project: population characteristics of ciliate protozoans from organically enriched Sea-Loch sediments. *J. exp. mar. Biol. Ecol.* **56:** 279-303

ACTA
PROTOZOOLOGICA

PACAP-38 Signaling in *Tetrahymena thermophila* Involves NO and cGMP

John LUCAS, Mark RIDDLE, Janine BARTHOLOMEW, Brendan THOMAS, Jason FORNI, L. Emery NICKERSON, Bradley Van HEUKELUM, Joshua PAULICK and Heather KURUVILLA

Cedarville University, Department of Science and Mathematics, Cedarville, OH, USA

Summary. Chemorepellents are signaling molecules, which have been shown to be important for mammalian neuronal development, and are presumed to have a role in protozoan defense. *Tetrahymena thermophila* represent a good model system in which to study repellents because of their ease of use in biochemical, behavioral, electrophysiological, and genetic analyses. In this study, we have used *Tetrahymena* as a model in which to study the chemorepellent, PACAP. Using behavioral and biochemical (EIA) assays, we have found that the NO/cGMP pathway plays an important role in PACAP signaling. An increase in intracellular calcium is also critical for PACAP avoidance, which appears to be mediated through a pertussis toxin-sensitive G-protein.

Key words: chemorepellent, G-protein, nitric oxide, PACAP-38.

Abbreviations: cGMP - guanosine 3'5' monophosphate, IMP - 2-imino-4-methylpiperidine, NO - nitric oxide, NOS - nitric oxide synthase, PACAP - pituitary adenylate cyclase activating polypeptide.

INTRODUCTION

Chemorepellents are compounds that cause a cell to exhibit avoidance. Some of these compounds have been shown to be important in human neuronal development (Zhu *et al.* 1999). Still, relatively little is known about repellents and how they work. Ciliate model systems, such as *Tetrahymena thermophila*, are a useful tool in which to study repellents because they exhibit a distinctive "avoidance behavior", easily seen under a dissection microscope. They have been widely used in genetics studies (Orias 1998), and can even be used in

electrophysiological experiments (Kuruvilla and Hennessey 1998, 1999; Kim *et al.* 1999).

Tetrahymena respond to a number of compounds as repellents, including ATP (Kim *et al.* 1999, Rosner *et al.* 2003), GTP (Kuruvilla *et al.* 1997, Iwamoto and Nakaoka 2002), and PACAP (Mace *et al.* 2000, Hassenzahl *et al.* 2001, Keedy *et al.* 2003), all of which appear to use different receptors. Although avoidance behavior to each of these compounds appears identical when observed under a dissection microscope, the intracellular pathways involved are not. Previous studies in our laboratory have implicated a G-protein linked receptor in PACAP signaling (Hassenzahl *et al.* 2001), which is similar to signaling pathways utilized by vertebrate PACAP receptors. ATP also appears to signal through a G-protein linked receptor (Rosner *et al.* 2003); however,

Address for correspondence: Heather Kuruvilla, Cedarville University, Department of Science and Mathematics, 251 North Main St. Cedarville, OH 45314, USA

GTP signaling appears to involve a tyrosine kinase pathway (Bartholomew *et al.,* submitted).

PACAP has myriad actions in vertebrates. Although originally isolated from brain, target cells include smooth muscle cells along with a number of different neuronal cell types (Forssmann and Said 1998). Vertebrate second messenger pathways activated by PACAP include protein kinases A and C, and pathways inhibited include the JNK/SAPK pathway (Forssmann and Said 1998).

In parallel with mammalian systems, PACAP-38 avoidance in *Tetrahymena* has previously been shown to involve an intricate pathway, which includes adenylyl cyclase and phospholipase C (Hassenzahl *et al.* 2001). Recent studies show that these pathways are also involved in ATP avoidance, along with an NO pathway (Rosner *et al.* 2003). In this study, we use pharmacological and EIA assays as evidence that the NO/cGMP pathway is also involved in PACAP-38 signaling in *Tetrahymena.* The PACAP-38 response is also shown to be calcium dependent and pertussis toxin sensitive. Finally, a model of PACAP-38 signaling attempts to pull together all of the pathways involved and postulates how these may contribute to avoidance.

MATERIALS AND METHODS

Cell cultures. *Tetrahymena thermophila* B, strain SB2086, a generous gift from T. M. Hennessey (SUNY at Buffalo) was used throughout the study. Cells were incubated under sterile conditions at 25°C for 48 h after inoculation, without shaking, in the axenic medium of Dentler (1988). No antibiotics were added to the media.

Chemicals and solutions. Behavioral bioassays were carried out in a buffer containing 10 mM Trizma base, 0.5 mM MOPS, 50 μM $CaCl_2$, pH 7.0. All repellents and inhibitors were dissolved in this buffer. Compounds which were insoluble in aqueous solution were first dissolved into a small quantity of DMSO, then immediately diluted into behavioral buffer at a dilution of 1:10,000 or higher.

PACAP-38 was obtained from the American Peptide Co. Sunnyvale, CA. The G-protein inhibitor, pertussis toxin, was obtained from Alexis Biochemicals, San Diego, CA. The calcium chelator, BAPTA-AM, the guanylyl cyclase inhibitor, NS-2028, and the Quantizyme Assay SystemÔ NO Kit were all obtained from BIOMOL Research Laboratories, Plymouth Meeting, PA. The NOS inhibitors, 1400W and 2-Imino-4-Methylpiperidine (IMP), the guanylyl cyclase inhibitor, LY-83583, and the cGMP EIA kit, were obtained from Cayman Chemical, Ann Arbor, MI. All other chemicals were obtained from Sigma Chemical Company, St. Louis, MO.

Behavioral bioassays. *In vivo* behavioral bioassays were carried out as previously described (Kuruvilla *et al.* 1997, Kim *et al.* 1999, Mace *et al.* 2000). Cells were first washed in the assay buffer and transferred to the first well of a 3-well spot microtiter plate. Cells were then transferred to the second well of the microtiter plate, which contained the inhibitor being tested, and were incubated for 10-

15 min, to allow time for cellular uptake of the inhibitor. If no inhibitor was being tested, cells were simply incubated in fresh buffer for 10-15 min. Individual cells were then transferred to the third well of the microtiter plate, which contained a combination of the chemorepellent (0.1 μM PACAP 38) and the test concentration of inhibitor. If no inhibitors were being tested, cells were simply transferred to the repellent. Each cell was then scored for avoidance (+ or -) for each trial. Each trial consisted of ten cells. The mean ± SD was calculated for at least three trials, and was expressed as "cells showing avoidance, (%)".

EIA assays. NO assays were carried out using two-day old cell cultures. Cells were washed twice in buffer and diluted to a final concentration of approximately 720 cells/ml. Cells were exposed to 9 μM PACAP 38 for approximately 30 seconds, then spun down in a benchtop microcentrifuge for 30 s. Supernatant was analyzed for NO using a kit from BIOMOL, according to the manufacturer's instructions.

cGMP assays were carried out using two day old cell cultures. Cells were concentrated to approximately 7.66×10^6 cells/ml. Cells were exposed to 1 μM PACAP 38 for approximately 30 seconds, then immediately lysed by freezing in liquid nitrogen and thawing. Theophylline (1 μM) was added to the lysate to inhibit phosphodiesterases. Lysate was spun at 16,000 g for 30 min. Supernatant was assayed for cGMP using a kit from Cayman Chemicals according to the manufacturer's instructions.

RESULTS

As seen previously (Mace *et al*. 2000, Hassenzahl *et al*. 2001, Keedy *et al*. 2003), *in vivo* behavioral bioassays indicate that PACAP-38 is an effective chemorepellent in *Tetrahymena* (Fig. 1). The potency of PACAP-38 was concentration dependent, and a maximum potency, causing 100% of cells to show avoidance, was seen at 0.1 μM. This concentration was used in the inhibitor studies which follow. The EC_{50} of this compound was approximately 0.01 μM.

In order to determine whether NO was involved in PACAP-38 avoidance, two NO inhibitors, 1400W and IMP were used. Both inhibitors (Figs 2, 3) blocked avoidance in a concentration-dependent manner. An avoidance response near baseline (10-20%; Mace *et al.* 2000) was achieved at 10 μM 1400W (23.3 ± 5.8%), and 500 nM IMP (20 ± 5%). The EC_{50} for 1400W was near 1 nM, and for IMP was near 0.1 nM. These data implicate the NO pathway in PACAP signaling. In order to confirm these results biochemically, EIA assays were performed on intact cells. Using 9 μM PACAP, our EIA assays showed a 148 ± 4.8% increase in NO levels compared to control cells, confirming NO involvement in the *Tetrahymena* response.

Since NO often activates guanylyl cyclase within cells, and since the presence of a membrane-bound
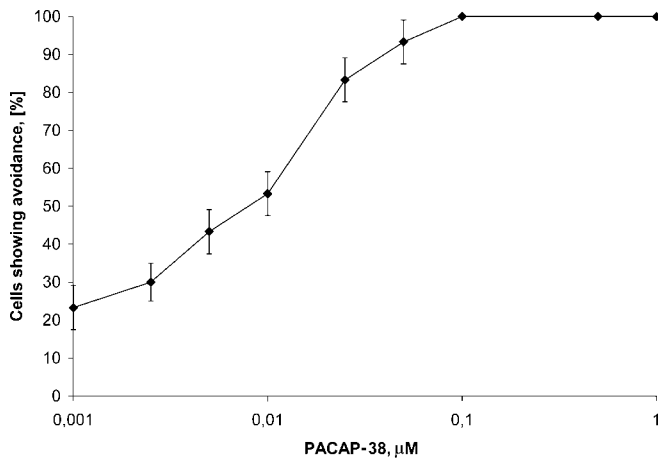
Fig. 1. PACAP-38 is an effective chemorepellent in *Tetrahymena.* *In vivo* behavioral bioassays (see Materials and Methods) were used to show the concentration dependencies for avoidance reactions to PACAP. The percentage of cells showing avoidance was determined by observation of a single cell after transfer to the test solution. Each trial consisted of ten cells, which were individually scored as to whether or not avoidance occurred. Each point represents the mean ± SD of three trials. Error bars, representing the standard deviation, are shown for each point. Minimum concentration required to give 100% avoidance was 0.1 μM for PACAP-38. This concentration was used in the inhibition studies that follow. The EC_{50} of this compound was approximately 0.01 μM.
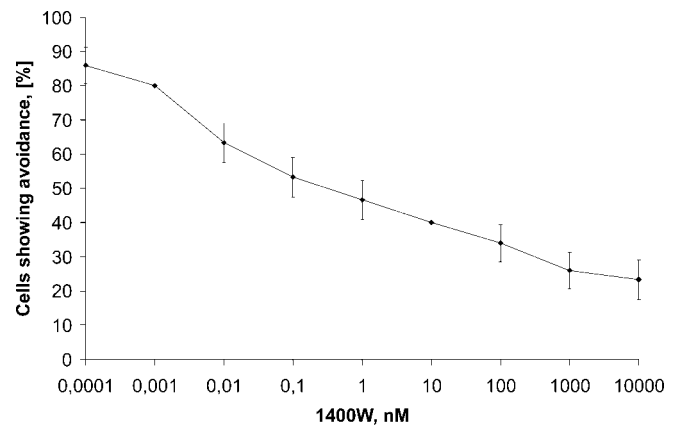

Fig. 2. *In vivo* behavioral assays (see Materials and Methods) show that the iNOS inhibitor, 1400W, reduced avoidance behavior to 0.1 μM PACAP to near baseline levels at a concentration of 10 μM 1400W. The IC_{50} of 1400W was approximately 1 nM.
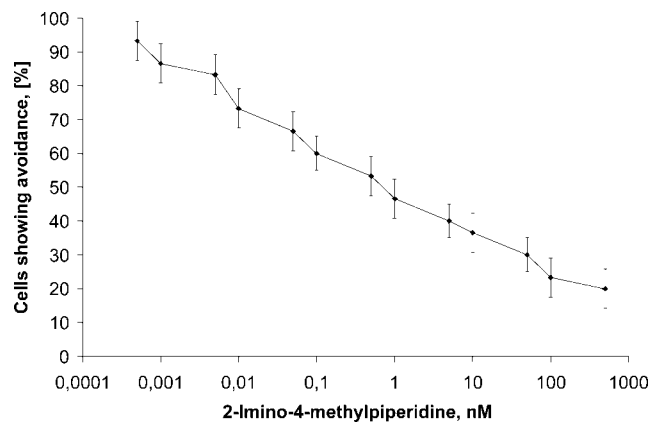

Fig. 3. *In vivo* behavioral assays (see Materials and Methods) show that the NOS inhibitor, IMP, reduced avoidance to 0.1 mM PACAP to baseline levels at a concentration of 500 nM IMP. The IC_{50} of IMP was approximately 1 nM.
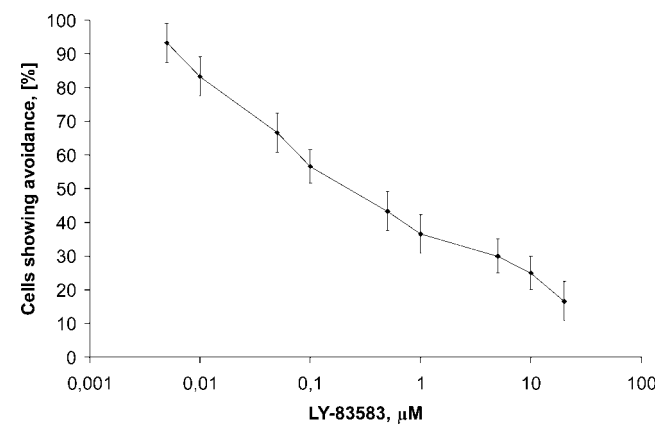
Fig. 4. *In vivo* behavioral assays (see Materials and Methods) show that the guanylyl cyclase inhibitor, LY-83583, reduced avoidance behavior to 0.1 mM PACAP to near baseline levels at a concentration of 20 mM LY-83583. The IC_{50} of LY-83583 was approximately 0.1 μM.

guanylyl cyclase in *Tetrahymena* has been documented (Linder and Schultz 2002), we used two guanylyl cyclase inhibitors, LY-83583, and NS-2028, in an attempt to inhibit PACAP-38 avoidance. Both inhibitors (Figs 4, 5) blocked avoidance in a concentration-dependent manner. An avoidance response near baseline was achieved using 20 μM LY-83583 (16.6 ± 5.8%), and 1 nM NS-2028 (13.3 ± 5.8%). The EC_{50} for LY-83583 was near 0.1 nM, and for NS-2028 was near 0.05 nM. These data implicate guanyl cyclase in PACAP-38 avoidance. In
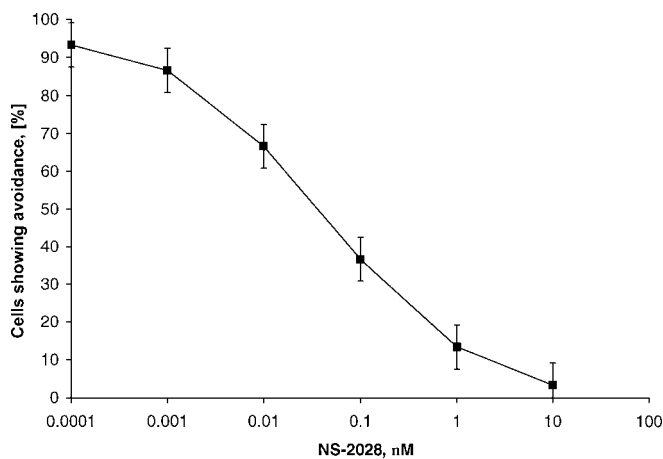
Fig. 5. *In vivo* behavioral assays (see Materials and Methods) show that the guanylyl cyclase inhibitor, NS-2028, effectively eliminated avoidance behavior to 0.1 mM PACAP at a concentration of 10 nM NS-2028. The IC_{50} of NS-2028 was approximately 0.05 nM.
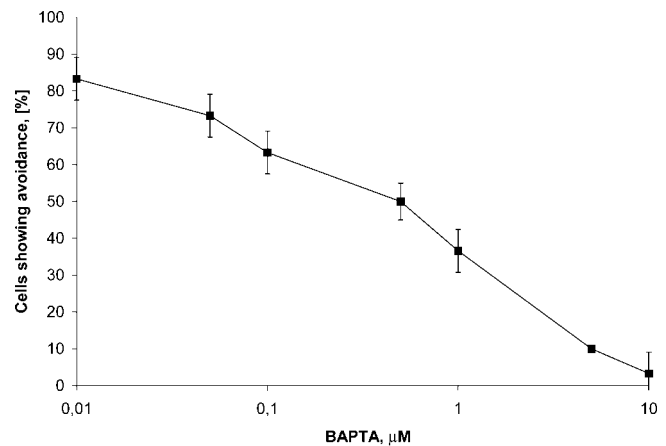
Fig. 6. *In vivo* behavioral assays (see Materials and Methods) show that the membrane-permeable calcium chelator, BAPTA-AM, effectively eliminated avoidance behavior to 0.1 mM PACAP at a concentration of 10 mM BAPTA-AM. The IC_{50} of BAPTA-AM compounds was 0.5 μM.
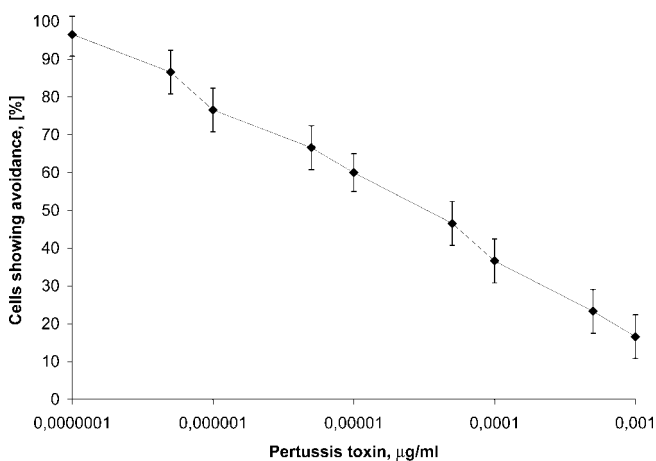

Fig. 7. *In vivo* behavioral assays (see Materials and Methods) show that pertussis toxin, an inhibitor of $G_{i/o}$ proteins, reduced avoidance behavior to 0.1 mM PACAP to baseline levels at a concentration of 0.001 mg/ml pertussis toxin. The IC_{50} of pertussis toxin was near 0.00001 mg/ml.

order to confirm these results biochemically, we used EIA assays performed on *Tetrahymena* lysate. Exposure to 1 μM PACAP-38 increased cGMP levels to 351 ± 4.6% of control levels.

Since many NO synthases are calcium-dependent, the membrane-bound guanylyl cyclase of *Tetrahymena* has been shown to be calcium dependent (Linder and Schultz 2002), and since *Tetrahymena* exhibit a calcium-

based depolarization when stimulated with lysozyme (Kuruvilla and Hennessey 1998), which presumably acts through the same receptor as PACAP (Mace *et al.* 2000, Keedy *et al.* 2003), we used the membrane-permeable calcium chelator, BAPTA-AM, to see whether avoidance would be blocked. As seen in Fig. 6, exposure to 5 μM BAPTA-AM was sufficient to achieve baseline avoidance. The EC_{50} of this compound was 0.5 μM.

Previous studies (Hassenzahl *et al.* 2001, Keedy *et al.* 2003) indicate that the PACAP receptor is a G-protein linked receptor. However, the pertussis toxin sensitivity of this receptor has not previously been tested. We found that pertussis toxin was an effective inhibitor of PACAP avoidance, requiring a concentration of just 0.01 μg/ml to achieve baseline avoidance (Fig. 7). The EC_{50} of this compound was approximately 0.0001 μg/ml.

A proposed model of PACAP avoidance, based on these and previous studies, is shown in Fig. 8. Arrows broken with a question mark represent hypothetical steps in the model, while unbroken arrows represent confirmed steps in the pathway.

DISCUSSION

PACAP-38 is a convenient ligand to use for *Tetrahymena* avoidance assays because low concentrations are

NOS in PACAP signaling **19**

required in order to achieve avoidance (Fig. 1; Mace *et al.* 2000, Hassenzahl *et al.* 2001, Keedy *et al.* 2003) and because the ligand has been well studied in other systems. In *Tetrahymena*, however, the pharmacological profile of the receptor is different from known PACAP receptors in other systems. For example, the antagonists, PACAP 6-27 and 6-38, which competitively inhibit many PACAP receptors actually serve as agonists for *Tetrahymena* PACAP receptors (Keedy *et al.* 2003). Previous studies (Hassenzahl *et al.* 2001) have shown that the PACAP-38 pathway in *Tetrahymena* is linked to a G-protein pathway which involves adenylyl cyclase and phospholipase C, presumably resulting in the formation of cAMP as well as the release of calcium from internal stores. Earlier studies (Kuruvilla and Hennessey 1998) link the lysozyme response, which presumably occurs through the same receptor as PACAP-38 (Mace *et al.* 2000) to a calcium-linked depolarization. However, the mechanism of avoidance has not yet been established. In this study, we present evidence that NO and cGMP are also critical for PACAP avoidance (Figs. 2-5). Intracellular calcium (Fig. 6) is also essential in order for avoidance to occur. A pertussis toxin-sensitive G protein is presumably involved (Fig. 7). How do all these data, together with that from other laboratories, come together to form a coherent model of PACAP avoidance? Questions remain, yet when the available data are compiled, a complex picture begins to emerge.

One of the first points made clear by the data is that calcium is critical for avoidance. When the membrane-permeable calcium chelator, BAPTA-AM, is introduced into the cells, avoidance ceases (Fig. 6). Interestingly, we have seen this same behavior with the repellents ATP and GTP (Rosner *et al.* 2003; Bartholomew *et al.,* submitted). This is consistent with past electrophysiological data (Kuruvilla and Hennessey 1998, Kim *et al.* 1999) showing that lysozyme, GTP, and ATP all exhibit calcium-based depolarizations. In addition, PACAP (Hassenzahl *et al.* 2001) and ATP (Rosner *et al.* 2003) also utilize the phospholipase C pathway, presumably releasing calcium from internal stores.

The roles for calcium in avoidance are also beginning to emerge. For example, many nitric oxide synthase isoforms are calcium dependent. Our pharmacological data with 1400W (Fig. 2) and IMP (Fig. 3) suggest a role for NO in PACAP avoidance, and our EIA detection assay confirms this result. We have seen similar results with ATP (Rosner *et al.* 2003) and GTP (Bartholomew *et al.,* submitted, personal comn.). Interestingly, 1400W is selective for iNOS isoforms, which are calcium inde-

pendent, and the low concentrations of IMP needed for inhibition are also characteristic of an iNOS. NO has previously been implicated in *Tetrahymena* survival (Christensen *et al.* 1996); however, the type of NOS involved is unknown. It is possible that the NOS of *Tetrahymena* is calcium-dependent. Our data seem to support this, since the rise in NO is instantaneous, correlating with the calcium depolarization and presumably the phospholipase C pathway as well. However, inducible nitric oxide synthases are turned on at the transcriptional level, requiring hours to take effect (for example, see Arimoto and Bing 2003). Future experiments are required to determine whether the NOS of *Tetrahymena* is calcium-dependent.

Another possible role of calcium in avoidance is the triggering of guanylyl cyclase. In *Tetrahymena*, a membrane bound isoform of this enzyme has been shown to be calcium-dependent (Linder and Schultz 2002). Our pharmacological studies indicate that guanylyl cyclase is involved in PACAP-38 avoidance, as the guanylyl cyclase inhibitors, LY-83583 and NS-2028, block avoidance to PACAP-38 (Figs 4, 5). Both of these inhibitors have been previously shown to block soluble forms of guanylyl cyclase. If the guanylyl cyclase activated by PACAP-38 is indeed a soluble isoform, its calcium dependence is unknown. If, however, the drugs were blocking the membrane-bound cyclase mentioned previously, then calcium would have a role in cGMP formation.

As detected by EIA, cGMP is also produced at higher levels in cells, which have been exposed to PACAP-38. We have seen similar EIA and pharmacological results for ATP and GTP (Rosner *et al.* 2003; Bartholomew *et al.,* submitted), suggesting that the cGMP pathway, like intracellular calcium, may be critical for ciliary reversal.

Another potential role of calcium in avoidance has emerged from recent data. Hennessey *et al.* (2003), have shown that calcium-dependent ciliary reversal in *Tetrahymena* depends on properly functioning inner arm dynein 1 (I1). Their hypothesis is that a "calcium sensor" protein binds to and activates I1. The calcium sensor protein may be regulated by the NO/cGMP pathway or another of the pathways involved in avoidance.

The G-protein involved in avoidance is also interesting to consider. Our data suggest that the G-protein is pertussis toxin-sensitive (Fig. 7), a characteristic of $G_{i/o}$ proteins. This same pattern is seen in the ATP chemoresponse of *Tetrahymena* (Rosner *et al.* 2003). In many mammalian cells, PACAP acts through a G_s protein; however, in smooth muscle, PACAP acti-

vates a calcium-dependent, membrane-bound NO synthase *via* a $G_{i1\text{-}2}$ protein (Murthy and Makhlouf 1996). Perhaps something similar is occurring during PACAP avoidance in *Tetrahymena.*

The diagram shown in Fig. 8 represents the pathways involved in PACAP-38 avoidance. As seen in the figure, the pathway is rather complex, and many questions still remain unanswered. This model represents a work of continuing research and will continue to develop as more is discovered regarding this specific signaling pathway and ciliary function in general.
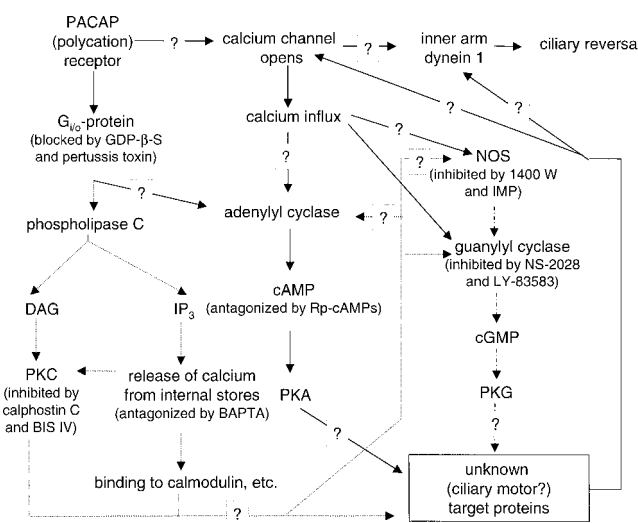

Fig. 8. Proposed mechanism for PACAP-38 avoidance in *Tetrahymena thermophila* based on current data. Dotted lines indicate components of the phospholipase C pathway. Dashed lines indicate components of the NO pathway. Arrows broken with a question mark indicate hypothetical components.

Further studies will be necessary to fully understand *Tetrahymena* avoidance behavior. The data we have obtained highlight the elegance and complexity of this model system for behavioral studies. Its adaptability for genetic experiments will make it an excellent candidate for future studies that may help us to understand protists better, as well as to gain a more complete knowledge of chemorepellent signaling in higher organisms.

REFERENCES

Arimoto T., Bing G. (2003) Up-regulation of inducible nitric oxide synthase in the substantia nigra by lipopolysaccharide causes microglial activation and neurodegeneration. *Neurobiol. Disease* **12:** 35-45

Christensen S. T., Kemp K., Quie H, Rasmussen L. (1996) Cell death, survival, and proliferation in *Tetrahymena thermophila*: effects of insulin, sodium nitroprusside, 8-bromo cyclic GMP, N^G-methyl-L-arginine, and methylene blue. *Cell Biol. International* **20:** 653-666

Dentler W. L. (1988) Fractionation of *Tetrahymena* ciliary membranes with Triton X-114 and the identification of a ciliary membrane ATPase. *J. Cell Biol.* **107:** 2679-2688

Forssmann W-G., Said S. I.; Eds. (1998) VIP, PACAP, and related peptides: Third International Symposium. *Ann. NY Acad. Sci.* 865

Hassenzahl D. L., Yorgey N. K., Keedy M. D., Price A. R., Hall J. A., Myzcka C. C., Kuruvilla H. G. (2001) Chemorepellent signaling through the PACAP/lysozyme receptor occurs through both cAMP and PKC in *Tetrahymena thermophila*. *J. Comp. Physiol. A* **187:**171-176

Hennessey T. M., Kim D.Y., Oberski D. J., Hard R., Rankin S. A., Pennock D.G. (2002) Inner arm dynein 1 is essential for Ca^{++}-dependent ciliary reversals in *Tetrahymena thermophila*. *Cell. Motil. Cytoskel.* **53:** 281-288

Iwamoto M., Nakaoka Y. (2002) External GTP binding and induction of cell division in starved *Tetrahymena thermophila*. *Eur. J. Cell Biol.* **81:** 517-524

Keedy M., Yorgey N., Hilty J., Price A., Hassenzahl D., Kuruvilla H. (2003) Pharmacological evidence suggests that the lysozyme/PACAP receptor of *Tetrahymena thermophila* is a polycation receptor. *Acta Protozool.* **42:** 11-17

Kim M. Y., Kuruvilla H. G., Raghu S., Hennessey T. M. (1999) ATP reception and chemosensory adaptation in *Tetrahymena thermophila*. *J Exp. Biol.* **202:** 407-416

Kuruvilla H. G., Hennessey T. M. (1998) Purification and characterization of a novel chemorepellent receptor from *Tetrahymena thermophila*. *J. Memb. Biol.* **162:** 51-57

Kuruvilla H. G., Hennessey T. M. (1999) Chemosensory responses of *Tetrahymena thermophila* to CB_2, a 24-amino acid fragment of lysozyme. *J. Comp. Physiol. A.* **184:** 529-534

Kuruvilla H. G., Kim M. Y., Hennessey T. M. (1997) Chemosensory adaptation to lysozyme and GTP involves independently regulated receptors in *Tetrahymena thermophila*. *J. Euk. Microbiol.* **44:** 263-268

Linder J. U., Schultz J. E. (2002) Guanylyl cyclases in unicellular organisms. *Mol. Cell. Biochem.* **230:** 149-158

Mace S. R., Dean J. G., Murphy J. R., Rhodes J. L., Kuruvilla H. G. (2000) PACAP-38 is a chemorepellent and agonist for the lysozyme receptor in *Tetrahymena thermophila. J. Comp. Physiol. A* **186:** 39-43

Murthy K. S., Makhlouf G. M. (1994) Vasoactive intestinal peptide/pituitary adenylate cyclase-activating peptide-dependent activation of membrane-bound NO synthase in smooth muscle mediated by pertussis toxin-sensitive $G_{i1\text{-}2}$. *J. Biol. Chem.* **279:** 15977-15980

Orias E. (1998) Mapping the germ-line and somatic genomes of a ciliated protozoan, *Tetrahymena thermophila. Genomic Research* **8:** 91-99

Rosner B. N., Bartholomew J. N., Gaines C. D., Riddle M. L., Everett H. A., Rulapaugh K. G., Nickerson L. E., Marshall M. R., Kuruvilla H. G. (2003) Biochemical evidence for a P2Y-like receptor in *Tetrahymena thermophila. J. Comp. Physiol. A* **189:** 781-789

Zhu Y., Li H., Zhou L., Wu J.Y., Rao Y. (1999) Cellular and molecular guidance of GABAergic neuronal migration from an extracortical origin to the neocortex. *Neuron* **23:** 473-85

ACTA
PROTOZOOLOGICA

The Effects of Release from Cold Stress on the Community Composition of Terrestrial Gymnamoebae: A Laboratory-based Ecological Study Simulating Transition from Winter to Spring

O. Roger ANDERSON

Biology, Lamont-Doherty Earth Observatory of Columbia University, Palisades, U. S. A.

Summary. Changes in community composition of terrestrial gymnamoebae were analyzed in laboratory microcosms established with thoroughly mixed soil from a northeastern U. S. A. site taken during the onset of winter 2002-2003, when the soil temperature was 5°C. The temperature of one of the microcosms, maintained in constant temperature chambers, was increased from 5°C to 25°C at 5 intervals of two weeks each for a period of 10 weeks. Another microcosm was maintained for the 10 weeks at 5°C to serve as a control for the lapse of time and to assess the effects of prolonged treatment at 5°C simulating winter conditions. Small subsamples (0.01 g) of the microcosm soil were taken using a modified 1 cm³ syringe with the tip cut off to make a cylindrical corer. Based on a culture enrichment technique, the morphospecies richness, heterogeneity of distribution within the samples (morphospecies uniqueness) and community patchiness were determined by microscopic observation of the morphospecies that grew out in the cultures of each 0.01 g sample. The data showed that with increasing temperatures up to 20°C, the richness and patchiness of morphospecies increased while the uniqueness did not change within statistical significance. Two-weeks treatment at 25°C simulating summer conditions, produced a marked decline in richness of morphospecies and a substantial increase in the percent that were encysted suggesting less favorable conditions for growth, perhaps resulting from thermal stress and depletion of nutrients and other resources. Overall, the evidence from this study indicated that release from cold stress during the transition from winter to spring produced increased richness of morphospecies and greater patchiness of the gymnamoeba communities. This "bloom," however, was followed by a period of less productivity and retrenchment with increasing numbers of encysted gymnamoebae as the temperature was increased above 20°C.

Key words: amoebae, biotic complexity, community structure, microcosm, seasonal temperature effects.

INTRODUCTION

Research on the ecology of terrestrial gymnamoebae is relatively limited compared to other protozoa such as testate amoebae, ciliates and flagellates (e.g., Heal 1964; Bamforth 1971; Lousier and Parkinson 1984;

Address for correspondence: O. Roger Anderson, Biology Lamont-Doherty Earth Observatory, Columbia University, Palisades, NY 10964, U. S. A.; Fax: 845 365-8150; E-mail ora@ldeo.columbia.edu

Foissner 1987, 1991, 1994; Darbyshire *et al.* 1989). More research appears to have been done on the role of gymnamoebae in the ecology of agricultural soils (e.g., Clarholm 1989, Griffiths 1994, Zwart *et al.* 1994, Anderson and Griffin 2001) and as bioindicators and regulators of soil pathogens (Old 1986, Foissner 1994). Recently, there have been increasing investigations of fundamental aspects of terrestrial gymnamoeba abundance, spatial distribution, and ecology (e.g., Sawyer 1989; Anderson and Bohlen 1998; Bischoff and Anderson 1998; Anderson 2000, 2002; Bass and Bischoff 2001; Bischoff

2002). However, little is known about major interactions of gymnamoebae with physical characteristics of the environment, especially terrestrial environments. Terrestrial gymnamoebae as is also the case for other protists exhibit a wide range of adaptive morphologies and sizes (e.g., Page 1988, Rogerson and Patterson 2000, Corliss 2002) including forms that are broad in outline and fan-shaped with sizes in the micron range, a variety of forms with peripheral extended pseudopodia in a size range of microns to hundreds of microns, limax (worm-shaped) species with sizes up to hundreds of microns, and reticulate plasmodial forms of very large sizes in the millimeter size range. These markedly different life forms and sizes suggest that terrestrial gymnamoeba species have highly varied niches and ecological roles that may vary across small spatial dimensions in the millimeter range. Nonetheless, only a few studies have focused on the distribution of terrestrial gymnamoebae in micro-size dimensions of soil particles (e.g., Anderson 2002, 2003). Furthermore, there is clear evidence that seasonal and climatic factors influence the abundance and diversity of protozoa, although much of the work has been done in aquatic environments (e.g., Baldock and Sleigh 1988, Schmidt-Halewicz 1994, Mathes and Arndt 1995) including studies focused on gymnamoebae (Anderson and Rogerson 1995). Annual variations in abundances of terrestrial testate amoebae have been studied rather carefully (e.g., Lousier and Parkinson 1984), but there has been less emphasis on time series studies of seasonal effects on terrestrial gymnamoebae (e.g., Anderson 2002). Moreover, there have been limited analyses of how differences in temperature associated with seasonal changes affect the composition of terrestrial gymnamoeba communities.

This study examined how the composition of terrestrial gymnamoeba communities, grown in laboratory microcosms, varied during release from cold stress simulating a transition from winter to spring. The change in community composition was analyzed using a biotic complexity model previously applied to a variety of terrestrial environments (Anderson 2003). This model is used to analyze changes in gymnamoeba abundances within small (0.01 g) soil samples in relation to three parameters: (1) the morphospecies richness (number of morphospecies in each small soil sample), (2) the heterogeneous spatial distribution (uniqueness) of individual morphospecies among the small soil samples, and (3) patchiness in the distribution of morphospecies across the soil samples. The purpose of this study was to demonstrate the application of the biocomplexity model

to ecological studies of amoeboid protists and to examine a hypothesis about the relationship of the variables in the biocomplexity model to the effects of temperature changes during release from cold-stress simulating winter conditions. The study was not intended to describe the ecology of an entire natural site, but rather to use microcosms to test a theory-based hypothesis

Based on prior findings that gymnamoeba communities are distributed in a patchy pattern in microbiocoenoces (Anderson 2000) and theory related to community biocomplexity (Anderson 2002), the following hypothesis was tested.

With increasingly favorable temperatures for growth, the richness of gymnamoebae morphospecies will increase leading to a proliferation of gymnamoebae in the most favorable niches, while less favorable niches are less populated, thus giving rise to increased patchiness of morphospecies across small spatial domains. Concomitantly, there will be a decline in the number of uniquely occurring individual morphospecies within the small-scale spatial domains. The latter is predicted due to the proliferation and migration of morphospecies throughout larger regions of the soil medium as the temperature became more favorable, thus reducing the uneven distribution of a particular morphospecies throughout the soil environment.

MATERIALS AND METHODS

Sample site and preparation of laboratory microcosms

Soil samples were obtained from a location covered by leaf litter beneath a sparse stand of deciduous trees on the Lamont-Doherty Earth Observatory campus in January, 2003 when soil temperature (*ca* 5°C) was representative of early winter conditions in coastal northeastern U. S. A. Three core samples were taken approximately 10 cm apart from beneath the leaf litter using a LaMotte model EP soil corer to a depth of approximately 5 cm. The soil samples were combined yielding approximately a 500 g mass that was thoroughly mixed to ensure greater initial homogeneity. Prior experience with microcosm studies of this kind (e.g., Anderson 2002) has shown that soil communities are very heterogeneous even within small dimensions of centimeters. Thus, to establish uniform initial conditions within the microcosms, it is important to thoroughly mix the soil samples before placing them in the Pyrex microcosm dishes. A portion of the soil (*ca* 200 g) was placed in each of two Pyrex culture dishes (9 cm diameter and 5 cm deep) that had been sterilized with 70 % (w/v) aqueous ethanol solution. Each of the soil-containing culture dishes served as a microcosm for the laboratory research. The dishes were covered with a sheet of parafilm™ and a Pyrex glass cover to control for loss of moisture. One dish served as a control and

was placed at 5°C for the duration of the experiment. Since this dish contained the same thoroughly mixed soil sample as the temperature-treated dish, but was not subjected to increasing temperatures during the course of the experiment, the enumeration of gymnamoebae from this dish served as a baseline measure of the density of gymnamoebae resulting from continuous treatment at 5°C during the duration of the experiment. The other dish, designated the temperature-treatment dish, was placed initially at 5°C, but every subsequent two weeks it was transferred to warmer temperatures (10°C, 15°C, 20°C, and 25°C) simulating cold release during transition from winter into spring and early summer. The duration of the experiment was 10 weeks. At each two-week interval, beginning with the 10°C temperature treatment, soil samples were taken for analysis as described below. The time-control dish kept at 5°C was sampled at the end of the experiment (10 weeks) when the final sample was taken. This served as the 5°C sample and simulated the effects of extended treatment of winter cold stress.

Analysis of soil samples

At each two-week sampling point, small cores of soil were extracted from the microcosms using a 1 ml syringe that had been modified by cutting off the tip to produce an open cylindrical corer (Anderson 2002). The plastic syringe cylinder was inserted into the soil while the plunger was withdrawn to create a slight vacuum during penetration into the soil, thus enhancing uptake of the soil into the corer. Four replicate cores were taken at each biweekly sample to assess the total number of viable morphospecies using a culture-enrichment technique (Anderson 2002) as follows. To obtain small *ca* 0.01 g subsamples of the soil core, each of the cores was gently extruded by use of the syringe plunger. As each increment was extruded, a small disc of the soil from the protruding tip (*ca* 2 mm length) was cut from the core using an ethanol-sterilized, thin razor blade. The disc was immediately cut into 4 pieces (each piece was *ca* 0.01 g as described previously in Anderson 2002). Each piece was placed in a culture well of a 24-well plastic sterile culture dish (Falcon 35-3047 multi-well tissue culture dish) where each well contained 2 ml of 0.45 µm pore-size Millipore-filtered pond water. A small cube of agar (*ca* 2 mm³) containing malt and yeast extract (Anderson 2002) was added to each well to promote growth of bacteria used as food by the gymnamoebae. After two weeks of culture at 25°C to permit outgrowth of viable morphospecies in each well containing the soil core sample, the culture dish was examined with a Nikon Diaphot inverted compound microscope using phase contrast optics and a phase contrast 40x objective. The purpose of maintaining the enrichment cultures at a uniform temperature of 25°C is to ensure a standard procedure for enumerating the categories of gymnamoebae that grow out from each of the 0.01 g samples. The number of different morphospecies that grow out is tallied, not the total number of gymnamoebae found in the well, hence the use of a constant temperature ensures a consistent measure of the total suite of morphospecies that grow out from each 0.01 g sample, but it does not bias the affect of the temperature treatment on the soil cultures in the microcosms. That is, this analysis (e.g., Anderson 2002) can only detect the number of morphospecies already present in the small soil sample and is intended to provide an optimum temperature and enrichment culture condition to reliably detect as many as possible of the existing morphospecies within each subsample of soil. Each well was thoroughly scanned and each morphospecies identified. Since it

is difficult to uniformly identify all of the observed gymnamoebae to species level based on taxonomic characteristics, morphospecies categories were used. Morphospecies are identified by noting the morphology, size and locomotion using methods previously published (e.g., Anderson and Rogerson 1995; Anderson 2000, 2002). A list of morphospecies occurring in each well was tabulated. The total number of individuals tallied during the 10 week experiment was *ca* 6,600 as observed in the 480 wells all-totaled for the 20 dishes (four replicate dishes per treatment) used for the assays in the five temperature treatments. Each kind of morphospecies occurring in each of the wells of the culture dish was tabulated in order to compute the indices as explained below. The list of morphospecies observed in each well of the culture dish represented morphospecies that were present in the small 0.01 g sample of soil and grew out from it. Based on this tabulation, the following indices are computed following the procedure of Anderson (2002). Mean values were computed for the four replicated samples taken for each temperature treatment.

Indices of gymnamoeba community composition and complexity

Morphospecies richness (I_R). The number of individual morphospecies enumerated per well was summed across all 24 wells and divided by the number of wells in the dish and multiplied by 100 to better scale the index. This index of richness (I_R) represents the mean number of morphospecies identified per small sample of soil from the core.

(1) $I_R = F_C / N \times 100$ where F_C is the total count of morphospecies and N is the number of wells.

Morphospecies spatial uniqueness (I_D). When the morphospecies identified in each well are fully tabulated, the data are examined to determine if there are any morphospecies that occurred in only one of the 24 wells in the culture dish. The number of such uniquely occurring species (F_U) is divided by the total number of morphospecies tabulated in the wells (F_C). This index of spatial uniqueness represents a form of spatial diversity across the soil samples and is symbolized as I_D.

(2) $I_D = F_U / F_C \times 100$ where F_U is the number of morphospecies that occurred in only one of the 24 wells in the culture dish.

Patchiness of morphospecies (I_P). The patchiness of the morphospecies identified from the small soil samples was assessed using an index applied to metazoan populations (e.g. Taylor 1984). The variance (V_F) in the morphospecies counts across the 24 wells is divided by the mean number of morphospecies per well (M_F).

(3) $I_P = (V_F / M_F) \times 100$ where V_F is the variance in the counts of morphospecies among the 24 wells and M_F is the mean count per well.

These three indices were used to characterize the community composition of the gymnamoebae in the soil samples. The three indices are tabulated for each treatment. Additionally, the values of the three indices are plotted as a three-dimensional graph where each index serves as one of the three axes of the Euclidean plot. Thus, the data for each sample is reduced to a plotted point in the field of the three-dimensional graph. Mean values of the four replicate samples for each of the three axes were used to plot the coordinates on the graph. The Euclidean distance of each point from the origin is used as an overall index of complexity (C) of the organization of the gymnamoeba communities. A standard Shannon-Wiener index of diversity (H) also was computed using the formula: $H = - \Sigma p_i \log_2 p_i$.

Where, p_i = the proportion of times a given morphospecies occurred compared to the total counts.

Estimation of encysted stages

In addition to the assay of the total number of morphospecies in a soil sample, the proportion of encysted forms also was determined. A replicate sample of the soil in each temperature treatment was taken with the syringe core sampler. However, each small segment of soil was added initially to a dry culture dish well without water. The soil particles were rapidly air dried for 15 min under gentle flowing air at ambient temperature before adding the 2 ml of micropore-filtered pond water to each well. The drying step has been shown to kill trophic stages but preserve the viability of encysted terrestrial gymnamoebae (Anderson 2000). The count of morphospecies that grew out from the dried samples after two weeks of culture divided by the counts obtained with the non-dried samples, expressed as a percent, provides evidence of the number of encysted morphospecies in the soil sample. This technique has been used successfully previously (Anderson 2000). It yields a strong correlation between the number of encysted forms and the extent of dryness of the soil sample.

Soil chemical and physical characteristics

The organic content, percent moisture, and pH of the soil in the microcosms was determined at the end of the 10 week experiment for the temperature-treated microcosm and the time-control microcosm kept at 5°C using methods previously published (Anderson 2000, 2002). There were no major differences between the two microcosm samples (moisture content = ca 43 to 44 %, organic content = 20 %, and pH = 6.0) indicating that these physico-chemical variables were not altered by the temperature increases compared to the constant temperature control. Organic content was determined by combustion. An air-dried portion of the soil was weighed and combusted for at least 16 h at a temperature of 375°C. The difference in weight between the air-dried and combusted sample was used to calculate the percentage of organic matter. Percent moisture was obtained by weighing a freshly collected portion of moist soil, oven drying the sample overnight at 109°C and re-weighing the fully dried sample. The difference in weight was used to determine moisture content expressed as a percent. To measure pH, 5 g of the soil from the microcosm was suspended in 50 ml of tap water and the pH of the slurry was determined using an Accumet model 15 pH meter (Fisher Scientific Co.).

Statistical analyses

The purpose of this study was to evaluate the hypothesis stated in the introduction using the microcosms as the sampling universe. A series of 4 samples each were taken independently from the dishes using a small coring device. It has been shown previously that samples of soil taken at centimeter distances apart are highly different in community composition; therefore, each core sample was considered sufficiently independent of the other samples to apply inferential statistical analyses. A linear regression model was used with each of the four complexity variables (I_R, I_P, I_D and C, the overall coefficient of complexity) as a dependent variable and the treatment temperatures as the independent variable for the regression analysis. A StatView 512+ computer program (Abacus Concepts, Calabasas, CA) was used.

RESULTS

The results of the measurements of the three indices of gymnamoeba community composition (I_R, I_P and I_D), and the overall index (C) are presented as mean values for each of the four replicate samples in Table 1. The percent of gymnamoebae that were encysted in each treatment condition and the Shannon-Wiener index of diversity (H) also are included in Table 1. There was a statistically significant increase in species richness (R = 0.8, p < 0.01, df = 14), patchiness (R = 0.6, p < 0.05, df = 14), and the overall complexity coefficient (C) (R = 0.9, p << 0.01, df = 14) during the release from cold as the temperature was increased from 5°C to 20°C simulating a transition from winter into spring. The mean index for richness (I_R) increased from 255 to 397, the mean index for patchiness (I_P) increased from 41 to 61, and the complexity coefficient (C) increased from 259 to 402. Concurrently, the mean index of uniqueness (I_D) decreased from 19 to 14, but this small decline was not statistically significant (R = - 0.3, p = 0.2, df = 14). After two additional weeks at 25°C, which was more typical of summer temperatures, the morphospecies richness declined rather markedly from 397 to 138, but the patchiness and uniqueness variables changed less markedly. The decline in richness of morphospecies at 25°C was accompanied by a major increase in encysted forms (ca 50%) relative to 20°C (31%). The two-week sustained treatment at 25°C appears to have produced less favorable growing conditions for the gymnamoebae. This may be due to thermal stress during the two-week incubation at 25°C, or perhaps due to depletion of nutrients and a decline in prey during the last two weeks of the entire 10-week experiment.

The data are plotted as a graph (Fig. 1) following the standard procedures used in the complexity model (Anderson 2002). However, only a two-dimensional graph is presented here since the third variable (I_D), expressing the degree of morphospecies uniqueness, was not significantly related to change in temperature. The Euclidean distance from the origin to each plotted point is used as a measure of overall complexity (C) as reported in Table 1. The clear trend of an increase in richness and patchiness is apparent in the pattern of plotted points.

Table 1. Temperature treatments and gymnamoeba community composition variables[a].

Temperature (°C)	Complexity (C)	I_R	I_P	I_D	R_C/R_T (%)[b]	H[c]
5	259 ± 34	255 ± 35	41 ± 5	19 ± 4	61	3.9
10	315 ± 17	278 ± 70	52 ± 13	25 ± 8	56	4.3
15	325 ± 27	304 ± 55	56 ± 8	20 ± 4	44	4.0
20	402 ± 23	397 ± 24	61 ± 18	14 ± 7	31	4.4
25	153 ± 24	138 ± 20	58 ± 24	24 ± 9	52	3.2

[a] The ± values are standard errors of the mean for the four samples. [b] Percent of encysted forms derived from the ratio of encysted forms (R_C) to total forms (R_T) observed to grow out in culture from the air dried sample and the undried sample, respectively, as explained in the Materials and Methods section. [c] Shannon-Wiener diversity coefficient.
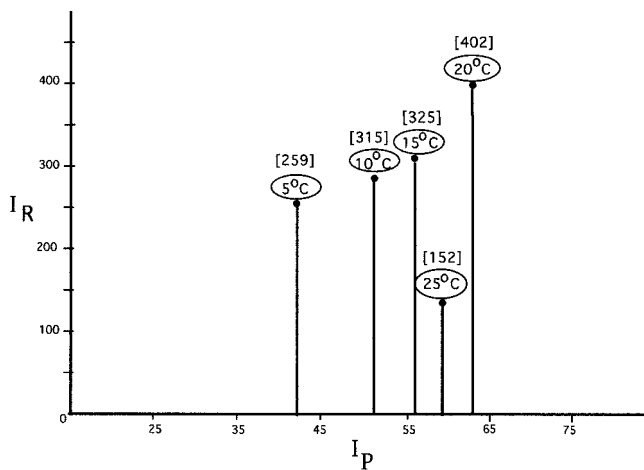

Fig. 1. Plot of the indices for richness (I_R) and patchiness (I_P), for each of the temperature treatments. The numbers in brackets are the complexity coefficient values (C). As temperature increased from 5°C to 10°C there was a statistically significant increase in richness and patchiness indicating a marked change in community composition. At 25°C, a major decrease in richness occurred, probably representing stress. There was a marked increase in encysted forms at 25°C. Data are based on a total of 6,600 observed individuals.

Overall, the combined data from Table 1 and Fig. 1 indicate that release from cold stress during the transition from winter temperatures (5°C) toward spring temperatures (20°C) is accompanied by increased richness and patchiness of the gymnamoeba community as predicted in the hypothesis. However, the predicted decline in the index for uniqueness was not statistically supported, though there is a trend in the predicted direction. The decline in percent of encysted individuals (*ca* 60% to 30%) during this sequence of temperature

treatments at constant moisture indicated that growth conditions improved markedly. These results suggest that there was a gradual proliferation of gymnamoeba species during improved growing conditions resulting in greater species richness within the soil samples, but patchiness also increased due to enhanced growth of gymnamoebae within those portions of the soil aggregates that particularly support population growth. That is, with increasingly favorable temperatures, those small soil aggregates that were most suitable to sustaining gymnamoeba populations gave rise to substantial increases in population richness, while other small aggregates with less favorable growth conditions were relatively sparsely populated. Hence the net result was increased patchiness within the soil communities.

Based on light microscopic morphology, 96 different morphospecies were identified and some could be assigned with confidence to the following genera: *Acanthamoeba*, *Mayorella/ Korotnevella*, *Vannella*, *Platyamoeba*, *Arachnula*, *Glaeseria*, *Saccamoeba*, *Hartmannella*, *Thecamoeba*, *Leptomyxa*, and *Cochliopodium*. As is increasingly clear from analyses of gymnamoebae in various environments, there are many examples of morphospecies that are taxonomically undefined based on current species descriptions. This is especially true for the smallest forms that are less than 10 µm. Undoubtedly, many of these unusual morphospecies observed in this experiment represent new taxa, but cannot be fully described without substantially more light microscopic and fine structural analyses. During the course of this experiment, there were no marked changes in the occurrence of categories of morphospecies in the samples, all tended to remain at about the same level or increased substantially in num-

bers. That is, there is no evidence that increasing temperature favored the abrupt appearance or disappearance of any of the morphospecies identified in this study.

DISCUSSION

The ecology of soils is highly complex, due in part to the large variations in particle size in the soil, varying diameters of soil pores, and the fine-scale variations in nutrients, moisture, and gases within the pore spaces of many soils (Tate 1995). Previous research on abundance of gymnamoebae in soils of varying porosity and organic content has shown that the number and diversity of terrestrial gymnamoebae can vary substantially across very small spatial scales within soil samples at a northeastern U. S. A. site (Anderson 2002). This evidence indicates that microniches for gymnamoebae can vary across small spatial dimensions of soil on the order of millimeters and within small volumes in the range of 0.01 g. Terrestrial microbial communities in temperate climates incur large extremes in growth conditions, especially major variations in temperature during the annual seasonal cycle. Soil temperatures in winter under litter and snow cover hover near or below freezing while in summer in the same location temperatures reach 25°C or higher depending on solar radiation. In addition to extremes of temperature, terrestrial environments incur large variations in moisture content. In some cases, the surface soil may dry out completely under drought conditions while extended precipitation can produce heavy water saturation of the soil. It is widely established that most terrestrial gymnamoebae produce cysts or other desiccation-resistant stages that permit survival of terrestrial species during periods of starvation and soil water stress (Fenchel 1987, Cowling 1994).

While considerable evidence has been gathered on the desiccation tolerance of gymnamoebae, there is less research on the ecological significance of temperature stress. The research reported here specifically addresses the question of how the composition of gymnamoeba communities is affected by release from cold stress in a laboratory simulation of the changes that occur during temperature transitions from winter to spring and into summer. A controlled experiment using microcosm cultures was used to ensure that only temperature and associated temperature effects were the key variables. The soil sample was thoroughly mixed prior to the

experiment to establish a uniform baseline for the experimental work. A laboratory study was done, since sampling from the natural environment introduces so many uncontrolled variables that it is not feasible to isolate temperature effects from co-occurring confounding variables. Moreover, plant cover and associated variations in rhizosphere, soil texture and organic content in the natural environment varies appreciably even within a small quadrat making it almost impossible to ensure that small core samples taken over a period of several months during a seasonal cycle come from portions of the soil medium that are sufficiently similar to control for non-temperature-related variables. Also, major changes in soil moisture in the natural environment may mask any effects of temperature. The composition of the gymnamoebae in the microcosm soil samples was determined by a culture enrichment technique (Anderson 2002). Laboratory culture enrichment techniques for enumerating protists have limitations. Only those morphospecies that grow out in laboratory culture can be analyzed by these techniques and there is always the possibility that some taxa that are not amenable to laboratory cultivation are missed. However, as noted in the Results section, 96 different morphospecies were detected by use of the culture enrichment technique including forms with unique characteristics that appear to be previously undescribed taxa. Moreover, all-totaled over 6,000 observations were tallied during the course of this experiment suggesting that this technique which has been used in various research settings provides a reasonable estimate of the major occurring gymnamoebae (e.g., Anderson and Rogerson 1995; Darbyshire *et al.* 1996; Bischoff and Anderson 1998; Anderson 2000, 2002; Anderson *et al.* 2001; Bass and Bischoff 2001).

The results of this study provide some insights into changes in communities of soil gymnamoebae when moisture is held constant and as cold stress is released over a range of temperatures simulating natural environmental changes from winter to spring. Morphospecies richness (the number of different kinds of gymnamoebae occurring in each 0.01 g of soil sample) increased markedly after the temperature reaches 10°C probably due to excystment and proliferation of species that are dormant at lower temperatures. This is consistent with prior research (Anderson 1996, Fig. 6) indicating that numerical abundances of gymnamoebae in aquatic environments also increase substantially after the temperature reaches 10°C.

In the study reported here, the statistically significant increase in morphospecies richness combined with an

increase in patchiness among the 0.01 g samples of soil support the predictions made in the hypothesis presented in the Introduction. Further research is needed to determine if there is a significant change in the uniqueness of morphospecies since no significant trend was found with the limited set of samples used in this study. This hypothesis is based on a theory that soil communities are compartmentalized into small biocoenoses existing in microscale soil aggregates as small as *ca* 0.01 g (Anderson 2002). These small domains vary substantially in the number and kind of microbiota that they can support. Optical examination of such small soil aggregates indicates that they are heterogeneous in composition and vary in mineral particle content, particle size and amount of bulk organic matter. Thus, some of these microdomains can potentially support larger populations of microbiota due to favorable nutrient composition, available surface area for attachment, and enhanced water-holding capacity compared to other microdomains. The number of encysted morphospecies available to support population growth undoubtedly varies across these small domains providing variations in potential for species richness among the small-scale niches available in the soil. When cold temperature stress decreases, giving rise to more favorable growth conditions, gymnamoebae excyst and proliferate. The most favorable niches support more luxuriant growth than less favorable ones, thus increasing the variance in the distribution of morphospecies richness across the microdomains leading to increased patchiness. This theory may account for the concomitant increase in gymnamoeba richness (I_R) and patchiness (I_p) as observed in this study.

It is interesting to note that the values of the Shannon-Wiener index (H), typically used to assess community diversity, increased during the increment in temperature from 5 to 10°C (Table 2), but remained fairly constant in the 10 to 20°C range and in this study at least, did not reflect major changes in the composition of the gymnamoeba communities. The biotic complexity measure used here, however, did reflect subtle changes that occur during release from cold stress above 10°C (Table 1).

Overall, this microcosm-based research indicated that during release from cold stress at constant moisture, the percent of active gymnamoebae versus encysted forms, morphospecies richness, and community patchiness increased as the temperature increased from 5°C to 20°C simulating a transition from winter to spring. However, since this work was based on only one soil sample,

further research is needed to determine the generality and reproducibility of these findings.

REFERENCES

Anderson O. R. (1996) The physiological ecology of planktonic sarcodines with applications to paleoecology: Patterns in space and time. *J. Eukaryot. Microbiol.* **43:** 261-274

Anderson O. R. (2000) Abundance of terrestrial gymnamoebae at a northeastern U. S. site: A four-year study, including the El Niño winter of 1997-1998. *J. Eukaryot. Microbiol.* **47:** 148-155

Anderson O. R. (2002) Laboratory and field-based studies of abundances, small-scale patchiness, and diversity of gymnamoebae in soils of varying porosity and organic content: Evidence of microbiocoenoses. *J. Eukaryot. Microbiol.* **49:** 17-23

Anderson O. R. (2003) A model of biocomplexity and its application to the analysis of some terrestrial and marsh eukaryotic microbial communities with an emphasis on amoeboid protists. *J. Eukaryot. Microbiol.* **50:** 86-91

Anderson O. R., Bohlen P. J. (1998) Abundances and diversity of gymnamoebae associated with earthworm (*Lumbricus terrestris*) middens in a northeastern U. S. forest. *Soil Biol. Biochem.* **30:** 1213-1216

Anderson O. R., Griffin K. L. (2001) Abundances of protozoa in soil of laboratory-grown wheat plants cultivated under low and high atmospheric CO_2 concentrations. *Protistology* **2:** 76-84

Anderson O. R., Rogerson A. (1995) Annual abundances and growth potential of gymnamoebae in the Hudson Estuary with comparative data form the Firth of Clyde. *Europ. J. Protistol.* **31:** 223-233

Anderson O. R., Gorrell, T., Bergen A., Kruzansky R., Levandowsky, M. (2001) Naked amoebas and bacteria in an oil-impacted salt marsh community. *Microb. Ecol.* **42:** 474-481

Baldock B. M., Sleigh M. A. (1988) The ecology of benthic protozoa in rivers seasonal variation in abundance in fine sediments. *Arch. Hydrobiol.* **111:** 409-422

Bamforth S. S. (1971) The numbers and proportions of testacea and ciliates in litters and soils. *J. Protozool.* **18:** 24-28

Bass P., Bischoff P. J. (2001) Seasonal variability in abundance and diversity of soil gymnamoebae along a short transect in southeastern USA. *J. Eukaryot. Microbiol.* **48:** 475-479

Bischoff P. J. (2002) An analysis of the abundance, diversity and patchiness of terrestrial gymnamoebae in relation to soil depth and precipitation events following a drought in southeastern U. S. A. *Acta Protozool.* **41:** 183-189

Bischoff P. J., Anderson O. R. (1998) Abundance and diversity of gymnamoebae at varying soil sites in northeastern U. S. A. *Acta Protozool.* **37:** 17-21

Clarholm M. (1981) Protozoan grazing of bacteria in soil. Impact and importance. *Microb. Ecol.* **7:** 343-350

Clarholm M. (1989) Effects of plant-bacterial-amoebal interactions on plant uptake of nitrogen under field conditions. *Biol. Fertil. Soils* **8:** 373-378

Corliss J. O. (2002) Biodiversity and biocomplexity of the protists and an overview of their significant roles in maintenance of our biosphere. *Acta Protozool.* **41:** 199-219

Cowling A. J. (1994) Protozoan distribution and adaptation. In: Soil Protozoa (Ed. J. F. Darbyshire). CAB International, Wallington, 5-42

Darbyshire J. F., Griffiths B. S., Davidson M. S., McHardy W. J. (1989) Ciliate distribution amongst soil aggregates. *Rev. Ecol. Biol. Sol* **26:** 47-56

Darbyshire J. F., Anderson O. R., Rogerson A. (1996) Protozoa. In: Methods for the Examination of Organismal Diversity in Soils

and Sediments (Ed. G. S. Hall). CAB International, Wallingford, 79-90

Fenchel T. (1987) Ecology of Protozoa: The Biology of Free-living Phagotrophic Protists. Science Tech Publishers, Madison, 53-68

Foissner W. (1987) Soil protozoa: fundamental problems, ecological significance, adaptations in Ciliates and Testaceans, bioindicators, and guide to the literature. In: Progress in Protistology, (Eds. J. O. Corliss and D. J. Patterson). Biopress Ltd., Bristol, **2:** 69-212

Foissner W. (1991) Diversity and ecology of soil flagellates. In: The Biology of Free-living Heterotrophic Flagellates (Eds. D. J. Patterson and J. Larsen). Clarendon Press, Oxford, 93-112

Foissner W. (1994) Soil protozoa as bioindicators in ecosystems under human influence. In: Soil Protozoa (Ed. J. F. Darbyshire). CAB International, Wallington, 147-193

Griffiths B. S. (1994) Soil nutrient flow. In: Soil Protozoa (Ed. J. F. Darbyshire). CAB International, Wallington, 65-91

Heal O. W. (1964) Observations on the seasonal and spatial distribution of Testacea (Protozoa: Rhizopoda) in *Sphagnum*. *J. Anim. Ecology* **33:** 395-412

Lousier J. D., Parkinson D. (1984) Annual populations dynamics and production ecology of Testacea (Protozoa, Rhizopoda) in an aspen woodland soil. *Soil Biol. Biochem*. **16:** 103-114

Mathes J., Arndt H. (1995) Annual cycle of protozooplankton (ciliates, flagellates and sarcodines) in relation to phyto- and metazooplankton in Lake Neumuehler See (Mecklenburg, Germany). *Arch. Hydrobiol*. **134:** 337-358

Old K. M. (1986) Mycophagous soil amoebae: Their biology and significance in the ecology of soil-borne plant pathogens. In: Progress in Protistology, (Eds. J. O. Corliss and D. J. Patterson). Biopress Ltd., Bristol, **1:** 163-194

Page F. (1988) A New Key to Freshwater and Soil Gymnamoebae. Freshwater Biological Association, U. K.

Rogerson A., Patterson D. J. (2000) Ramicristate amoebae (Gymnamoebae) In: The Illustrated Guide to the Protozoa (2nd Ed.) (Eds. J. J. Lee, G. F. Leedale, P. Bradbury) Society of Protozoologists, Lawrence, KS, 1023-1052

Sawyer T. K. (1989) Free-living pathogenic and non pathogenic amoebae in Maryland USA Soils. *Appl. Environ. Microbiol*. **55:** 1074-1077

Schmidt-Halewicz S. E. (1994) Composition and seasonal changes of the heterotrophic plankton community in a small oligotrophic reservoir. *Arch. Hydrobiol. Beih*. **40:**197-207

Tate R. L. (1995) Soil Microbiology. John Wiley and Sons, New York

Taylor L. R. (1984) Assessing and interpreting the spatial distributions of insect populations. *Ann. Rev. Entomol*. **29:** 321-357

Zwart K. B., Kuikman P. J., Van Veen J. A. (1994) Rhizosphere protozoa: Their significance in nutrient dynamics. In: Soil Protozoa (Ed. J. F. Darbyshire). CAB International, Wallington, 93-121

ACTA
PROTOZOOLOGICA

Sibling Species Within *Paramecium jenningsi* Revealed by RAPD

Bogumiła SKOTARCZAK, Ewa PRZYBOŚ², Beata WODECKA¹ and Agnieszka MACIEJEWSKA¹

¹Department of Genetics, Faculty of Biology, Szczecin University, Szczecin; ²Institute of Systematics and Evolution of Animals, Polish Academy of Sciences, Kraków, Poland

Summary. The studies with application of the classical genetic method (strain crosses) and a molecular technique (RAPD-PCR fingerprinting, primer Ro 460-04) revealed the presence of separate sibling species within *P. jenningsi*. One of these is confined to six genetically related strains originating from Japan, separated from other group (results of strain crosses) and showing only one characteristic band pattern. The other of these includes strains from India, Saudi Arabia and China (Przyboś *et al.* 2003). We wanted to verify the RAPD markers specific for *P. jenningsi* and to prove the existence of two sibling species within it (revealed by one primer only), by application of others Ro-type primers. The conducted RAPD-PCR fingerpring analysis revealed that the genomes of the studies strains of *P. jenningsi* have polymorphic DNA sequences complementary to the four applied primers. The band patterns can be used as species-specific markers for *P. jenningsi*. DNA amplification by four primers used differentiates *P. jenningsi* into two groups of strains, one of which includes the Indian, Saudi Arabian and Chinese strains, the other the Japanese strains. Our results are congruent with inter-strain crossing experiments in which reproductive isolation was found when continental and Japanese strains were tested. This is further evidence for the existence of two sibling species, whose reproductive isolation is genetically induced.

Key words: *Paramecium jenningsi*, primers, RAPD-PCR analysis, sibling species, species markers.

INTRODUCTION

Paramecium jenningsi Diller *et* Earl,1958 was described from India (Bangalore). Later, several strains of this species were also found in different, mainly tropical regions, i.e. Uganda, Madagascar, Florida (USA), Panama, but also from the Kaliningrad district (Russia), Tajikistan and Japan (Przyboś *et al*. 1999). In 1999 and 2000 new strains were collected from Saudi Arabia, China and again from Japan (Table 1). An expansion of

the range of *P. jenningsi* prompted studies on intraspecific differentiation, i.e. ascertainment if strains originating from remote and isolated habitats represent one sibling species or more. The existence of one sibling species (syngen) of *P. jenningsi* was accepted (Sonneborn 1958, 1970; Przyboś 1986) and confirmed by genetic, karyological and cytological studies (Przyboś 1975, 1978, 1980, 1986; Jurand and Przyboś 1984) carried out on strains from India, Uganda and Madagascar. Biochemical investigations of esterases and acid phosphotases by Allen *et al*. (1983) were performed on strains from India, Panama and the USA (Florida).

However, a preliminary analysis of *P. jenningsi* strains from India, Madagascar, Uganda, Florida and one

Address for correspondence: Ewa Przyboś, Institute of Systematics and Evolution of Animals, Polish Academy of Sciences, Sławkowska 17, Kraków 31-016, Poland; Fax: (48) 12 422 42 94; E-mail: przybos@isez.pan.krakow.pl

strain from Japan (Przyboś *et al*. 1999) using the RAPD-PCR method (primer Ro 460-04) revealed the existence of three different DNA genotypes (band patterns) within the species. Three groups of strains were distinguished; one group consisting of strains from India and Madagascar, the second one of strains from Uganda and Florida, and a third from Japan (Hagi).

The differentiation of subsequent strains from Saudi Arabia, China, six strains from Japan and one from India (Bangalore) was investigated (Przyboś *et al*. 2003). These studies were carried out with the classical genetic method (strain crosses) and a molecular technique (RAPD-PCR fingerprinting, primer Ro 460-04). They revealed the presence of separate sibling species within *P. jenningsi*. One of these is confined to six genetically related strains originating from Japan, separated from other groups (results of strain crosses) and showing only one characteristic band pattern. The other sibling species of *P. jenningsi* includes strains from India, Saudi Arabia and China.

The aim of the present study was the verification of RAPD markers specific for *P. jenningsi*. We also wanted to prove the existence of two separate species within *P. jenningsi* (revealed by one primer only) by the application of four Ro-type primers. Therefore, the adequacy of the primers in differentiating strains within the species could be assessed.

MATERIALS AND METHODS

Paramecium DNA was isolated from the 9 strains listed in Table 1 (two cultures each) using QIAamp DNA Mini Kit (Qiagen, Germany) as described by Przyboś *et al.* (2003). Random amplified polymorphic DNA-PCR (RAPD-PCR) was performed with primers Ro 460-04 (5' GCAGAGAAGG 3'), Ro 460-06 (5' GTAGCCATGG 3'), Ro 460-07 (5' AACGTACGCG 3') and Ro 460-10 (5' CTAGGTCTGC 3') (Roth, Karsruhe, Germany) by the method described by Stoeck and Schmidt (1998), using Taq polymerase (Fermentas, Lithuania). The products of the PCR reaction were separated by electrophoresis in 1.5% agarose for 3.5 h at 85 V together with a DNA molecular weight marker (SmartLadder, Bioline, Germany), stained with ethidium bromide and visualized in UV light. The images were stored in computer memory using the program Biocapt (Vilbert Lourmat, France).

All RAPD-PCR reactions for each strain and culture were repeated several times for verification. Phylogenetic analysis was performed by comparing the molecular weight of DNA obtained by the RAPD-PCR method using the Bio 1D program (Vilbert Lourmat, France). The similarity index according to Nei and Li (1979) applied in the program was calculated by the equation: $a=2nxy/(nx+ny)$; where: nx and ny describe the numbers of bands appearing in the RAPD patterns of x and y, respectively; while nxy describes the number of DNA-bands with similar molecular weight shared by the two patterns. Phylogenetic trees were constructed on the basis of a similarity matrix with the values from the above equations.

RESULTS

RAPD-PCR fingerprints (band patterns) revealed by primers Ro 460-04, Ro 460-06, Ro 460-07 and Ro 460-10 from nine strains (two cultures each) of *P. jenningsi* are presented in Figs 1-4. Schematic band patterns were constructed on the basis of photographs of gel separation products, characterizing strains from particular geographic localities, and also the applied primers. The approximate molecular weight of RAPD-PCR products reveals 100% concordance in all 9 strains (two cultures per strain).

RAPD-PCR fingerprint analysis for the Ro 460-04 primer (Fig. 1) revealed a pervasive 483 bp band for all strains, and another band (1466 bp) appearing in all samples with the exception of China. A band of 900 bp occurred in all strains except the Arabian and Japanese Okinawa strain. Another band (206 bp) common to all but two Japanese strains (Shinnamyou and Okinawa) was recorded. Specific Japanese markers of *P. jenningsi* with a molecular weight of 1348 and 743 bp were also discovered. Three non-Japanese strains (India, Saudi Arabia and China) shared common bands of 1090, 750, 700 and 645 bp.

Analysis of RAPD-PCR fingerprints for the Ro 460-06 primer did not reveal a common band for the entire species (Fig. 2). All continental strains and two of the Japanese strains (Hagi and Ube) shared a 1272 bp band, as well as a 1156 bp band in all continental strains and two of the Japanese strains (Yamaguchi and Ube). Moreover, four of the continental strains and one Japanese (Okinawa) had specific bands not present in other strains and recognized as markers. The Indian band had a molecular mass of 2253 and 1824 bp, the Saudi Arabian a 2370 and 2000 bp band, the Chinese a 852 and 448 bp band, and 685 and 331 bp band in the Okinawa strain.

Results of RAPD-PCR fingerprints for primer Ro 460-07 (Fig. 3) were almost identical to Ro 460-06 (Fig. 2). A common band for the entire species was not present. Neither the Japanese, nor the continental strains shared bands. Continental strains and some of the Japanese strains shared bands, as in fingerprints for Ro 460-06.

Table 1. *Paramecium jenningsi* strains.

Origin and collector's name	References
Saudi Arabia, neighbourhood of Riyadh; K.A.S. AL-Rasheid, July 1999	Fokin *et al.* 2001
India, Bangalore; [1,2] P.B. Padmavathi, 1955	Diller and Earl 1958, Przyboś 1975, 1978, 1986
China, Shanghai; M. Fujishima, November 1999	Fokin *et al.* 2001
Japan, Honshu Island, Yamaguchi prefecture, Ube City; M. Fujishima, October 2000	Present paper
Japan, Honshu Island, Yamaguchi prefecture, Nagato City; M. Fujishima, September 2000	Present paper
Japan, Honshu Island, Yamaguchi prefecture, Shinnamyou; M. Fujishima, October 2000	Present paper
Japan, Honshu Island, Yamaguchi prefecture, Hagi City; [1]S. Fokin, September 1997	Przyboś *et al.* 1999
Japan, Honshu Island, Yamaguchi prefecture, Yamaguchi City; S. Fokin, November 1999	Fokin *et al.* 2001
Japan, Okinawa Island, Okinawa prefecture, Hujigawa; M. Fujishima 2000	Present paper

[1]Strains studied by RAPD-PCR previously (Przyboś *et al.* 1999); [2]Strain from India was studied genetically and karyologically (Przyboś 1975, 1978, 1986).
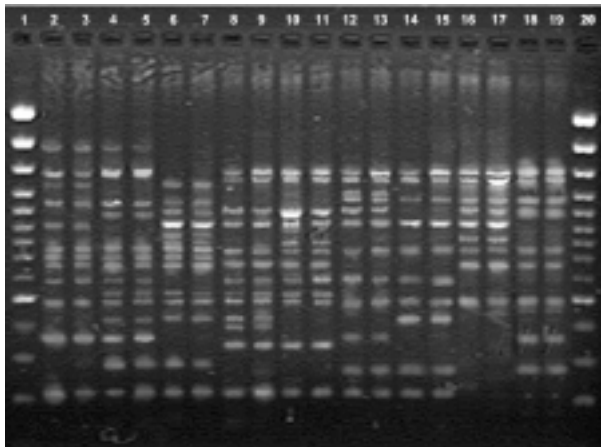

Fig. 1. RAPD reaction products for primer Ro 460-04 separated in an agarose gel. Lanes: 1 and 20 - weight marker; 2, 3 - Indian strain (Bangalore); 4, 5 - Saudi Arabian strain; 6, 7 - Chinese strain (Shanghai); 8, 9 - Japanese strain (Hagi); 10, 11 - Japanese strain (Yamaguchi); 12, 13 - Japanese strain (Ube); 14, 15 - Japanese strain (Nagato); 16, 17 - Japanese strain (Shinnamyou); 18, 19 - Japanese strain (Okinawa, Hujigawa).
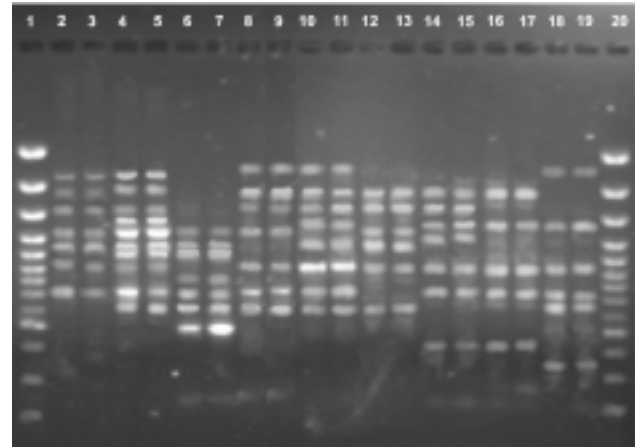

Fig. 2. RAPD reaction products for primer Ro 460-06 separated in an agarose gel. Lanes: 1 and 20 - weight marker; 2, 3 - Indian strain (Bangalore); 4, 5 - Saudi Arabian strain; 6, 7 - Chinese strain (Shanghai); 8, 9 - Japanese strain (Hagi); 10, 11 - Japanese strain (Yamaguchi); 12, 13 - Japanese strain (Ube); 14, 15 - Japanese strain (Nagato); 16, 17 - Japanese strain (Shinnamyou); 18, 19 - Japanese strain (Okinawa, Hujigawa).

Analysis of RAPD-PCR fingerprints revealed a 1031 bp band, present in all strains, when the primer Ro 460-10 was applied (Fig. 4) and it can also be used as a molecular marker for *P. jenningsi*. RAPD-PCR profiles in all strains shared a band of 1304 bp, with the exception of those from the Arabian locality. Analogously, all strains except the Japanese Yamaguchi strain had a band of 677 bp. Another band (513 bp) was present in all strains except for the Japanese Hagi and Yamaguchi. All continental strains (India, Saudi Arabia, China) pos-

sessed a 1200 bp band, acknowledged as a geographical marker. Additionally, all continental strains and two of the Japanese strains (Ube and Okinawa) shared a 912 bp band. Amplification with primer Ro 460-10 did not produce a band specific only for Japanese strains. A 1975 bp band was revealed in all Japanese strains except for Okinawa. Only the Chinese strain had a specific 1129 bp band, which can be used as a marker for this strain. Two of the continental strains (India and Saudi Arabia) had a conspicuous 443 bp band.
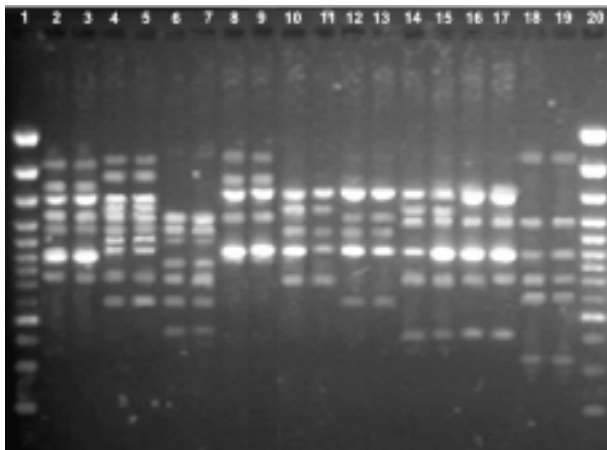
Fig. 3. RAPD reaction products for primer Ro 460-07 separated in an agarose gel. Lanes: 1 and 20 - weight marker; 2, 3 - Indian strain (Bangalore); 4, 5 - Saudi Arabian strain; 6, 7 - Chinese strain (Shanghai); 8, 9 - Japanese strain (Hagi); 10, 11 - Japanese strain (Yamaguchi); 12, 13 - Japanese strain (Ube); 14, 15 - Japanese strain (Nagato); 16, 17 - Japanese strain (Shinnamyou); 18, 19 - Japanese strain (Okinawa, Hujigawa).
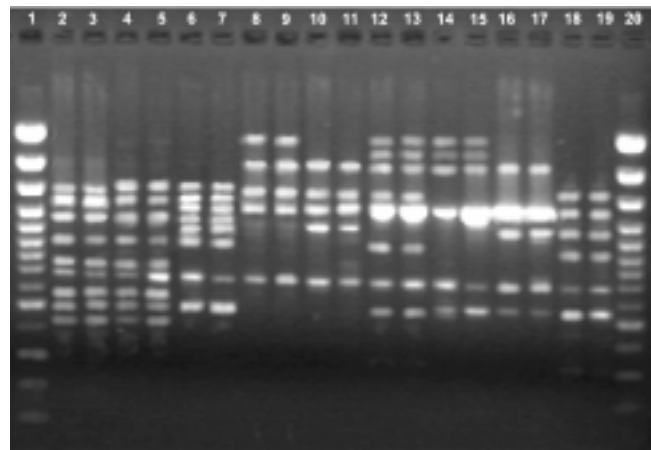
Fig. 4. RAPD reaction products for primer Ro 460-10 separated in an agarose gel. Lanes : 1 and 20 - weight marker; 2, 3 - Indian strain (Bangalore); 4, 5 - Saudi Arabian strain; 6, 7 - Chinese strain (Shanghai), 8, 9 - Japanese strain (Hagi), 10, 11 - Japanese strain (Yamaguchi); 12, 13 - Japanese strain (Ube), 14, 15 - Japanese strain (Nagato), 16, 17 - Japanese strain (Shinnamyou), 18, 19 - Japanese strain (Okinawa, Hujigawa).
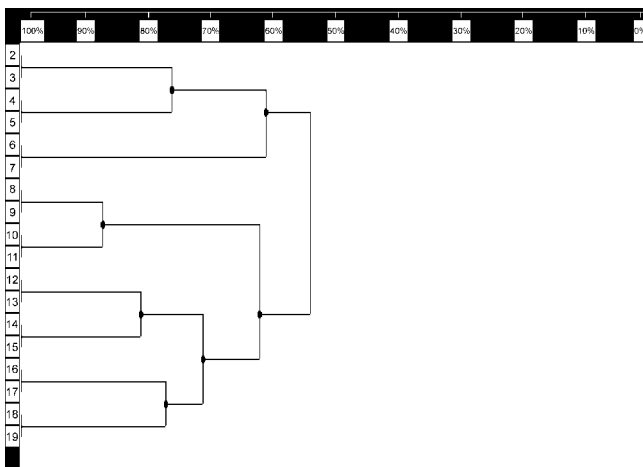

Fig. 5. Dendrogram representing phylogenetic relationships among strains of *P. jenningsi* with RAPD fingerprint data from the Ro 460-04, Ro 460-06, Ro 460-07, Ro 460-10 primers (2, 3 - Indian strain; 4, 5 - Saudi Arabian strain; 6, 7 - Chinese strain; 8, 9 - Japanese strain from Hagi; 10, 11 - Japanese strain from Yamaguchi; 12, 13 - Japanese strain from Ube; 14, 15 - Japanese strain from Nagato; 16, 17 - Japanese strain from Shinnamyou; 18, 19 - Japanese strain from Okinawa).

Results of genetic kinship analysis. On the basis of band patterns obtained from RAPD-PCR fingerprinting with primers Ro 460-04, Ro 460-06, Ro 460-07 and Ro

460-10, using the program Bio 1D (Vilber Lourmat), dendrograms were constructed depicting the genetic relatedness of the different geographical strains of *P. jenningsi* following Nei and Li's (1979) similarity coefficients. The confidence limit of the performed analyses was 1%.

The Fig. 5 depicts a dendrogram obtained from the results of RAPD fingerprinting with the primers Ro (460-04, 460-06, 460-07, 460-10). The 9 strains of *P. jenningsi* are divided into 2 main groups: the first large group includes all continental strains; the second encompasses the Japanese strains (similarity value of 54%). The first group contains an Indian and Arabian subgroup and another with only the Chinese strain (similarity of 62%). The Japanese strains are additionally divided into two subgroups (similarity of 63%): the first includes the Hagi and Yamaguchi strains, while the second involves two lines composed of Ube / Nagato and Shinnamyou / Okinawa strains, respectively (similarity of 73%).

DISCUSSION

Species from the *Paramecium aurelia* group, which includes *P. jenningsi*, show morphological similarity

making them difficult to identify. *Paramecium* is acknowledged as a model organism in many fields of experimental biology, and also considered an indicator in ecological studies, i.e. in littoral zone dynamics of aquatic ecosystems. Therefore, a precise and quick method is needed to identify the species of *Paramecium*. The primers applied in this study can be considered suitable for the identification of *P. jenningsi* and also can be used to analyze genetic relatedness and phylogenetic relationships amongst strains originating from remote and isolated geographic localities. The conducted RAPD-PCR fingerprint analysis revealed that the genomes of most of the 9 studied strains of *P. jenningsi* have polymorphic DNA sequences complementary to the 4 applied primers. The observed genetic variability did not occur among individuals belonging to the same strain, which was repeatedly confirmed by studies involving many isolates descending from cultures of different strains of *P. jenningsi*. The band patterns obtained from the RAPD-PCR analysis can be used as species-specific markers for the separation of *P. jenningsi* from other species in the genus and also as strain-specific markers determining the geographic origins of strains in a sample.

The Ro 460-04 primer produced band patterns for each of the 9 different strains and can prove useful as a strain-specific marker for geographic differentiation. Additionally, one band was shared by all strains (483 bp); therefore it is considered a marker for the entire species. Two bands were obtained for Japanese strains (1348 bp and 743 bp) and four bands for continental strains (1090 bp, 750 bp, 700 bp, 645 bp). All of these traits deem the primer Ro 460-04 useful in RAPD analysis for species and strain identification in *P. jenningsi*.

The band pattern acquired in this study as well as in a previous one (Przyboś *et al*. 2003) allowed for strain-specific identification, disclosed a band shared by all strains, and a few bands differentiating continental and Japanese strains. RAPD-PCR fingerprinting with the primer Ro-460-04 in *P. jenningsi* was first carried out in 1999 (Przyboś *et al*. 2003). The study incorporated two Indian strains, the Japanese Hagi strain, Madagascan, Ugandan and Floridian strains. Band patterns were identical for all strains examined and were clearly different from patterns obtained from other *Paramecium* species (*P. aurelia* complex, *P. nephridiatum*, *P. dubosqui*, *P. calkinsi*, *P. woodruffi*, *P. multimicronucleatum*, *P. caudatum*). The diversity in band pattern between the different strains of *P. jenningsi* was considered as genotypic variation in one species.

Additionally, this analysis confirmed the results of morphometric and cytological studies allowing the inclusion of the Japanese strain into *P. jenningsi* (Przyboś *et al*. 1999). The current investigation yielded band patterns similar to the ones of Przyboś *et al*. (1999), who applied the 460-04 primer for the Indian and Japanese Hagi strains, used in both studies. However, a difference in RAPD product molecular mass of several tens of base pairs in magnitude was noticed, probably on account of the proximate character of these values estimated by their position relative to the position of the mass marker. Many factors contribute to electrophoretic mobility and the observed differences in mass and band pattern are considered negligible.

The DNA polymorphism revealed by the RAPD technique (Przyboś *et al*. 2003) inclined us to undertake successive studies on *P. jenningsi* using the same strains from India, Saudi Arabia, China and Japan (6 different strains). In the above-cited paper (Przyboś *et al*. 2003), the primer Ro 460-04 disclosed the presence of three types of band patterns (Indian and Arabian strains; Chinese strain; Japanese strains). These band patterns were differentiated by the presence/absence of specific bands. All patterns contained more bands than revealed by the current study. However, the position of the key bands, intensively visible in UV light, was the same in both investigations. The molecular mass of the products was similar and exhibited minimal deviation.

It seems especially meaningful to compare band patterns of *P. jenningsi* with analogous studies carried out on other species of the *P. aurelia* complex (Stoeck and Schmidt 1998, Stoeck *et al*. 1998, 2000). This comparison is further advocated by the close relationship of the two species as revealed by similar reorganization processes in the nucleus (Fokin *et al*. 2001) and sequencing studies incorporating the SSrRNA gene in the subclass *Peniculia* (Strüder-Kypke *et al*. 2000). Differences between *P. jenningsi* and the *P. aurelia* species complex in band pattern expression indicates that the pattern observed for primer Ro 460-04 is specific for *P. jenningsi*. RAPD-PCR fingerprinting with this primer is an excellent tool for fast and accurate identification of this species, i.e. in environmental samples.

Analysis of RAPD-PCR fingerprints for the Ro 460-06 primer did not reveal a common band for the entire species. However RAPD-PCR profiles for the Ro 460-06 primer distinguish between two groups of strains: one containing continental and part of the Japanese strains, the other the remaining Japanese strains. This primer cannot be used to distinguish the species, however, the

profiles show a large degree of variation and are good strain markers, important for confirmation purposes.

RAPD-PCR fingerprints for primer Ro 460-07 were almost identical to Ro 460-06 (Fig. 2). A common band for the entire species was not present. Neither the Japanese, nor the continental strains shared bands. Continental strains and some of the Japanese strains shared bands, as in fingerprints for Ro 460-06. Interestingly, the molecular mass of products from primers Ro 460-06 and 460-07 is very similar, resulting in almost identical band profiles, differing only in the position of one band in the Arabian strain and by the presence of a few additional bands in the Hagi, Yamaguchi and Ube profiles for Ro 460-06.

Analysis of RAPD-PCR fingerprints with the primer Ro 460-10 revealed a common band (1031 bp) present in all strains and it can also be used as a molecular marker for *P. jenningsi*. All continental strains (India, Saudi Arabia, China) possessed a 1200 bp band, acknowledged as a geographical marker. Amplification with primer Ro 460-10 did not produce a band specific only for Japanese strains. However the band pattern acquired in this study allowed for species-specific identification, disclosed a band shared by all strains, so it can be consider as a good general species marker. A single marker obtained for continental strains of *P. jenningsi* and absence of specific one for the Japanese strains does not render it helpful in differentiating between continental and Japanese strains.

This paper is the first to apply the primers Ro 460-06, 460-07 and 460-10 in *P. jenningsi* and consequently, because of the lack of published research concerning their use, a comparative analysis of results is impossible.

Many investigators point out the problems associated with repeatability of RAPD-PCR fingerprinting (Skroch and Nienhuis 1995, Woodburn *et al.* 1995; after Foissner *et al.* 2001). Because of the variation in intensity of bands in parallel samples, interpretation of results is problematic and demands extensive experience, being prone to subjective judgment (Foissner *et al.* 2001). Stoeck and Schmidt (1998) proved that the intensity of bands could change in subsequent experiments in relation to template DNA. Relatively weak bands may not show up at all in successive runs. This is why reliable results required the analysis of several isolates of each strain of *P. jenningsi* in multiple replicates.

Phylogenetic analysis of the 9 strains of *P. jenningsi* based on RAPD-PCR fingerprints permit genetic simi-larity assessment and the construction of dendrograms reflecting phylogenetic relationships in this species. DNA amplification by four used primers used in RAPD-PCR differentiates *P. jenningsi* into two groups of strains, one of which includes the Indian, Saudi Arabian and Chinese strains, the other the Japanese strains.

An evaluation of the applicability of the primers for identification of *P. jenningsi* demonstrated the usefulness of Ro 460-06, Ro 460-07, Ro 460-10 and the previously tested Ro 460-04. Similarity coefficients (Nei and Li 1979) between particular strains were calculated on the basis of the results of RAPD-PCR fingerprinting with 4 primers. These values were computer analysed and used in dendrogram construction in order to elucidate population structure, the evolutionary history and relationships in *P. jenningsi*. Phylogenetic analysis employing the RAPD data from primer Ro 460-04, Ro 460-06, Ro 460-07 and Ro 460-10 separates the species into two groups: an Indian, Chinese and Saudi Arabian assemblage and a Japanese group. These results agree with an earlier phylogenetic analysis (Przyboś *et al.* 2003), which revealed the presence of two sibling species incorporating the continental and Japanese groups, respectively. In the first group, Indian and Arabian strains had similar band patterns, while the Chinese was slightly different (Przyboś *et al.* 2003).

Our results are congruent with inter-strain crossing experiments in which reproductive isolation was found when continental and Japanese strains were tested (Przyboś *et al.* 2003). This is further evidence for the existence of two sibling species, whose reproductive isolation is genetically induced. Ro primers can be expected to verify these results.

Taking into account the fact that the values of the similarity indexes are not absolute but rather relative - they change depending on the applied primer (Chapco *et al.* 1992, Przyboś *et al.* 1999) - they cannot accurately describe the phylogenetic structure of this species. Landry and Lapoite (1996) concluded that at least 12 primers were needed for appropriate phylogenetic reconstruction. Still, the arrangement of groups and subgroups established on the basis of the similarity matrices is relatively constant and probably reflects actual phylogenetic relationships in *P. jenningsi*.

The genetic structure revealed by RAPD-PCR fingerprinting is closely linked to the life strategy of the species and its evolutionary history. Genetic variation between continental and Japanese strains of *P. jenningsi*,

reflected by the presence of two sibling species, is therefore a result of the geographic dispersal of this species.

REFERENCES

Allen S. L., Rushford D. L., Nerad T. A., Lau E. T. (1983) Intraspecies variability in the esterases and acid phosphatases of *Paramecium jenningsi* and *Paramecium multimicronucleatum*: assignment of unidentified paramecia, comparison with the *Paramecium aurelia* complex. *J. Protozool.* **30:** 155-163

Chapco W., Ashton N. W., Martel R. K. B., Antonishyn N. (1992) A feasibility study of random amplified polymorphic DNA in the population genetics and systematics of grasshoppers. *Genome* **35:** 569-574

Diller W. F., Earl P. R. (1958) *Paramecium jenningsi*, n. sp. *J. Protozool.* **5:** 155-158

Foissner W., Stoeck T., Schmidt H., Berger H. (2001) Biogeographical differences in a common soil ciliate, *Gonostomum affine* (Stein), as revealed by morphological and RAPD-fingerprint analysis. *Acta Protozool.* **40:** 83-97

Fokin S. I., Przyboś E., Chivilev S. M. (2001) Nuclear reorganization variety in *Paramecium* (Ciliophora: Peniculida) and its possible evolution. *Acta Protozool.* **40:** 249-261

Jurand A., Przyboś E. (1984) A new method of study of chromosome numbers in *Paramecium. Folia Biol. (Kraków)* **32:** 295-300

Landry P. A., Lapointe F. J. (1996) RAPD problems in phylogenetics. *Zool. Scr.* **25:** 283-290

Nei M., Li W.- H. (1979) Mathematical model for studying genetic variation in terms of restriction endonucleases. *Proc. Natl. Acad. Sci. U. S. A.* **76:** 5269-5273

Przyboś E. (1975) Genetic studies of *Paramecium jenningsi* strains (Diller & Earl, 1958). *Folia Biol. (Kraków)* **23:** 425-471

Przyboś E. (1978) Cytological and karyological studies of *Paramecium jenningsi. Folia Biol.* (*Kraków*) **26:** 25-29

Przyboś E. (1980) The African strain of *Paramecium jenningsi.* Cytological and karyological investigations. *Folia biol.* (*Kraków*) **28:** 391-397

Przyboś E. (1986) Chromosomes in *Paramecium jenningsi* (Diller & Earl, 1958): A serial section study. *Folia Biol.* (*Kraków*) **34:** 133-160

Przyboś E., Fokin S., Stoeck T., Schmidt H. J. (1999) Occurrence and ecology of *Paramecium jenningsi* strains. *Folia Biol.* (*Kraków*) **47:** 53-59

Przyboś E., Skotarczak B., Wodecka B. (2003) Phylogenetic relationships of *Paramecium jenningsi* strains (classical analysis and RAPD studies). *Folia biol.* (*Kraków*) **51:** 85-95

Skroch P., Nienhuis J. (1995) Impact of scoring error and reproductibility of RAPD data on RABD based estimates of genetic distance. *Theor. Appl. Genet.* **91:** 1068-1091

Sonneborn T. M. (1958) Classification of sibling species of the *Paramecium aurelia- multimicronucleatum* complex. *J. Protozool.* **4(Suppl.):** 17-18

Sonneborn T. M. (1970). Methods in *Paramecium* reserach. In: Methods in Cell Physiology, (Ed. D. M. Prescott). Academic Press, New York, **4:** 242-339

Stoeck T., Schmidt H. J. (1998) Fast and accurate identification of European species of the *Paramecium aurelia* complex by RAPD-fingerprints. *Microb. Ecol.* **35:** 311-317

Stoeck T., Przyboś E., Schmidt H. J. (1998) A combination of genetics with inter- and intra-strain crosses and RAPD-fingerprints reveals different population structures within the *Paramecium aurelia* species complex. *Europ. J. Protistol.* **34:** 348-355

Stoeck T., Przyboś E., Kusch J., Schmidt H. J. (2000) Intra-species differentiation and level of inbreeding of different sibling species of the *Paramecium aurelia* complex. *Acta Protozool.* **39:** 15-22

Strüder-Kypke M. C., Wright A.-D. G., Fokin S. I., Lynn D. H. (2000) Phylogenetic relationships of the subclass Peniculia (Oligohymenophorea, Ciliophora) inferred from small subunit rRNA gene sequences. *J. Eukaryot. Microbiol.* **47:**419-429

Woodburn M. A., Youston A. A., Hilu K. H. (1995) Random amplified polymorphic DNA fingerprinting of mosquito-pathogenic and nonpathogenic strains of *Bacillus sphaericus. Int. J. Bact.* **45:** 212-217

ACTA
PROTOZOOLOGICA

Free-living Amoebae May Serve as Hosts for the *Chlamydia*-like Bacterium *Waddlia chondrophila* Isolated from an Aborted Bovine Foetus

Rolf MICHEL[1], Michael STEINERT[2], Lothar ZÖLLER[1], Bärbel HAURÖDER[1] and Klaus HENNING[3]

[1]Department of Microbiology / Parasitology, Central Institute of the Federal Armed Forces Medical Service, Koblenz; [2]Institut für Molekulare Infektionsbiologie, Wuerzburg; [3]Federal Research Centre of Virus Diseases of Animals, Wusterhausen, Germany

Summary. *Chlamydia*-like endocytobionts are commonly observed in protozoan hosts. Therefore, we examined the potential of 21 different species of free-living amoebas to serve as hosts of a newly found bacterium, *Waddlia chondrophila*. The *Chlamydia*-like bacterium *Waddlia chondrophila* 2032/99 was originally isolated from an aborted bovine foetus in Rheinstetten, Germany. The inoculum of the obligate intracellular agent was prepared from Buffalo Green Monkey (BGM) cells. The infection of *Hartmannella vermiformis* OS101 revealed typical morphological stages of a *Chlamydia*-like life cycle, including the presence of elementary and reticulate bodies. The following infection studies with a *Hartmannella*-adapted *Waddlia* isolate showed that also *Acanthamoeba* sp. Gr. II HLA, *Vahlkampfia ovis* Rhodos, *H. vermiformis* C3/8, *Hyperamoeba*-like amoeba B1,2-100PE and *Dictyostelium discoideum* Sö-P2 supported the growth of *Waddlia*. An interesting finding was that *Hartmannella*-adapted *Waddlia* exhibited a broader host range when compared to the BGM cell isolate. The concept that *Waddlia* may fall into the group of environmentally preadapted pathogens is discussed.

Key words: *Acanthamoeba, Chlamydia,* endoparasite, *Hartmannella,* host spectrum, *Hyperamoeba, Neochlamydia, Simkania,* ultrastructure, *Waddlia chondrophila.*

INTRODUCTION

Chlamydiae are important obligate intracellular pathogens. They are known to be the causative agents of a variety of diseases including infections of the eye, and the respiratory and genital tracts. The life cycle of Chlamydiae is characterized by the development of reticulate bodies, which divide intracellularly by binary fission, and the elementary bodies, which are specialized for transmission (Stephens 1999).

The recent isolation of several novel *Chlamydia*-related bacteria from free-living amoebae, contaminated cell culture and an aborted bovine foetus led to the reclassification of the Chlamydiales and the establishment of the families Parachlamydiaceae, Simkaniaceae, and Waddliaceae (Everett *et al*. 1999, Poppert *et al.* 2002). The clinical significance of the so-called environmental chlamydiae is still unclear. This is also true for *Waddlia chondrophila*, which was isolated from the lung and liver of an aborted bovine foetus (Dilbeck *et al*. 1990, Rurangirwa *et al*. 1999). A second isolation of this species from an aborted bovine foetus in

Germany suggests that it may be associated with abortions in cattle (Henning *et al.* 2002). However, since this second case was associated with Neosporosis the direct influence of *W. chondrophila* on reproductive failure remains to be established.

Within the Chlamydiales it was shown that the Parachlamydiaceae naturally infect amoebae (Everett *et al.* 1999). In addition we previously isolated the *Chlamydia*-like strains Bn9 from *Acanthamoeba* sp. (Michel *et al.* 1994) and A1Hsp1 from *Hartmannella vermiformis* that were later described as novel species *Parachlamydia acanthamoebae* and *Neochlamydia hartmannellae* respectively (Amann *et al.* 1997, Horn *et al.* 2002). For *Acanthamoeba* spp., approximately one of five isolates from both environmental and medical samples contains bacterial endocytobionts (Fritsche *et al.* 1993). In addition it has been shown that *Chlamydia*-like endosymbionts are able to enhance the amoebic cytopathogenicity *in vitro* which may have clinical significance (Fritsche *et al.* 1998).

In this study we evaluated the amoebae host spectrum of the German *W. chondrophila* isolate 2032/99. The findings presented here may help to identify the environmental reservoir and to analyze the epidemiological importance of this organism.

MATERIALS AND METHODS

Isolation and maintenance of *Waddlia chondrophila*. *Waddlia chondrophila* strain 2032/99 was isolated from a bovine fetus, which was aborted on day 228 of gestation. Buffalo Green Monkey (BGM) cells were used for the isolation and cultivation of the bacteria. The cell culture medium was composed of RPMI 1640 and PFEK-1 medium (Biochrom, Berlin, Germany) (1 : 1/v : v) containing 20 mmol HEPES, 5% new-born calf serum, 50 µg/ml gentamycin, 100 µg/ml vancomycin, 2.5 µg/ml amphotericin B, 1% vitamins, 1% amino acids, and 2% glutamine (Henning *et al.* 2002). Infected BGM cells were incubated at 37°C. The cultures were examined for inclusions by phase-contrast microscopy or by staining according to the method of Giménez (1964).

Protozoan strains and culture. The protozoa used in this study are listed in Tables 1 and 2. *Naegleria gruberi* (CCAP 1518/1e) and *N. lovaniensis* (Aq/9/45D) were kindly provided by Johan De Jonckheere, the *Balamuthia mandrillaris* strain CDC: VO39 was provided by Klaus Janitschke. The *Acanthamoeba* strain HLA was isolated from the cornea of a keratitis patient and has been provided by Horst Aspöck. The *Dictyostelium* strain Sö-P2 was isolated from soil. The protozoan cultures were maintained on NN-agar seeded with *Enterobacter cloacae* according to Page *et al.* (1988). *N. gruberi, N. lovaniensis*, and *Hartmannella vermiformis* (OS 101) were grown axenically on SCGYE-medium according to De Jonckheere (1977).

Growth of bacteria within protozoa. The cell suspension of a 6-8 days old infected BGM culture was passed through a membrane filter with a pore size of 1.2 µm. Alternatively, the bacterial inoculum was prepared from infected *H. vermiformis* OS101 by freeze-thawing and passage through a 1.2 µm filter. Bacterial elementary bodies from 100 ml filtrate and trophozoites of log-phase protozoa were coincubated on NN-agar or in SCGYE-medium. After 48 h the infected cell cultures were inspected daily for a time period of 10 days. Morphological alterations and symptoms of infection were compared with non-infected host cells.

Electron microscopy. Infected host cells were harvested after 5 days post infection. The cell suspension was centrifuged for 10 min at 600 g. The resulting pellet was fixed in 3% glutaraldehyde (1 h), transferred to 0.1M cacodylate buffer, postfixed in 1% osmium tetroxide and embedded in Spurr resin. Sections were stained with uranyl acetate and Reynold's lead citrate and examined using a Leo EM 910 electron microscope.

RESULTS

Cocultivation of *W. chondrophila* and protozoa. To evaluate whether *Acanthamoeba* sp., *H. vermiformis* OS 101, *N. gruberi* and *N. lovaniensis* are suitable hosts for *W. chondrophila* isolate 2032/99, we analyzed the intracellular multiplication of the bacteria by light microscopy, phase contrast microscopy and transmission electron microscopy. The bacterial inocula were prepared from infected BGM cells and the results of the coincubations on NN-agar plates and in axenic SCGYE-medium are summarized in Table 1. After 5 days of cocultivation *H. vermiformis* OS101 showed characteristic signs of infection including glassy appearance, prevention of cell migration and the presence of intracellular coccoid bacteria. These features resemble previous observations of *Neochlamydia* infected host cells (Horn *et al.* 2000). Subsequent subculture showed that the association of *Waddlia* and its experimental host *H. vermiformis* was stable. *Acanthamoeba* sp. Gr II, *N. gruberi* and *N. lovaniensis* were not susceptible to infection with *Waddlia*. The inspection of the *Naegleria* Nbeck led to the detection of intracellular *Waddlia*. However the cocci were regularly lost after the subculture of the host.

Transmission electron microscopy of *W. chondrophila* infected *Hartmannella* trophozoites revealed that numerous coccoid bacteria were located either within the cytoplasm or within membrane bound vacuoles (Fig. 1). At higher magnification typical morphological characteristics of the Chlamydiales were observed and the two developmental stages could be visualized simul-

Table 1. Cocultivation of free-living amoebae with *Waddlia chondrophila* isolated from BGM cell culture.

Host amoeba	Source	Intracellular replication
NN-agar plates[1]		
Acanthamoeba sp. Gr. II C3 ATCC50739	Potable water reservoir	-
Acanthamoeba sp. Gr. II HLA	Keratitis patient	-
Naegleria sp. Nbeck	Aquarium	(+)[3]
Hartmannella vermiformis OS101	Hospital tap water	+++
SCGYE medium (axenic)[1]		
Naegleria gruberi CCAP:1518/1e	Unknown	-
Naegleria lovaniensis Aq/9/1/45D	Aquarium	-
Hartmannella vermiformis OS101	Hospital tap water	++

[1] Infection medium. [2] Intracellular replication of *W. chondrophila* was determined by microscopic inspection. [3] Intracellular bacteria were regularly lost after subculture of the host.

Table 2. Cocultivation of protozoa with *Waddlia chondrophila* isolated from *Hartmannella vermiformis* OS101.

Host protozoa	Source	Intracellular replication[1]
Acanthamoeba sp. Gr. II C$_3$ ATCC50739	Water reservoir	-
Acanthamoeba lenticulata Gr. III 89	Nasal mucosa	-
Acanthamoeba lenticulata Gr. III 45, ATCC50703	Nasal mucosa	-
Acanthamoeba lenticulata Gr.III 72, ATCC50704	Nasal mucosa	-
Acanthamoeba sp., Gr. II HLA	Keratitis patient	+++
Acanthamoeba comandoni Gr. I Pb30/40	Greenhouse	-
Naegleria gruberi CCAP:1518/1e	Unknown	+[2]
Naegleria gruberi Nbeck	Aquarium	-
Naegleria lovaniensis Aq/9/1/45D	Aquarium	-
Vahlkampfia ovis Rhodos	Puddle/Rhodos	+++[3]
Willaertia magna A1,2PbFl2	Greenhouse	-
Willaertia magna NI4Cl1	Pond/India	-
Hartmannella vermiformis OS 101	Hospital water	+++
Hartmannella vermiformis C3/8	Water reservoir	+++
Echinamoeba sp. PVC/Mühlh.	Potable water	-
Vannella miroides DentG1	Dental unit	-
Comandonia operculata WBT	Water reservoir	-
Balamuthia mandrillaris CDC:Vo39	*Papio sphinx*	-
Hyperamoeba-like amoeboflagellate B1,2-100PE	Water reservoir	+++
Dictyostelium discoideum Berg 25	Nasal mucosa	+[2]
Dictyostelium discoideum Sö-P2	Soil, Würzburg	+++

[1] Intracellular replication of *W. chondrophila* was determined by microscopic inspection. [2] Intracellular bacteria were regularly lost after subculture of the host. [3] Infected cultures were able to produce cysts.

taneously. The highly condensed coccoid stages (approximately 0.4 µm) were identified as elementary bodies (Fig. 2). The thin walled particles (approximately 0.6 µm) some of which show binary fission were identified as reticulate stages. These results show that *W. chondrophila* can infect and develop within *H. vermiformis*.

Infection of different protozoa species by *Hartmannella*-adapted *Waddlia*. In order to determine the host range of *Waddlia*, 21 different protozoan
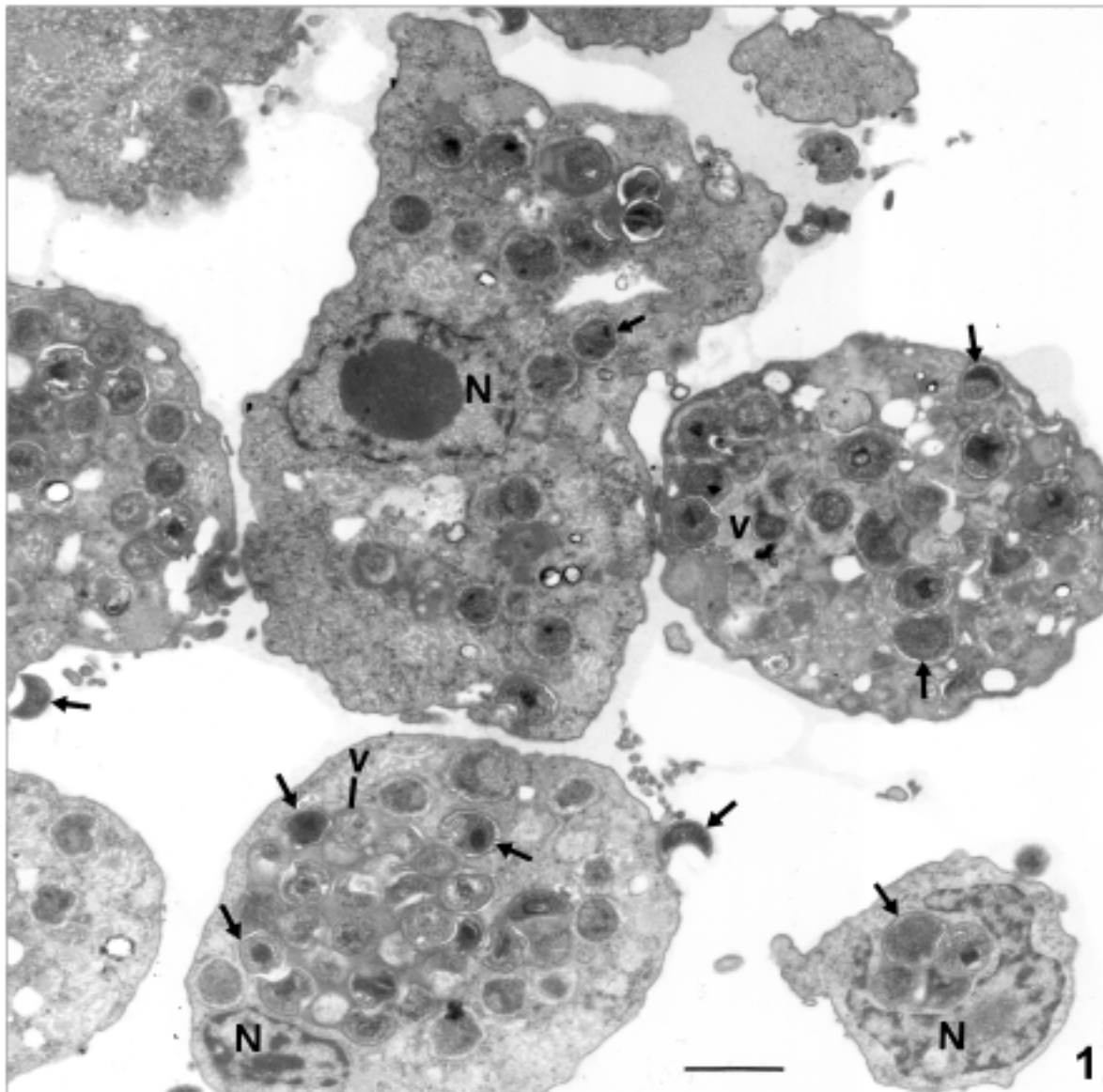
Fig. 1. Transmission electron micrograph of intracellular *Waddlia chondrophila* 2032/99 within *Hartmannella vermiformis* OS101. The protozoan trophozoites harbour numerous coccoid endocytobionts (arrows). The bacteria are located either within the cytoplasm or within vacuoles (v). N - nucleus of the host amoeba. Scale bar 1.0 µm.

species belonging to the genera *Acanthamoeba*, *Naegleria*, *Hartmannella*, *Vahlkampfia*, *Willaertia*, *Echinamoeba*, *Vannella*, *Comandonia*, *Balamuthia*, the *Hyperamoeba*-like amoeba and *Dictyostelium* were tested in cocultivation assays. The bacterial inoculum was prepared after the cultivation of *Waddlia* in *H. vermiformis*. After five transfers of infected hartmannellae into fresh axenic medium the trophozoites were submitted to freeze-thawing and subsequent filtering through a millipore filter. The filtrate with *Hartmannella*-adapted endocytobionts was then added

to the different protozoan species on NN-agar. The successful infection of *H. vermiformis* strain OS101 was used as positive control.

Daily monitoring by microscopy showed that *Acanthamoeba* sp. Gr. II, HLA, *V. ovis* Rhodos, *H. vermiformis* C3/8, the *Hyperamoeba*-like amoeba, and *D. discoideum* Sö-P2 harboured numerous replicating *Waddlia* endocytobionts (Table 2). The infection by endocytobionts resulted in the inhibition of cyst formation in the free-living amoebae and fruiting body development in *Dictyostelium*, respectively. The only exception was
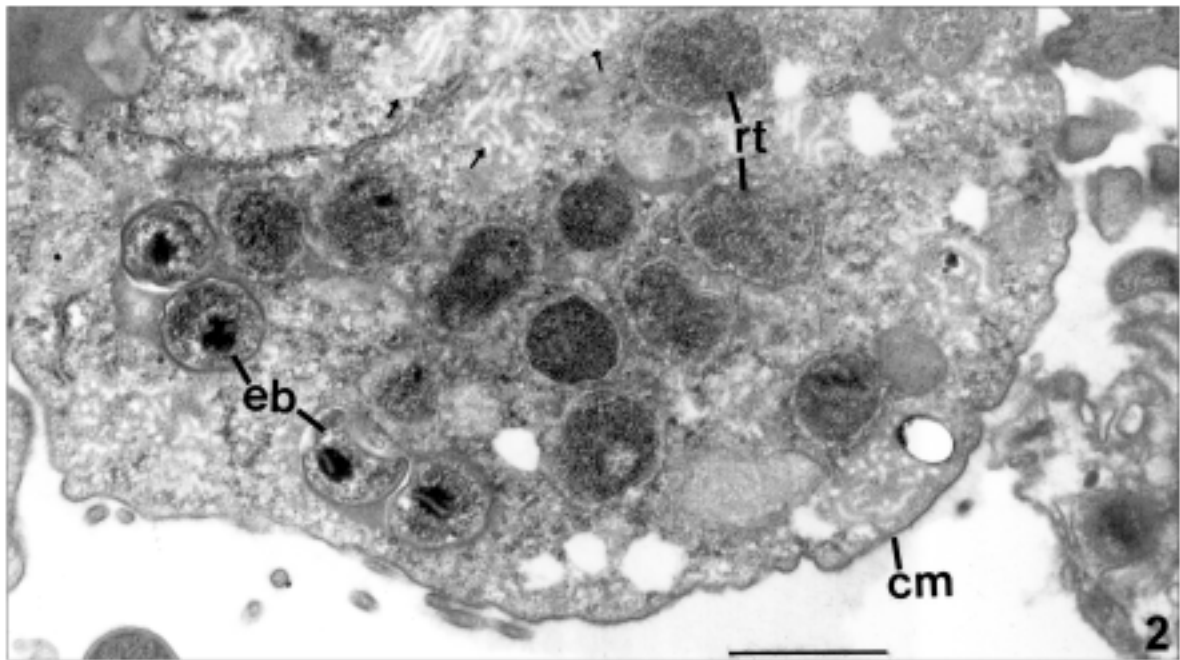
Fig. 2. Transmission electron micrograph of intracellular *Waddlia chondrophila* 2032/99 within *Hartmannella vermiformis* OS101. The detail of a sectioned *Hartmannella trophozoite* shows the differentiation of the endocytobiont into reticulate stages (rt) and elementary bodies (eb). Arrows indicate mitochondria. Cm - cell membrane of the trophozoite. Scale bar 1.0 µm.

found with *V. ovis* since infected cultures of this host were still able to differentiate into regular cysts. Very weak and transitory infections were observed with *N. gruberi* CCAP and *D. discoideum* Berg 25. Interestingly, a heavy infection was observed with *Acanthamoeba* sp. Gr. II HLA. This observation is remarkable since *Acanthamoeba* spp., Gr. II, HLA was originally resistant to infection by *Waddlia*. This result and the transitory infection of *N. gruberi* CCAP1518/1e suggest that the adaptation of *Waddlia* to *Hartmannella* results in a broader host spectrum of the endocytobiont.

DISCUSSION

Chlamydia-like endocytobionts are commonly observed in protozoa (Michel *et al.* 1994, Amann *et al.* 1997, Horn *et al.* 2000, Fritsche *et al.* 2000, Michel *et al.* 2001). The ability to grow intracellularly within protozoa could have preadapted these bacteria as pathogens of higher eukaryotes (Corsaro *et al.* 2002). Accordingly it is likely that protozoa may also represent a reservoir for the chlamydia-like bacterium *W. chondrophila*. In order to evaluate the amoebae host spectrum we transferred this obligate intracellular endocytobiont from BGM cells

into *H. vermiformis*. Detailed transmission electron microscopy of *Waddlia* infected *Hartmannella* cells revealed typical morphological stages of a *Chlamydia*-like life cycle, including the presence of elementary and reticulate bodies. The following coculture assays with 21 different protozoa species revealed that species of the genera *Acanthamoeba*, *Vahlkampfia*, *Hartmannella*, *Hyperamoeba* and *Dictyostelium* were able to support bacterial growth. The infected cells were killed and lysed by the replicating bacteria. However the amoebae generation time was obviously shorter than the period between infection and host cell lysis since infected cultures could easily be maintained.

The observed host range of *Waddlia* is unequally wider when compared to the *Chlamydia*-like *Hartmannella* endocytobiont *Neochlamydia hartmannellae* (Horn *et al.,* 2000). This previously analyzed strain was not able to propagate within closely related protozoa except the original host, two more *H. vermiformis* strains and *D. discoideum*. However, in contrast to *Waddlia*, which inhibited the formation of *Dictyostelium* fruiting bodies, *Neochlamydia* did not interfere with the underlying differentiation processes.

An interesting finding of this study was that *Hartmannella*-adapted *Waddlia* exhibited a broader

host range when compared to the BGM cell isolate. This suggests that *Waddlia* possesses an adaptive potential to broaden its host range. The aggressive behaviour of the endocytobionts within the tested protozoa and the ability to prevent cyst formation also strengthen the view of a limited evolutionary specialization of *Waddlia*. Another possible hypothesis is that *Waddlia* survives within a yet unrecognized reservoir. The best-adapted host identified so far appears to be *V. ovis*. This host exhibited high intracellular bacterial numbers and infected cells maintained their ability to differentiate into cysts.

Many protozoa are not very selective with respect to the uptake of bacteria (Görtz and Michel 2003). In evolutionary time frames this behaviour may help environmental bacteria to overcome host specificities. We therefore must be aware that the adaptation of environmental bacteria to certain protozoa species may generate new pathogens. This speculation is supported by the observation that the respiratory pathogens *Chlamydia pneumoniae* and *Simkania negevensis* multiply within *Acanthamoeba* under laboratory conditions (Essig *et al.* 1997, Kahane *et al.* 2001). Since *Waddlia* was isolated from an aborted bovine fetus but also multiplies within protozoa it is conceivable that this microbe also falls into the group of environmentally preadapted pathogens.

REFERENCES

Amann R. Springer N., Schönhuber W., Ludwig W., Schmid E. N., Müller K.-D., Michel R. (1997) obligate intracellular bacterial parasites of acanthamoebae related to *Chlamydia* spp. *Appl. Environ Microbiol.* **63:** 115-121

Corsaro D., Venditti D., Valassina M. (2002) New chlamydial lineages from freshwater samples. *Microbiology* **148:** 343-344

De Jonckheere J. F. (1977) Use of an axenic medium for differentiation between pathogenic an non-pathogenic *Naegleria fowleri* isolates. *Appl. Environ. Microbiol.* **33:** 751-757

Dilbeck P. M., Evermann J. F., Crawford T .B., Ward A. C. S., Leathers C. W., Holland C. J., Mebus C. A., Logan L. L., Rurangirwa F. R., McGuire T.C. (1990) Isolation of a previously undescribed rickettsia from an aborted fetus. *J. Clin. Microbiol.* **28:** 814-816

Essig A., Heinemann M., Simnacher U., Marre R. (1997) Infection of *Acanthamoeba castellanii* by *Chlamydia pneumoniae. Appl. Environ. Microbiol.* **63:** 1396-1399

Everett K. D., Bush R. M., Andersen A. A. (1999) Emended description of the order Chlamydiales, proposal of Parachlamydiaceae fam. nov. and Simkaniaceae fam. nov., each containing one monotypic genus, revised taxonomy of the family Chlamydiaceae, including a new genus and five new species, and standards for the identification of organisms. *Int. J. Syst. Bacteriol.* **49:** 415-440

Fritsche T. R., Gautom R. K., Seyedirashti S., Bergeron D. L., Lindquist T. D. (1993). Occurrence of bacteria endosymbionts in Acanthamoeba spp. isolated from corneal and environmental specimens and contact lenses. *J. Clin. Microbiol.* **31:** 1122-1126

Fritsche T. R., Sobek D., Gautom R. K. (1998) Enhancement of the *in vitro* cytopathogenicity by *Acanthamoeba* spp. following acquisition of bacterial endosymbionts. *FEMS Microbiol. Lett.* **166:** 231-236

Fritsche T. R., Horn M., Wagner M., Herwig R. P., Schleifer K.-H., Gautom R. K. (2000) Phylogenetic diversity among geographically dispersed Chlamydiales endosymbionts recovered from clinical and environmental isolates of *Acanthamoeba* spp. *Appl. Environ. Microbiol.* **66:** 2613-2619

Giménez D. F. (1964). Staining rickettsiae in yolk sac cultures. *Stain Technol.* **39:** 135-140

Görtz H.-D., Michel R. (2003) Bacterial Symbionts of Protozoa in Aqueous Environments - Potential Pathogens? In: Emerging Pathogens, Oxford Biology

Henning K., Schares G., Granzow H., Polster U., Hartmann M., Hotzel H., Sachse K., Peters M., Rauser, M. (2002) *Neospora caninum* and *Waddlia chondrophila* strain 2032/99 in a septic stillborn calf. *Vet. Microbiol.* **85:** 285-292

Horn M., Wagner M., Müller K.-D., Schmid E. N., Fritsche T. R., Schleifer K.-H., Michel R. (2000) *Neochlamydia hartmannellae* gen. nov., sp. nov. (*Parachlamydiaceae*), an endoparasite of the amoeba *Hartmannella vermiformis. Microbiology* **146:** 1231-1239

Kahane S., Dvoskin B., Mathias M., Friedmann M. G. (2001) Infection of *Acanthamoeba polyphaga* with *Simkania negevensis* and *S. negevensis* survival within amoebal cysts. *Appl. Environ. Microbiol.* **67:** 4789-4795

Michel R., Hauröder-Philippczyk B., Müller K.-D., Weishaar I. (1994) *Acanthamoeba* from human nasal mucosa infected with an obligate intracellular parasite. *Europ. J. Protistol.* **30:** 104-110

Michel R., Henning K. Steinert M., Hauroeder B., Hoffman R., Zoeller L. (2001) Cocultivation of free-living amoebae and the first European isolate of *Waddlia chondrophila* (Chlamydiales). X International Congress of Protozoology-ICOP, Salzburg, Austria, July 15-19

Page F. C. (1988) A New Key to Freshwater and Soil Gymnamoebae. Freshwater Biological Association, Ambleside

Poppert S., Essig A., Marre R., Wagner M., Horn M. (2002) Detection and differentiation of *Chlamydiae* by fluorescence in situ hybridization. *Appl. Environ. Microbiol.* **68:** 4081-4089

Rurangirwa F. R., Dilbeck P. M., Crawford T. B., McGuire T. C., McElwain T. F. (1999) Analysis of the 16S rRNA gene of microorganism WSU 86-1044 from an aborted foetus reveals that it is a member of the order Chlamydiales: Proposal of Waddliaceae fam. nov., *Waddlia chondrophila* gen. nov., sp. nov. *Int. J. Syst. Bacteriol.* **49:** 577-581

Stephens R. S. (ed.). (1999) Chlamydia: Intracellular Biology, Pathogenesis, and Immunity. American Society for Microbiology, Washington, D. C.

ACTA PROTOZOOLOGICA

Morphometric and Cladistic Analyses Of The Phylogeny of *Macropodinium* (Ciliophora: Litostomatea: Macropodiniidae)

Stephen L. CAMERON[1,2] and Peter J. O'DONOGHUE[1]

[1]Department of Microbiology and Parasitology, The University of Queensland, Brisbane, 4072, Australia; [2]Department of Integrated Biology, Brigham Young University, Provo, Utah, United States of America.

Summary. Phylogenetic studies of the genus *Macropodinium* were conducted using two methods; phenetics and cladistics. The phenetic study of morphometrics suggested that the genus could be divided into 3 groups attributable mostly to cell size and shape. The cladistic study also split the genus into 3 groups related to cell size but groups were further distinguished by patterns of ornamentation. Reconciliation of both approaches revealed considerable congruence, however, it also suggested the existence of convergences in the phenetic study and a lack of resolution in the cladistic study. The morphological diversity of *Macropodinium* is probably due to evolutionary trends such as increasing body size, allometry and polymerisation of structures. None of these trends, however, was uniformly directional and differential effects were observed in different regions of the phylogenetic tree. Comparison of the phylogeny of *Macropodinium* to a consensus phylogeny of the macropodids revealed limited incongruence between the 2 trees. The ciliate groups could be related to 2 host groups; the wallaby genera and the kangaroo and wallaroo subgenera. The association with these host groups may be the result of phyletic codescent, ecological resource tracking or a combination of both. Further studies of both host and ciliate phylogeny are necessary to resolve these effects.

Key words: Ciliophora, cladistic analysis, endosymbionts, phylogeny, *Macropodinium, Megavestibulum*.

INTRODUCTION

The Macropodiniidae are endosymbiotic ciliates which inhabit the enlarged, fermentative forestomachs of macropodid marsupials (kangaroos and wallabies) (Dehority 1996; Cameron *et al.*, 2001, 2002; Cameron and O'Donoghue 2002, 2003a). Two genera have been described: *Macropodinium* Dehority, 1996 with 13 species; and *Megavestibulum* Cameron *et* O'Donoghue, 2003 with 2 species. Of the two genera *Megavestibulum*

is clearly more plesiomorphic and grossly similar to other trichostome ciliates inhabiting the macropodid stomach, such as the amylovoracids or polycostids (Cameron and O'Donoghue 2003a). In contrast, *Macropodinium* species have a highly derived and variable morphology which made species diagnosis easy and suggested the possibility of studying the evolution of the genus by phylogenetic studies. The aim of this study was therefore to elucidate the phylogeny of the genus *Macropodinium* using continuous morphometric characters in a phenetic analysis and discrete cell features in a cladistic analysis and to use the resultant phylogenies to investigate character trends within the genus and the evolution of host relationships.

Address for correspondence: Stephen L. Cameron, Department of Integrated Biology, 401 WIDB, Brigham Young University, Provo, UT, 84602, U. S. A.; Fax: (800) 422 0090; E-mail: slc236@email.byu.edu

MATERIALS AND METHODS

For full details of collection, preservation and staining methods see Cameron *et al*. (2001, 2002). Terminology used throughout is that of Cameron *et al*. (2002).

Morphometric analyses. A morphometric analysis of 10 standardised linear measurements [cell length, cell width, macronucleus length, macronucleus width, vestibulum width, vestibulum depth, cytostome width, ventral bar (VB) width, dorsal bar (DB) width, width between longitudinal grooves] and 2 count variables (number of longitudinal grooves left and right) was conducted to assess phenetic distinctiveness within *Macropodinium* (see Fig. 1 for definitions). Species which lacked either VB or DB were scored as having a width of 0 for this feature. The measurements of individual cells used to generate summary morphometric statistics in our previous papers (Cameron *et al*. 2001, 2002) were used again in this study. Only individual cells from which all linear measurements could be obtained were used in this study. The 12 *Macropodinium* species described or redescribed in Cameron *et al*. (2001, 2002) were used: *M. setonixium*, *M. titan*, *M. petrogale*, *M. ocallaghani*, *M. yalanbense*, *M. ennuensis*, *M. moiri*, *M. hallae*, *M. marai*, *M. bicolor*, *M. tricresta* and *M. spinosus*. *M. baldense* Dehority, 1996, was the only species in the genus omitted due to a lack of appropriately stained specimens. Within-species variation was assessed by inclusion of the 3 host groups of *M. yalanbense* (eastern-grey kangaroo, EG; western-grey kangaroo, WG; and Kangaroo Is. grey kangaroo, KI) and the two forms of *M. ennuensis* (forma *ennuensis* and *dentis*). Discriminant analysis was performed to determine the morphometric distinctiveness of each species or subspecies group. Cluster observations were then performed to determine the phenetic similarity of each species or subspecific group. Multivariate statistics were performed using the software package Minitab® ver. 11 (1996).

Morphological cladistics. The thirteen species of *Macropodinium* were examined by light and electron microscopy and a matrix of 21 characters developed (Table 2). A generalised *Megavestibulum* sp. was used as an outgroup and characters which did not occur in *Megavestibulum* were coded as a separate character state "not applicable"; otherwise character polarity was determined relative to *Megavestibulum*. Characters for which the character state could not be determined were coded as '?'. Taxa with multistate characters were scored as possessing both character states. The list of characters and their transformations are listed in Appendix 1. Characters sets were coded as either unordered or ordered and duplicate analyses performed in PAUP 4.0b10 (Swofford 2002) and character state changes assigned to nodes by MacClade ver4 (Maddison and Maddison 2000).

RESULTS

Multivariate analysis using cluster observations yielded 9 discrete groups. Of the 15 taxa included, only 3 (*M. tricresta*, *M. titan*, *M. moiri*) formed monophenetic groups. The remaining species appeared intermingled in the dendrogram and did not form distinct clusters (not shown). For this reason, a discriminant analysis of the

data set was performed to determine the distinctiveness of each taxon. Discriminant analysis compares *a priori* defined groups, in this case the species or subspecific groups, against the groupings supported by the morphometric data. The results of the discriminant analysis are presented in Table 1. In this analysis, 9 of the 12 species were found to be distinct and supported by all specimens assigned to that species. *M. marai*, *M. hallae* and *M. ocallaghani* each had a single specimen which appeared to be aberrant and be more similar to members of another group, *M. setonixium*, *M. petrogale* and *M. yalanbense* KI respectively. The *M. ennuensis* forms, despite slight overlap in the cluster observation, were found to be completely distinct in the discriminant analysis. In contrast, the three host groups of *M. yalanbense* were highly overlapping in the cluster observations and indistinct in the discriminant analysis. The cluster observation suggested that the genus has three broad groups: group 1 comprising *M. titan* and *M. moiri*; group 2 comprising *M. setonixum*, *M. marai*, *M. bicolor*, *M. hallae* and *M. tricresta*; and group 3 comprising *M. ennuensis*, *M. ocallaghani*,
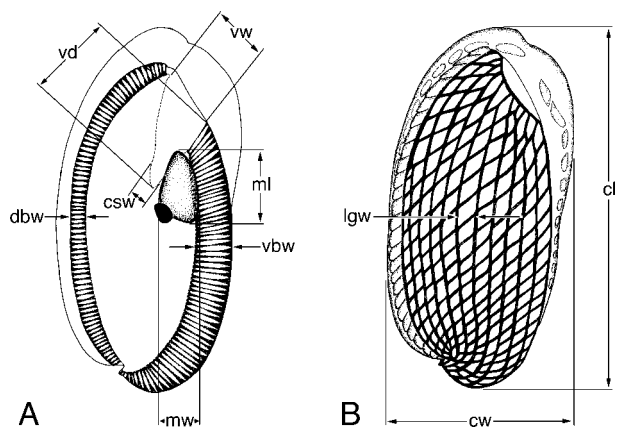

Fig. 1. Diagram of measurements. **A** - internal cell features. **B** - external cell features. cl - cell length, csw - cytostome width, cw - cell width, dbw - dorsal bar width, lgw - lateral groove width, ml - macronucleus length, mw - macronucleus width, vbw - ventral bar width, vd - vestibulum depth, vw - vestibulum width.
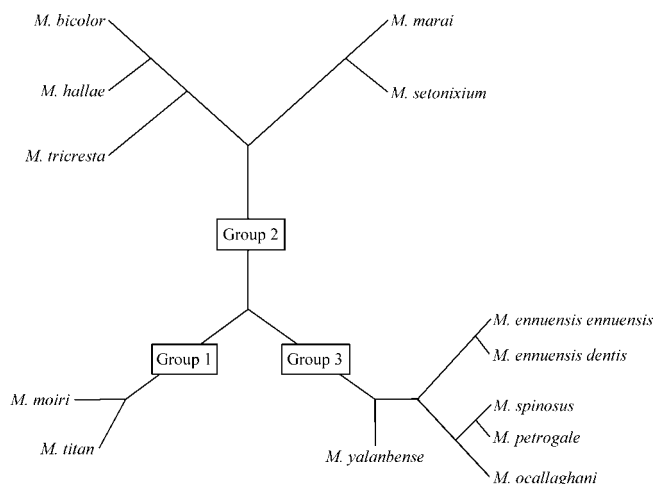
M. petrogale, *M. spinosus* and *M. yalanbense*. There are also strong phenetic associations between taxa within these groups. The unrooted network of phenetic relationships suggested by the morphometric analysis is presented in Fig. 2.

The results of both cladistic analyses are presented in Fig. 3 (ordered data set) and Fig. 4 (unordered data set).

Table 1. Summary of classifications suggested by discriminant analysis of *Macropodidium* morphometric data.

Group	Suggested group	1	2	3	4	5	6	7	8	9	10	11	12	13	14	15
1	*M. petrogale*	12														
2	*M. titan*		3													
3	*M. spinosus*			22												
4	*M. tricresta*				28											
5	*M. marai*					14										
6	*M. yal.* EG						25	3	1							
7	*M. yal.* KI						1	21	6					1		
8	*M. yal.* WG						3	5	20							
9	*M. enn. dentis*									20						
10	*M. enn. ennuensis*										20					
11	*M. bicolor*											10				
12	*M. hallae*												9			
13	*M. ocallaghani*													28		
14	*M. moiri*														18	
15	*M. setonixium*					1										15
Total		12	3	22	28	15	30	30	27	20	20	10	10	30	18	15
Nº. Correct		12	3	22	28	14	25	21	20	20	20	10	9	29	18	15

Heuristic analysis of the ordered data set yielded 6 equally parsimonious trees, 69 steps long, CI = 0.522, RI = 0.593 and RC = 0.309. The analysis of the unordered data set yielded 7 equally parsimonious trees with a length of 61 steps, CI = 0.590, RI = 0.615 and RC = 0.363. The unordered tree is significantly less structured than the ordered tree with a large basal polytomy within the genus and only recovering 2 clades which were both in common with the ordered consensus

Table 2. Character matrix - *Macropodinium* (*M.*) morphology.

	5	10	15	20	
Megavestibulum	00000	00000	00000	00000	0
M. setonixium	01000	12101	12210	10000	1
M. marai	01001	11202	22210	01000	1
M. tricresta	12111	11112	22111	11001	2/3
M. spinosus	12011	12212	22111	01000	2
M. bicolor	02021	12211	22211	01100	2/3
M. hallae	21001	12112	22210	10000	1
M. ocallaghani	22011	11111	11100	00000	0
M. petrogale	01111	12211	12100	00000	0
M. yalanbense	22011	21111	11100	00010	0
M. ennuensis	21111	21111	21200	00000	0
M. moiri	02311	11212	22210	00010	1
M. baldense	210?1	111?2	22210	10000	3
M. titan	02201	13101	21200	00110	0

Fig. 2. Phenetic cluster diagram based on morphometric similarity.

tree clade 6 (*M. ocallaghani* + *M. yalanbense* + *M. ennuensis*) and clade 4 (*M. bicolor* + *M. tricresta* + *M. spinosus*).

DISCUSSION

Both methods used to analyse the phylogeny of *Macropodinium* in this study have methodological concerns which affect the conclusions that can be drawn.
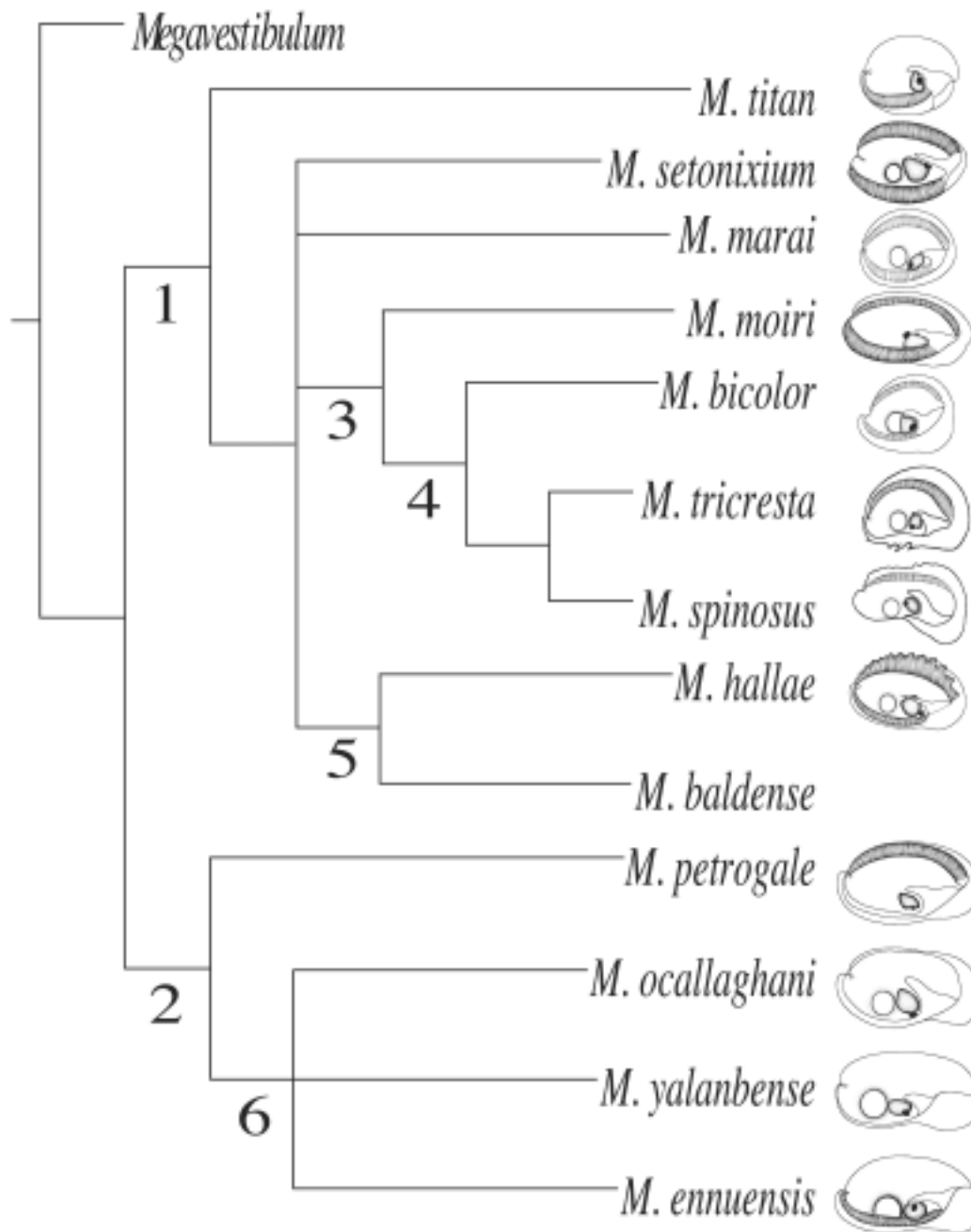
Fig. 3. Cladistic analysis, ordered data set. Numbers indicate clades of interest. Figures are internal right side views of each species except *M. baldense* and are not drawn to scale.

Cluster observation is a phenetic method of analysing morphometric data. Phenetic methods cannot be used to directly infer phylogenies because they group taxa based on total similarities between them. It is insensitive to the differences between shared derived features (synapomorphies) and shared primitive features (sympleisomorphies). For this reason, cladistic methods are more applicable to discrete data sets, and phenetic methods for continuous data sets such as morphometrics. The resultant dendrogram thus cannot be interpreted as
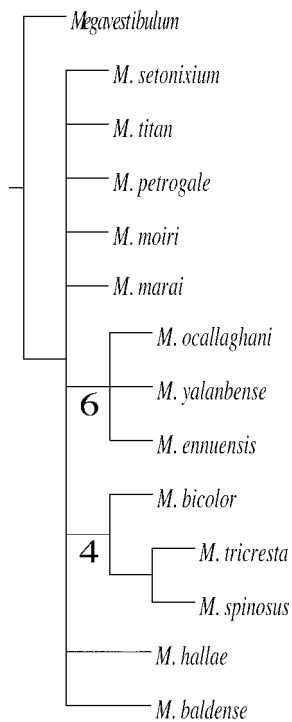
Fig. 4. Cladistic analysis, unordered data set. Numbers indicate clades shared with Fig. 3.

Fig. 5. Co-phylogenetic comparison of *Macropodinium* species (right hand tree) and macropodid hosts (left hand tree). Lines linking taxa represent host/parasite relationships. Macropodid phylogeny redrawn after Flannery (1989).

indicative of phylogenetic relationships between the specimens included (and therefore is omitted). If the dendrogram was read in a directly phylogenetic context, the considerable intermingling between the clusters would suggest that few of the *Macropodinium* species are monophyletic. This is not the case as demonstrated by the discriminant analysis in which the distinctiveness of each of the species was well supported despite a few outlying specimens which resembled other species.

The cluster observation result can be used to produce a network of phenetic similarities (Fig. 2). The groups within this network correspond to broadly similar morphotypes. Group 1 (*M. moiri*, *M. titan*) is composed of the largest species within the genus and may be an artefactual grouping based mostly on the extremely large size of the individual cells in these two species. Group 2 (*M. setonixium*, *M. marai*, *M. tricresta*, *M. hallae*, *M. bicolor*) is composed of species broadly oval in outline with prominent ventral and dorsal bars. Group 3 (*M. yalanbense*, *M. ennuensis*, *M. ocallaghani*, *M. petrogale*, *M. spinosus*) is composed of elongate species, most of which lack or have short ventral and dorsal bars and have large vestibular openings. The lack
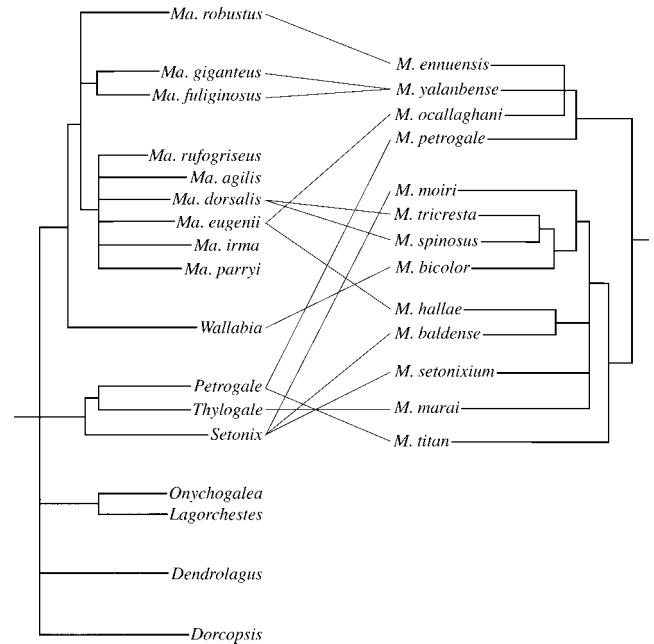
of solid resolution within the dendrogram precludes making conclusions on branching orders within the groups.

One of the tenets of Darwinian evolution is gradualism; species diverge from each other slowly in response to directional selection within the environment (Patterson 1978). Darwinian gradualism is well demonstrated in comparisons of body form between closely related taxa such as this morphometric analysis of the genus *Macropodinium*. It is common to see both the trends observed in this study. First, closely related species overlap in body form; only 3 of the 12 species did not overlap with any other species in the analysis. Secondly, internal groups can be related to particular correlated characters e.g. the 3 superspecific groups identified above. Morphometric analysis of *Macropodinium* suggests the diversity of body form within the genus may be the result of Darwinian gradualism. The closely related species have been diverging for a shorter period and so still overlap in morphospace (MacLeod 1999). It is also equally possible that the observed pattern is the result of morphological convergences. The weakness of phenetic methods, such as cluster observations, is that they are unable to indicate which effect best explains the data.

Analysis of the two cladistic datasets (ordered *vs.* unordered) differed mostly in the degree of resolution recovered, the unordered dataset resulting in a significantly less structured tree. There are however similarities in the clades which are recovered in each tree, the only clades recovered by the unordered analysis (clades 4 and 6) are also recovered by the ordered analysis. This suggests that these relationships are insensitive to data manipulation but the other proposed relationships described in Fig. 3 need further exploration. The use of *Megavestibulum* as an outgroup is less than ideal due to the absence of many of the characters used in this analysis from this genus. Five of the 21 characters are coded as not applicable or absent in *Megavestibulum* while all *Macropodinium* species possess that character. While coding of this type reduces signal within a data set, as the comparison to outgroup taxa has no resolving power within the ingroup (Strong and Lipscomb 1999), it is superior to either of the 2 alternatives. A hypothetical taxon in which all character states are set to 0 could be used. In this case, character polarity is subjective and the resolving power of comparison to an outgroup absent. The risk of circularity in such an approach is very high. Secondly, species within the ingroup could be used arbitrarily as outgroups. In the absence of some phylogenetic information this is entirely subjective. Small, simple species are often chosen as most evolutionary patterns proceed from small and simple to large and complex, but what if that is not the case? These analyses indicate that both very small and large *Macropodinium* species, *M. petrogale* and *M. titan*, are early branching within the two major clades within the genus. Use of either would significantly alter the result as they are virtually diametric opposites; *M. petrogale* is small and simple whereas *M. titan* is large and complex. Arbitrary choice of outgroup is thus almost certain to bias a phylogenetic analysis. Despite its faults, *Megavestibulum* is the best outgroup available at this time. The most notable feature of the ordered analysis (Fig. 3) is the suggestion of a 2 sub-groups within the genus which broadly correspond to general morphological types and host occurrence. Node 1 is composed of ornamented with marginal spines or crenullations which have small oral apertures and cover the range of cell sizes for the genus. Node 2 is composed of medium sized elongate species, totally lacking in marginal ornamentation which have large oral apertures.

Both the cladistic and cluster observation methods suggested that the genus *Macropodinium* could be divided into species groups on the basis on their morphology. Phenetic clustering suggested groups which corresponded strongly to cell size and shape whereas the cladistic analysis suggested groups which corresponded to cell ornamentation and size. There was considerable overlap in the two studies; Node 1 corresponds to Group 1 plus Group 2 and Node 2 corresponds to Group 3. The only major difference is in the position of *M. spinosus* which is strongly supported as the sister group of *M. tricresta* in both cladistic analyses but falls well within Group 3 (= node 2) in the phenetic analysis. In both analyses, *M. titan* is a highly divergent species and its association with *M. moiri* in the phenetic cluster is loose and probably only due to the large size of both species rather than indicative of a close relationship.

The major difficulty confronting the use of morphological data in the inference of relationships between taxa is the potential existence of convergent evolution. Phenetic methods are particularly susceptible to convergence as the directionality of evolution (as implied in cladistics by the use of outgroups or character ordering) is omitted. The similarity of *M. spinosus* to *M. petrogale* and *M. ocallaghani* in the phenetic clusters is probably the result of convergent evolution; all 3 are small, elongate species. *M. spinosus*, however, shares many characters with *M. tricresta*, cell ornamentation, pellicular windows and possession of a DB but no VB. The cladistic analysis shows that the features shared with *M. tricresta* are derived features whereas those shared with *M. petrogale* and *M. ocallaghani* are either convergent or pleisiomorphic.

Lynn (1978) applied theories about evolutionary patterns within lineages to ciliates and identified 3 main patterns within colpodids: size increase, body allometry and polymerisation. The phylogeny of *Macropodinium* suggests that size increase has not been a universally directional force with the evolution of this genus. Two taxa are consistently basal within the 2 major clades of the genus, *M. petrogale* and *M. titan*, the former species is one of the smallest within the genus whereas *M. titan* is the largest. It is thus possible that the genus has either increased in size through evolutionary time (evolution from forms similar to *M. petrogale*) or decreased in size (evolution from forms similar to *M. titan*). Early branching taxa are not necessarily representative of the primitive forms within a group (Yeates 1995); early branching taxa can be very derived due to long periods of directional divergence. It is probable that *M. titan* is one such early branching, highly

derived taxon. Even within the *Macropodinium* groups, size direction has not been uniform. In Node 3, the earliest diverging species, *M. moiri*, is large whereas in Node 2, the basal taxon, *M. petrogale*, is the smallest in the node and in Node 4 there is no apparent size difference for any of the members. Because the factors favouring size increase in ciliates proposed by Lynn (1978) (predator avoidance, food acquisition and metabolic efficiency) are probably not acting uniformly across all the diverse ecological range of hosts of *Macropodinium* spp., a trend towards size increase is not apparent.

Body allometry is the evolutionary trend of differential growth rates of body parts relative to total body size. It has been demonstrated in ciliates for colpodids (Lynn 1978) and *Paramecium* spp. (Fokin and Chivilev 2000) and it is apparent in *Macropodinium*. Mouth size is proportionately larger in the Node 6 species relative to the remaining *Macropodinium* species. Polymerisation is a net increase in the number or complexity of a particular organelle through evolutionary time. Polymerisation was observed in relation to the number of longitudinal grooves (*M. titan* and the Node 3 species), presence and extent of marginal ornamentations (Node 1 species) and the dorso-ventral groove (*M. tricresta*). A special case of polymerisation is metamerism, the complete duplication of a complex structure and all its constituent parts. The evolution of *M. tricresta* from a species resembling *M. spinosus* is best explained as a case of serial metamerisation. The main difference between the two species is the presence of a second complete dorsal groove, complete with identical marginal ornamentation and somatic ciliary bands associated with each groove. Net increase in the diversity of form within *Macropodinium* can be related to all of the factors identified by Lynn (1978), however, none of these factors provides a strong unidirectional trend. The absence of such a trend is probably due to environmental heterogeneity (the species are spread across 9 host species with the full range of herbivorous diets and the entire Australian continent) which fails to produce unidirectional selective pressures.

A sophisticated array of computer programs and algorithms have been proposed to examine parasite phylogenies in relation to host phylogenies including Brooks parsimony (Brooks 1981), Treemap (Page 1994) and generalised parsimony methods (Ronquist 1995). All of these methods require accurate, resolved phylogenies of both parasite and host, prerequisites which are lacking

for both *Macropodinium* and the macropodids. For both host and ciliate, the phylogenetic trees have areas of uncertainty in the form of polytomies. For this reason, two phylogenies have simply been mapped together and linkages between the two indicated rather than use inappropriate computer models (Fig. 5). We compared the most resolved and robust phylogeny (the ordered cladistic analysis) against the most widely accepted phylogeny of the macropodids (Flannery 1989). There is poor concordance between the two phylogenies, however, patterns of host association are apparent. Node 1 species are all associated with wallabies, members of the genera *Setonix*, *Thylogale*, *Wallabia* and *Macropus* (*Notamacropus*). The wallabies are all small bodied (< 10 kg), mostly mixed foragers and rarely feed in mobs. Phylogenetically, the wallabies form a paraphyletic assemblage, are considered basal within the macropodids and have an early appearance in the fossil record (Archer 1984). Node 6 species are mostly associated with the kangaroos and wallaroos, *Macropus* (*Macropus*) and *Macropus* (*Osphranter*). The hosts are large bodied macropodids (>15 kg), selective grazers and often live in mobs. The exception is *M. ocallaghani* which is an obvious host switch probably facilitated by the usually close habitat ranges of *Ma. eugenii* (the tammar wallaby) and *Ma. fuliginosus fuliginosus* (Kangaroo Is. Grey Kangaroo) on Kangaroo Island, South Australia. The phylogenetic relationships of the two subgenera are unresolved as is their origin from one of the wallaby taxa (Kirsch *et al*. 1997, Burk *et al*. 1998). Interestingly the most basal branch of both clades 1 and 2, *M. titan* and *M. petrogale* respectively, are associated with rock-wallabies of the genus *Thylogale* a group which has been proposed as one of the more primitive macropodid groups (Flannery 1989) The associations of the ciliate groups with host groups are broadly consistent with phylogenetic branching order only because of the lack of resolution within the macropodid phylogeny. Additional resolution in both trees will greatly enhance our understanding of the phyletic associations of *Macropodinium* and its hosts.

A second possibility is that the association of ciliates with hosts is not the result of phylogenetic co-descent, but rather due to resource tracking. The diets of the wallaby genera are broadly similar; they are all classified as intermediate feeders (Langer 1988) and selectively consume browse and fresh graze. In contrast, both the kangaroos and wallaroos are specialist grazers which exclusively consume grasses both fresh and moderately

desiccated. The association of the ciliates with one host group or the other may be in response to these dietary differences. The host switching event evident in Node 6, *M. ocallaghani*, suggests that resource tracking, if any, is not absolute as the putative source host, *Ma. fuliginosus* is a grazer and the new host, *Ma. eugenii* is a browser. The observed pattern of host association is probably a product of 3 factors: deficiencies in the phylogenies of both host and ciliate; phylogentic codescent and ecological based host tracking.

The evolution of parasite species is currently considered to result from a balance between 4 factors: host switching; failure to colonise descendent host species; sympatric speciation (in relation to host species not necessarily habitat); and co-speciation (Paterson and Gray 1997). We have good evidence that all 4 factors contributed to the evolution of *Macropodinium* species. Host switching between macropodids and their ciliates definitely occurred with *Cycloposthium edentatum* (Cameron *et al.* 2000a) and is suggested by the 3 macropodiniid species associated with the quokka. The detection of the equid associated ciliate, *C. edentatum*, in the black-striped wallaby suggests two extreme positions on the possibility of ciliate host switching in macropodids. First, host switching may be quite easy as it was accomplished despite radical differences between hosts, transmission strategy and gut structures. Alternatively, host switching between similar hosts may be quite difficult due to competition with resident ciliates whereas host switching between diverse hosts (e.g. horse → wallaby) may have been favoured in this instance by unique factors (e.g. vacant niche, lack of competitors, specialised diet). In all probability, reality is somewhere between these two poles of "easy" and "hard" host switching.

Amongst endemic ciliate species, the 3 *Macropodinium* species from quokkas (*M. moiri*, *M. baldense* and *M. setonixium*) are widely divergent and none formed bigeminate pairs suggesting that at least 2 colonised this host as the result of host switching. *M. setonixium* was revealed as one of the earliest branching species and if the quokka is as primitive a macropodid as is presently believed (Archer 1984, Flannery 1989, Kirsch *et al.* 1997) then *M. setonixium* is likely to be the original species and *M. baldense* and *M. moiri* are the products of subsequent switches. The bigeminate pair *M. baldense* and *M. hallae* (Fig. 4 Node 5) suggests geographical host switching. Both hosts, the quokka and tammar wallaby respectively,

occur on the offshore islands of south-western Australia and were probably sympatric on areas of the continental shelf which were exposed during the Pleistocene ice ages when sea levels dropped (Frakes *et al.* 1987). Another case of geographical host switching appears to be the close phyletic association of *M. ocallaghani* and *M. yalanbense*. Their hosts, the tammar wallaby and western-grey kangaroo, occur sympatrically only on Kangaroo Island off South Australia. Examination of tammar wallabies from mainland sites, and additional offshore sites would aid our understanding of these host switching events including which are source, and which are sink, host species.

There are also examples of host speciations which have failed to result in ciliate speciation. Most extreme is the red-necked wallaby, *M. rufogriseus*, which lacks ciliates altogether in the wild, although it is a suitable host of ciliates in a captive situation (Cameron and O'Donoghue 2003b). Comparison with nematodes reveals that it has a depauperate fauna relative to other *Notamacropus* wallabies entirely lacking in *Cloacina* spp., the most speciose strongyloid genus (Spratt *et al.* 1991). It does seem that there is something "odd" in the development of this macropodid. The biogeographic history of the red-necked wallaby (see Littlejohn *et al.* 1993) provides no clue. Many other macropodid species lack a *Macropodinium* species symbiont. These absences do not conform to a phyletic pattern and thus it appears that failure to colonise descendent species or "missing the boat" (Paterson *et al.* 1999) was a relatively common event during the evolution of the contemporary Australian trichostome fauna.

A range of speciation responses have occurred in response to host vicariation events. *M. yalanbese* has apparently failed to speciate in response to the speciation of its hosts *Ma. giganteus* and *Ma. fuliginosus*, a bigeminate pair which diverged due to Pleistocene ice age separation of populations to the south eastern and south western fringes of the Australian continent respectively (Flannery 1989). There were no discriminating differences between populations of *M. yalanbense* recovered from either host or from the 2 subspecies of *Ma. fuliginosus*. A similar pattern was found with the other trichostomes found in these hosts, *Amylovorax dehorityi* and *Bitricha oblata* (Cameron *et al.* 2000b). In contrast, *M. ennuensis* associated with the wallaroo, *Ma. robustus*, appears to have diverged more despite less conspicuous host divergence. Two distinct forms of *M. ennuensis* (forma *ennuensis* and forma *dentis*)

were found in the western and eastern subspecies (*Ma. r. erubescens* and *Ma. r. robustus* respectively). Divergence between these two forms of *M. ennuensis* is modest in comparison to the differences found between *Macropodinium* species (Cameron *et al.* 2001, 2002) however they were found to be completely distinct by discriminant analysis (Table 1). *Ma. robustus* is more xerically adapted than either *Ma. giganteus* or *Ma. fuliginosus* (Strahan 1995) and so was probably less effected by ice age expansions of Australia's central deserts. *M. ennuensis* appears to match the divergence of it's host in that there is modest differentiation but apparent failure to speciate.

Speciation in the absence of host speciation (sympatric parasite speciation) appears to have occurred in the case of *M. tricresta* and *M. spinosus*. Combes and Théron (2000) outlined a process by which sympatric speciation could occur within a host species by aggregation within different organs to ensure breeding success. This would result in strengthening organ specificity and eventual speciation. We have no evidence of habitat segregation for any species of trichostome ciliate. Furthermore, Combes and Théron's (2000) scheme is most applicable to parasites which use short range pheromones to attract mates. There is some evidence that pheromones are used as mate recognition factors in ciliate conjugation (Dini and Luporini 1985), however, in the absence of compartmentalisation of the macropodid stomach such aggregation based speciation appears unlikely. A second method compatible with sympatric speciation is the so-called 'instant chromosomal evolution' (Eldridge and Close 1993). Under this process, chromosome duplications or fusions can instantly create differences in ploidy such that the homologous pairs cannot join and fertilisation fails; sexual isolation is thus instantaneous. However, conjugation does not involve the joining of homologous chromosomal pairs thus changes in chromosome number should have no effect on conjugation success. Instead changes to the genes responsible for conjugation compatibility could result in instantaneous speciation within ciliates; asexual reproduction would increase the population size necessary to sustain the new species.

The accepted method of parasite speciation is, as with most animals, allopatric speciation; small populations of hosts become isolated from their conspecifics and because of their shorter generation times the parasites have greater capacity to speciate than their hosts. Subsequent shifts which remove the isolation reincorpo-

rate a new parasite species into the larger host population (Inglis 1971). Parasite speciation can thus appear to be sympatric when the actual process was allopatric. The differences in generation time should result in larger numbers of parasite species than host species; this method was suggested by Beveridge and Spratt (1996) as responsible for a large proportion of nematode speciations in macropodid stomachs and the excess of nematode species relative to host species. The biogeographical history of *Ma. dorsalis* has not been studied extensively but its present restriction to thick hill scrub (Strahan 1995) suggests that it would have been sensitive to habitat changes during the Pleistocene. Ice age desertification would most likely have split the habitat range into isolated montane scrublands along the spine of the Great Dividing Range separated by xeric grasslands. There would have been ample opportunities for a small population to become isolated and speciation of ciliates to result. *M. tricresta* is probably derived from an ancestor morphologically similar to *M. spinosus* by metamerism of the dorsal element of the DVG. The remaining changes are ones of scale; the cells are of similar size but *M. tricresta* is stouter, and the marginal ornamentations are similar but thicker in *M. tricresta*. A few basic changes in development could account for major morphological difference, the extracalary groove, and the remaining differences, size and spines, could be the result of random genetic drift. If this were true, the two putative species may still be conjugation intercompatible but have radically different forms.

The three examples presented show the range of possible outcomes of host isolation events on parasite evolution. Host vicariance may result in host speciation in the seeming absence of parasite speciation or even morphological divergence (e.g. *Ma. giganteus/ Ma. fuliginosus* and *M. yalanbense*). Secondly, host vicariance may result in host division into subspecific groups and increased morphological diversity within the parasite possibly to the extent of semicryptic speciation (e.g. *Ma. robustus* subspecies and the *M. ennuensis* forms). Finally, host vicariance may fail to result in host speciation but still result in parasite speciation (e.g. *Ma. dorsalis* and *M. tricresta/ M. spinosus*). This diversity of parasite response to host vicariance suggests that isolation is not a generalised force which will always favour parasite speciation at a faster rate than host speciation. The characteristics of the isolation must be taken into consideration. As has been found for animal and plant taxa "bottleneck effects" can significantly

increase the chances of speciation (Page and Holmes 1998); *M. tricresta*/ *M. spinosus* may be the result of just such an isolation of a small number of hosts. In contrast, continental scale vicariation events, such as occurred for *Ma. giganteus*/*Ma. fuliginosus* in the last ice age, may capture all of the parasite species' genetic diversity in both host populations and buffer against genetic drift. If isolation events do not result in net changes in habitat or diet of the host there will not be differential selective pressure acting on the two parasite populations. Speciation is thus limited to what can be achieved by random genetic drift alone. The period of isolation will determine the extent of genetic drift and thus speciation. As parasites and hosts respond to different components of the environment, different selective pressures can act independently on the two and generation time cannot be taken as directly indicative of speciation chance.

REFERENCES

Archer M. (1984) The Australian mammal radiation. In: Vertebrate Zoogeography and Evolution in Australasia (Eds. M. Archer and G. Clayton). Hesperian Press, Perth, WA, 633-808

Beveridge I., Spratt D. M. (1996) The helminth fauna of Australasian marsupials: origin and evolutionary biology. *Adv. Parasit.* **37:** 135-254

Brooks D. R. (1981) Hennig's parasitological methods: a proposed solution. *System. Zool.* **30:** 229-249

Burk A., Westerman M., Springer M. (1998) The phylogenetic position of the musky rat-kangaroo and the evolution of bipedal hopping in kangaroos (Macropodidae: Diprotodonta). *System. Zool.* **47:** 457-474

Cameron S. L., O'Donoghue P. J. (2002) The ultrastructure of *Macropodinium moiri* and revised diagnosis of the Macropodiniidae (Litostomatea: Trichostomatia). *Europ. J. Protistol.* **38:** 179-194

Cameron S. L., O'Donoghue, P.J. (2003a) Trichostome ciliates from Australian marsupials. III. *Megavestibulum* gen. nov. (Litostomatea: Macropodiniidae). *Europ. J. Protistol.* **39:** 123-138

Cameron S. L., O'Donoghue P. J. (2003b) Trichostome ciliates from Australian marsupials. IV. Distribution of the ciliate fauna. *Europ. J. Protistol.* **39:** 139-148

Cameron S. L., O'Donoghue P. J., Adlard R. D. (2000a) The first record of *Cycloposthium edentatum* Strelkow, 1928 from the black-striped wallaby, *Macropus dorsalis. Parasit. Res.* **86:** 158-162

Cameron S. L., O'Donoghue P. J., Adlard R. D. (2000b) Novel endosymbiotic ciliates (Vestibulifera: Isotrichidae) from Australian macropodid marsupials (Marsupialia: Macropodidae). *System. Zool.* **46:** 45-57

Cameron S. L., O'Donoghue P. J., Adlard R. D. (2001) Four new species of *Macropodinium* (Ciliophora: Litostomatea) from wallabies and pademelons. *J. Euk. Microbiol.* **48:** 542-555

Cameron S. L., O'Donoghue P. J., Adlard R. D. (2002) Species diversity within *Macropodinium* (Litostomatea: Trichostomatia): Endosymbiotic ciliates from Australian macropodid marsupials. *Mem. Queensland Museum* **48:** 27-47

Combes C., Théron A. (2000) Metazoan parasites and resource heterogeneity: constraints and benefits. *Int. J. Parasit.* **30:** 299-304

Dehority B. A. (1996) A new family of entodiniomorph protozoa from the marsupial forestomach, with descriptions of a new genus and five new species. *J. Euk. Microbiol* **43:** 285-295

Dini F., Luporini P. (1985) Mating-type polymorphic variation in *Euplotes minuta* (Ciliophora: Hypotrichida). *J. Protozool.* **32:** 111-117

Eldridge M., Close R. (1993) Radiation of chromosome shuffles. *Curr. Opinion Gen. Develop.* **3:** 915-922

Fokin S. I., Chivilev S. M. (2000) Brackish water *Paramecium* species and *Paramecium polycarum*. Morphometrical analysis and some biological peculiarities. *Acta Protozool.* **38:** 105-117

Flannery T. (1989) Phylogeny of the Macropodoidea: a study in convergence. In: Kangaroos, Wallabies and Rat-Kangaroos (Eds. G. Grigg, P. Jarman and I. Hume). Surrey Beatty and Sons, Chipping Norton, NSW, **1:** 1-46

Frakes L. A., McGowran B., Bowler J. M. (1987) Evolution of Australian environments. In: Fauna of Australia. General Articles (Eds. G. R. Dyne and D.W. Walton). Australian Government Publishing Services, Canberra, NSW, **1A:** 1-16

Inglis W. G. (1971) Speciation in parasitic nematodes. *Adv. Parasit.* **9:** 185-223

Kirsch J., Lapointe F., Springer M. (1997) DNA hybridisation studies of marsupials and their implications for metatherian classification. *Aust. J. Zool.* **45:** 211-280

Langer P. (1988) The Mammalian Herbivore Stomach: Comparative Anatomy, Function and Evolution. Gustav Fischer, Stuttgart, DU

Littlejohn M. J., Roberts J. D., Watson G. F., Davies M. (1993) Family Myobatrachidae. In: Fauna of Australia Amphibia and Reptilia (Eds. C. J. Glasby, G. J. B. Ross and P. L. Beesley). Australian Government Publishing Service, Canberra, ACT, **2A:** 41-57

Lynn D. H. (1978) Size increase and form allometry during evolution of ciliate species in the genera *Colpoda* and *Tillina* (Ciliophora: Colpodida). *BioSystems* **10:** 201-211

MacLeod N. (1999) Generalizing and extending the eigenshape method of shape space visualization and analysis. *Paleobiology* **25:** 107-138

Maddison W., Maddison D. (2000) MacClade ver 4. Sinauer Associates. Sunderland, MA

Minitab ver 11. (1996) MINITAB User's Guide: Data Analysis and Quality Tools. Minitab Inc, State College, PE

Page R. D. M. (1994) Maps between trees and cladistic analysis of historical associations among genes, organisms and areas. *System. Biol.* **43:** 58-77

Page R. D. M., Holmes E. (1998) Molecular Evolution: a Phylogenetic Approach. Blackwell Science, Oxford, UK

Patterson C. (1978) Evolution. Cornell University Press, Ithaca, NY

Paterson A. M., Gray R. D. (1997) Host-parasite cospeciation, host switching and missing the boat. In: Host-Parasite Evolution: General Principles and Avian Models (Eds. D. H. Clayton and J. Moore). Oxford University Press, Oxford, UK, 236-250

Paterson A. M., Palma R. L., Gray R. D. (1999) How frequently do avian lice miss the boat? Implications for coevolutionary studies. *System. Biol.* **48:** 214-223

Ronquist F. (1995) Reconstructing the history of host-parasite associations using generalized parsimony. *Cladistics* **11:** 73-89

Spratt D. M., Beveridge I., Walter E. L. (1991) A catalogue of Australasian monotremes and marsupials and their recorded helminth parasites. *Rec. South Austr. Mus. Monograph Series* **1:** 1-105

Strahan R. (1995) The Mammals of Australia. New Holland Publishers, Sydney, NSW

Strong E. E., Lipscomb D. (1999) Character coding and inapplicable data. *Cladistics* **15:** 363-371

Swofford D. L. (2002) PAUP*. Phylogenetic Analysis Using Parsimony (*and Other Methods). Version 4. Sinauer Associates, Sunderland, MA

Yeates D. K. (1995) Groundplans and exemplars: Paths to the tree of life. *Cladistics* **11:** 343-357

Appendix 1. Characters and their transformation states used to construct the character matrix used for morphological cladistics in Table 2. Character state transformations are optimized on the tree presented in Figure 4.

1. Body shape	0	Oval
	1	Wedge
	2	Reniform
2. Body symmetry	0	Not applicable
	1	Equal
	2	Unequal
3. Cell curvature	0	Absent
	1	Left anterior
	2	Left concave
	3	Left posterior ventral
4. Anterior window shape	0	Absent
	1	Single and strap-like
	2	Bilobed and triangular
5. Mouth orientation	0	Anterior
	1	Anterio-ventral
6. Mouth size	0	Not applicable
	1	Limited
	2	Entire
7. Longitudinal groove numbers	0	Absent
	1	Equal numbers right and left
	2	More left than right
	3	More right than left
8. Cytoproct shape	0	Hole
	1	Slot
	2	Cup
9. Preoral cilia	0	Absent
	1	Present
10. DVG depth dorsal	0	Absent
	1	Shallow
	2	Deep
11. DVG depth ventral	0	Absent
	1	Shallow
	2	Deep
12. Dorsal bars	0	Not applicable
	1	Absent
	2	Present
13. Ventral bars	0	Not applicable
	1	Absent
	2	Present
14. Ornamentations right dorsal	0	Absent
	1	Present
15. Ornamentations left dorsal	0	Absent
	1	Present
16. Ornamentations right ventral	0	Absent
	1	Present
17. Ornamentations left ventral	0	Absent
	1	Present
18. Tail bulge	0	Absent
	1	Present
19. Posterior spine	0	Absent
	1	Present
20. Intercalary row	0	Absent
	1	Present
21. Ornamentation type	0	None
	1	Crenulations
	2	Spines
	3	Teeth

ACTA PROTOZOOLOGICA

A New Marine Ciliate, *Erniella wilberti* sp. n. (Ciliophora: Hypotrichida), from Shrimp Culturing Waters in North China

Xiaofeng LIN and Weibo SONG

Laboratory of Protozoology, KLM, Ocean University of China, Qingdao, P. R. China

Summary. The morphology and infraciliature of a new marine hypotrichous ciliate, *Erniella wilberti* sp. n., collected from a shrimp culturing pond near Qingdao (Tsingtao), China, are investigated using living observations and protargol silver impregnation method. The new species is characterized by: 80-180 × 25-70 µm *in vivo* with elongated body shape and thin hyaline margin encircling the whole cell; arc-shaped cortical structures arranged in 3 rows on dorsal side; bipartite adoral zone each with 8-12 and 16-20 membranelles respectively; 4-6 frontal, 1 buccal and 2-5 transverse cirri; 2 ventral cirral rows extending to posterior half of body; 3 dorsal kineties; 2 macronuclear nodules and 1-3 micronuclei.

Key words: *Erniella wilberti* sp. n., Hypotrichida, marine ciliate, morphology.

INTRODUCTION

The hypotrichous genus *Erniella* was established by Foissner (1987), which is characterized by: bipartite adoral zone of membranelles; with one left and one right marginal rows; two to several ventral rows, several frontal and transverse cirri present, no caudal cirri (Foissner 1987). It differs from other related genera in the following combined features of: (1) AZM in 2 clearly separated parts, (2) apart from several differentiated frontal cirri, most somatic ciliary organelles are in rows (ventral rows) and (3) transverse cirri present. Until now, only one species is known in this genus, *E. filiformis* Foissner, 1987, which was found in soil.

During a survey of the ciliate fauna in mariculture waters in northern China, an unknown ciliate was isolated from a shrimp-culturing pond near Qingdao in the summer of 2002. Subsequent observations and studies demonstrated that it represents a new member of the monotypic genus *Erniella*. Its morphology and infraciliature are documented as follows.

MATERIALS AND METHODS

Samples were collected on August 10, 2002 from a shrimp-culturing pond near Qingdao (Tsingtao, 36°08'N; 120°43'E), China.

Address for correspondence: Weibo Song, College of Fisheries, Ocean University of China, Qingdao, 266003, P. R. China; E-mail: wsong@ouc.edu.cn

The ciliate was isolated and examined under a compound microscope with bright field and differential interference contrast equipments. The protargol silver staining method (Wilbert 1975) was used to reveal the infraciliature.

All drawings were performed at a magnification of 1250× with the aid of a camera lucida. Measurements were carried out with an ocular micrometer. Terminology mainly follows Corliss (1979) and Foissner (1982).

RESULTS

Erniella wilberti sp. n. (Figs 1-23; Table 1)

Diagnosis: Marine *Erniella*, with elongated body shape and thin hyaline margin encircling the whole cell; *in vivo* 80-180 × 25-70 µm; with arc-shaped cortical structures arranged in 3 rows on dorsal side; bipartite adoral zone each with 8-12 and 16-20 membranelles respectively; 4-6 frontal, 1 buccal and 2-5 transverse cirri; 2 ventral cirral rows extending to posterior half of body; 3 dorsal kineties; 2 macronuclear nodules and 1-3 micronuclei.

Dedication: We dedicate this species to Prof. Dr. Norbert Wilbert, Zoological Institute of the Bonn University, Germany, to express our special respects for his great contribution to the studies on the ciliatology and fatherly kindness to the junior author.

Type location and ecological features: Clear coastal water, salinity 18.5‰; water temperature 27°C; pH about 8.0.

Type slides: One holotype and one paratype slides of protargol impregnated specimens (No. Lin-02-08-10-A, B) are deposited in the Laboratory of Protozoology, Ocean University of China, P. R. China.

Morphology and infraciliature (Figs 1-9, 14-23): Size rather variable, 80-180 × 25-70 µm *in vivo*, but mostly about 120 µm long; body shape elongated with length: width about 3-4:1; both ends rounded, body widest in anterior 1/4-1/3; dorsoventrally flattened *ca* 2.5:1 (Figs 1-5). Body non-flexible and not contracted. Characteristically, cell clearly divided into 2 areas when observed dorsoventrally: central and marginal areas, of which the thin and hyaline margin is *ca* 5-8 µm in width, while the central portion is opaque and about twice to triple as thick as the margin area (Figs 1-3, 14). Buccal field narrow, about 2/5 to 1/4 of body length (Fig. 1). Pellicle conspicuously rigid, no typical cortical granules observed, but on dorsal side, some colorless arc-shaped structures loosely arranged in 3 rows, which are about 10-15 µm long and conspicuously recognizable even at low magnification (Figs 2, 18, 23, arrowheads). Cyto-plasm colorless to grayish, with many large and differently-sized globules (3-10 µm across) making the central area opaque to completely dark (Figs 1, 4, 5, 14). Contractile vacuole not observed.

Two large macronuclear nodules (Ma), ovoid to ellipsoid, about 20 × 10 µm in size after protargol impregnation, lying in mid-body, containing many large spherical nucleoli (Fig. 8); 1-3 micronuclei (Mi) globular, about 4 µm in length, adjacent to macronuclei (Figs 8, 22, arrowheads).

Locomotion relatively fast, crawling on the bottom of Petri dish or on debris, with short and frequent pauses and then changing the moving direction (Fig. 6).

Adoral zone of membranelles (AZM) genus typic: one huge gap between bipartite AZMs (Fig. 9, arrow). Bases of membranelles in AZM_1 about 3 µm long, which are conspicuously shorter than that in AZM_2 (*vs.* 4-8 µm) and locating on ventral side (Fig. 3, arrow). Cilia of AZM_1 about 15 µm long. Paroral membrane (PM) long and slightly curved; endoral membrane (EM) relatively short and terminated anteriorly at about mid-PM (Figs 7, 17). 4-6 frontal cirri (FC); less than half of specimens (6 out of 16) having 4 slightly enlarged FC (Fig. 7), in which the posterior two (Fig. 17, arrowheads) are continuous with the distal end of AZM_1. In most cases, two more frontal cirri positioned posterior to the 4 anterior ones, which are located near the anterior end of the left ventral row and hence often difficult to detect (Fig. 19, arrows). Single buccal cirrus (BC) situated near mid-way of paroral membrane (Figs 7, 17, arrow). 2-5 transverse cirri (TC) (Fig. 20, arrow) with cilia *ca* 12-15 µm long, only slightly enlarged and close to the posterior end of right marginal row (Fig. 9). Two ventral rows, of which the left row (LVR) consists of 20-36 cirri, terminating posteriorly at 2/5 of cell length, while the right one (RVR) is composed of 31-47 cirri and terminates subcaudally (Figs 9, 15, 20). Usually 1-2 ventral cirri located near transverse ones (Figs 9, 20, arrowhead). Two marginal rows separated posteriorly, the left row (LMR) composed of 21-36 cirri and terminating subcaudally (Fig. 1, arrow), while the right one (RMR) with 18-39 cirri, extending to almost the cell end (Figs 9, 15).

Dorsal cilia bristle-like, about 3-5 µm long, consistently arranged in 3 rows, which extend over entire length of body (Figs 3, 8, 16, 21, arrowheads).

Some morphogenetic features during binary division (Figs 10-13): As a less-commonly occurring genus, the morphogenetic process of *Erniella* remains unknown. In the present work, one specimen in the
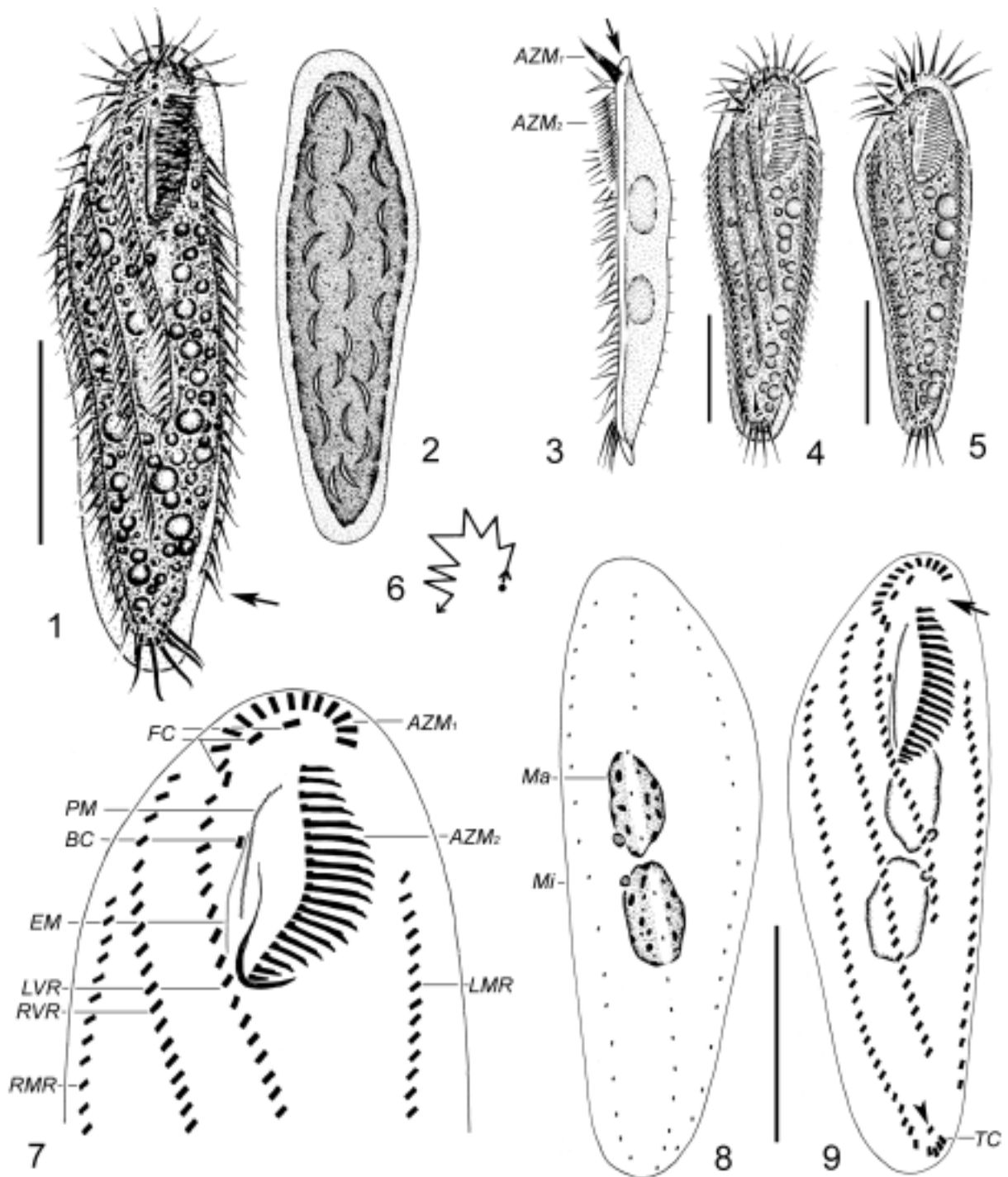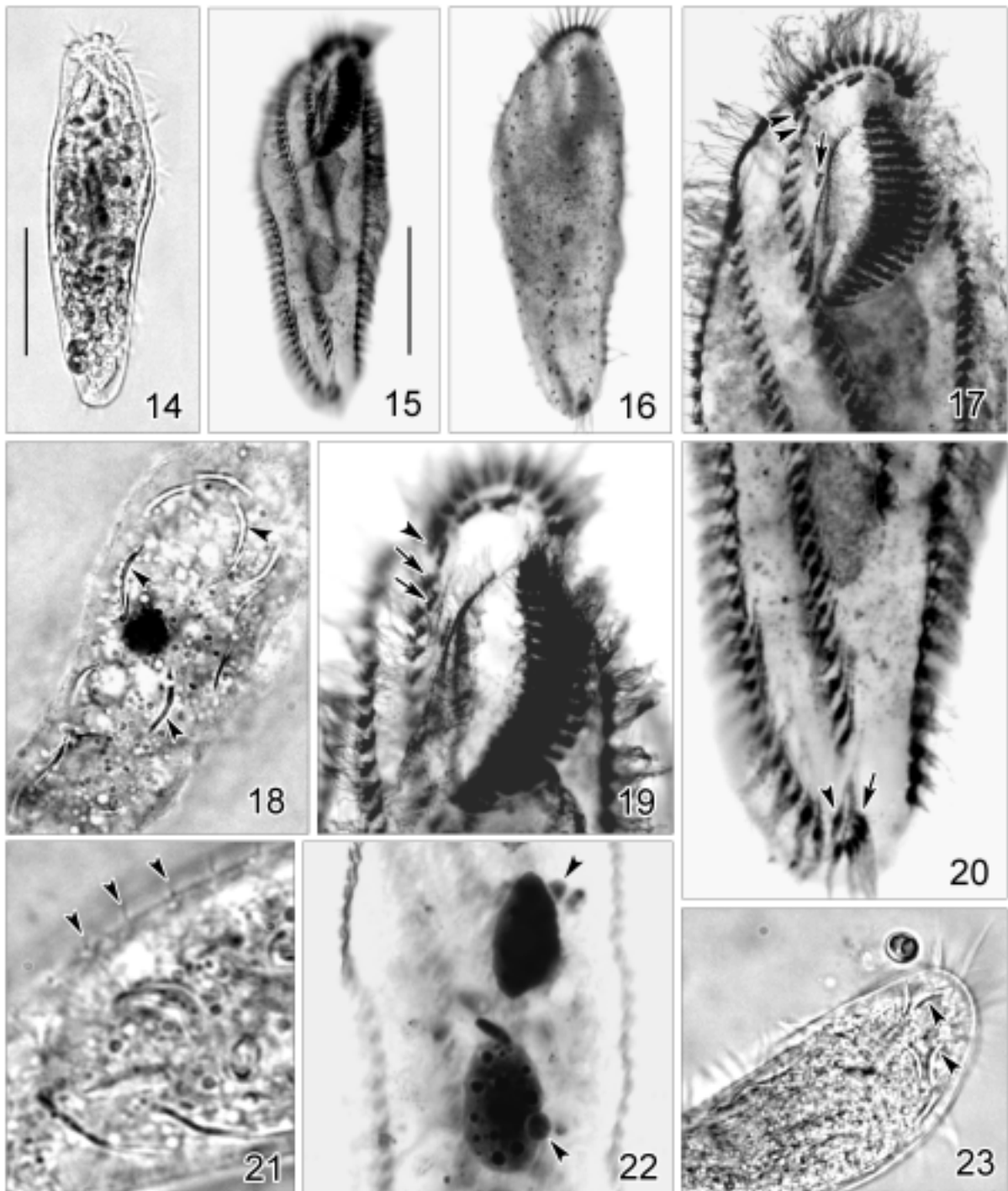
Figs 1-9. Morphology (1-6) and infraciliature (7-9) of *Erniella wilberti* sp. n., from life (1-5) and after protargol impregnation (7-9). **1 -** ventral view of a typical individual, arrow marks the end of left marginal row; **2 -** dorsal view, showing the arrangement of the arc-shaped cortical structures and hyaline cell margin; **3 -** lateral view, arrow indicates the cell margin, note that the membranelles in AZM_1 are located on the ventral side; **4, 5 -** ventral views, to show different body shapes; **6 -** diagram, to illustrate the movement; **7 -** infraciliature of the anterior part, to show the buccal apparatus; **8, 9 -** infraciliature of dorsal (8) and ventral (9) sides of the same specimen, arrow and arrowhead in Fig. 9 mark the gap between AZMs and the ventral cirrus anterior to the transverse cirri, respectively. AZM_1 - frontal part of adoral zone of membranelles, AZM_2 - posterior part of adoral zone of membranelles, BC - buccal cirrus, EM - endoral membrane, FC - frontal cirri, LMR - left marginal row, LVR - left ventral row, Ma - macronuclear nodules, Mi - micronuclei, PM - paroral membrane, RMR - right marginal row, RVR - right ventral row, TC - transverse cirri. Scale bars 40 μm.
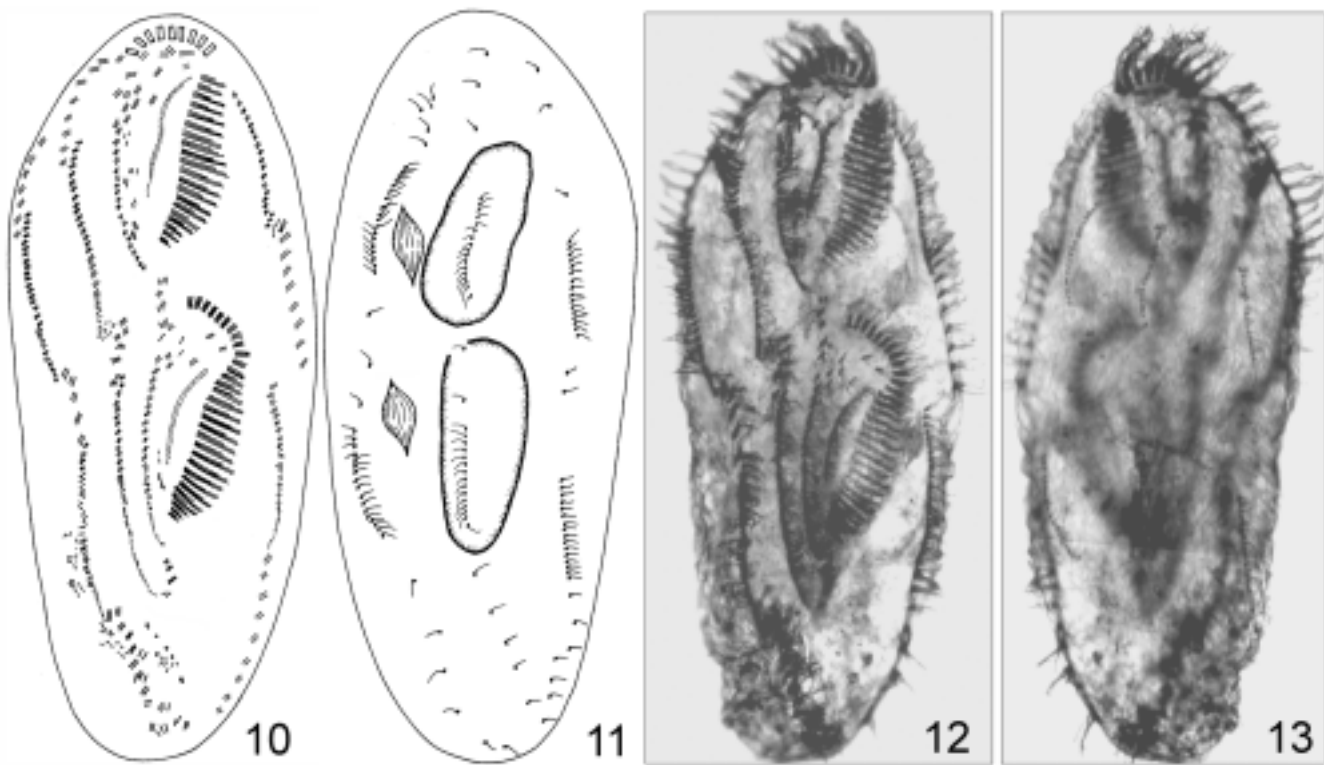
Figs 10-13. Ventral (10, 12) and dorsal (11, 13) views of a specimen in the middle morphogenetic stage.

Table 1. Morphometrical data of *Erniella wilberti* sp. n. All data are based on protargol impregnated specimens. Measurements in µm. Abbreviation: AZM$_1$ - frontal part of the adoral zone of membranelles; AZM$_2$ - posterior part of the adoral zone of membranelles; CV - coefficient of variation; M - median, Max - maximum, Mean - arithmetic mean, Min - minimum, n - sample size, SD - standard deviation.

Character	Min	Max	Mean	M	SD	CV	n
Body length	92	160	121.1	124	21.37	17.6	16
Body width	28	60	42.9	44	10.01	23.4	16
Length of buccal field	20	32	26.8	27	3.29	12.3	16
Number of AZM$_1$	8	12	9.8	10	0.98	10.0	16
Number of AZM2	16	20	18.9	20	1.45	7.7	16
Number of frontal cirri	4	6	5.3	4	1.00	19.1	16
Number of buccal cirri	1	1	1	1	0	0	50
Number of transverse cirri	2	5	4.3	4	0.86	20.2	16
Number of cirri in left ventral row	20	36	25.2	25	3.92	15.6	16
Number of cirri in right ventral row	31	47	35.1	37	4.01	11.4	16
Number of cirri in left marginal row	21	36	29.4	31	3.93	13.4	16
Number of cirri in right marginal row	18	39	31.9	31	5.23	16.4	16
Number of ventral cirri anterior to transverse cirri	0	2	1.3	1	0.58	46.2	16
Number of macronuclei	2	2	2	2	0	0	50
Length of macronuclei	10	38	21.9	22	8.29	37.8	16
Width of macronuclei	7	20	11	11	3.98	36.2	16
Number of micronuclei	1	3	2	2	0.41	20.4	13
Length of micronuclei	3	6	3.8	3	1.09	28.6	16
Width of micronuclei	2	5	2.8	2	0.84	30.3	16
Number of dorsal kineties	3	3	3	3	0	0	50

Figs 14-23. Photomicrographs of the morphology and infraciliature of *Erniella wilberti* sp. n., from life (14, 18, 21, 23) and after protargol impregnation (15-17, 19, 20, 22). **14 -** general appearance of a living cell; **15, 16 -** infraciliature of the ventral (15) and dorsal (16) sides of the same specimen; **17 -** ventral view, to show the oral apparatus; arrowheads indicate two frontal cirri, which are continuous with the distal end of AZM_1, arrow marks the buccal cirrus; note the intersecting of paroral and endoral membrane; **18 -** dorsal side, to demonstrate the arc-shaped cortical structures (arrowheads); **19 -** infraciliature of the anterior portion; arrowhead indicates a pair of frontal cirri; arrows mark last pair of frontal cirri, which near the anterior end of the left ventral row; **20 -** ventral view of the posterior portion; arrowhead and arrow indicate the ventral and transverse cirri, respectively; **21 -** to show the bristle-like dorsal cilia (arrowheads); **22 -** nuclear apparatus, arrowheads mark the micronuclei; **23 -** dorsal view of the anterior portion; arrowheads indicate the cortical structures. Scale bars 40 µm.

middle morphogenetic stage was observed (Figs 10-13). Based on this stage, the following conclusions can be made: (1) the developing pattern of the fronto-ventral transverse cirri is very likely a 5-anlagen-mode; (2) the right ventral row seems developing independently within the parental structure and separated from other cirri; (3) the parental oral structure is possibly partly renewed (?, only the AZM_2 will be renewed) or completely retained for the proter and (4) one anlage develops within each of the 3 parental dorsal kineties in both proter and opisthe (Figs 11, 13).

DISCUSSION

Since the genus *Erniella* was established, only one terrestrial species, *E. filiformis* Foissner, 1987, has been reported (Foissner 1987). The new form, *E. wilberti* differs from it in the following features: (1) different habitat (marine *vs.* soil); (2) smaller size (80-180 × 25-70 µm *vs.* 200-300 × 25-35 µm); (3) lower number of macronuclei (2 *vs.* 31-61); (4) more dorsal kineties (3 *vs.* 1); (5) lower number of ventral rows (2 *vs.* 3) and (6) single buccal cirrus (1 *vs.* 3-6). In addition, the presence of the arc-shaped cortical structures in the new species is, as to authors' knowledge, unique. Hence, the two organisms can be clearly separated.

As mentioned in the description, most specimens possess 6 frontal cirri. In this case, the last 4 are arranged like two pairs of cirri, i.e. a minimum zig-zag pattern (Fig. 19). This arrangement might indicate that this organism (this genus?) could be an intermediate form between urostylids and stichotrichs: it possibly represents a primary pattern of mid-ventral rows, which are seen in most typical urostylids (Hemberger 1982, Song 1990, Eigner and Foissner 1994, Shi *et al.* 1999).

REFERENCES

Corliss J. O. (1979) The Ciliated Protozoa: Characterization, Classification and Guide to the Literature. 2nd ed. Pergamon Press, New York

Eigner P., Foissner W. (1994) Divisional morphogenesis in *Amphisiellides illuvialis* n. sp., *Paramphisiella caudata* (Hemberger) and *Hemiamphisiella terricola* Foissner, and redefination of the Amphisiellidae (Ciliophora, Hypotrichida). *J. Eukaryot. Microbiol.* **41:** 243-261

Foissner W. (1982) Ökologie und Taxonomie der Hypotrichida (Protozoa: Ciliophora) einiger österreichischer Böden. *Arch. Protistenkd.* **126:** 19-143

Foissner W. (1987) Neue und wenig bekannte hypotriche und colpodide Ciliaten (Protozoa: Ciliophora) aus Böden und Moosen. *Zool. Beit.* **31:** 187-228

Hemberger H. (1982) Revision der Ordnung Hypotrichida Stein (Ciliophora, Protozoa) an Hand von Protargolpräparaten und Morphogenesedarstellungen. Dissertation Universität Bonn

Shi X., Song W., Shi X. (1999) Systematic revision of the hypotrichous ciliates. In: Progress in Protozoology (Eds. W. Song *et al.*) Ocean University Press, Qingdao (in Chinese)

Song W. (1990) Morphologie und Morphogenese des Bodenciliaten *Periholosticha wilberti* nov. spec. (Cilophora, Hypotrichida). *Arch. Protistenkd.* **138:** 221-231

Wilbert N. (1975) Eine verbesserte Technik der Protargolimprägnation für Ciliaten. *Mikrokosmos* **64:** 171-179

ACTA
PROTOZOOLOGICA

Notes on a New Marine Peritrichous Ciliate (Ciliophora: Peritrichida), *Zoothamnopsis sinica* sp. n. from North China, with Reconsideration of *Zoothamnium maximum* Song, 1986

Daode JI and Weibo SONG

Laboratory of Protozoology, KLM, Ocean University of China, Qingdao, People's Republic of China

Summary. The morphology, infraciliature and silverline system of a new marine peritrichous ciliate, *Zoothamnopsis sinica* sp. n., isolated from an abalone-farming pond off the coast of Qingdao, China, are investigated. *Z. sinica* is characterized by: colony dichotomously branched, zooids elongated and vase-shaped measuring 70-105 × 40-55 µm *in vivo*, double-layered peristomial lip; contractile vacuole located apically; number of transverse silverlines from peristomial area to aboral ciliary wreath *ca* 82-98, from aboral ciliary wreath to scopula, 48-55. Based on a reexamination on the slides deposited in the Laboratory of Protozoology, Ocean University of China, and on the original records, an updated and supplementary description on the infraciliature and morphology of *Zoothamnium maximum* Song, 1986 is supplied.

Key words: Marine Ciliophora, Peritrichida, *Zoothamnium maximum, Zoothamnopsis sinica* sp. n.

INTRODUCTION

Colonial peritrichous ciliates are common and dominant in marine waters, especially in littoral eutrophic biotopes (Kahl 1933, 1935; Precht 1935; Sommer 1951; Stiller 1971; Küsters 1974; Jankowski 1976, 1985). Compared with the forms found in freshwater habitats, however, most of marine species remain extremely less-known or only insufficiently described, which often

Address for correspondence: Weibo Song, Laboratory of Protozoology, KLM, Ocean University of China, Qingdao 266003, People's Republic of China; Fax: +86 532 203 2283; E-mail: wsong@ouc.edu.cn

render great difficulties in related fields, e.g. ecological and pathogenic studies involved in aquaculture (Song 1986, 1991a, 1992a, b; Hu and Song 2001; Song *et al.* 2002). As accepted by taxonomists, criteria for species identification in this group at least comprise: (1) branching style and features of stalk, (2) zooid shape (including feature of peristomial lip) and size, (3) number of transverse silverlines (i.e. after silver nitrate impregnation), (4) infraciliature (i.e. position of epistomial membrane and detail arrangement of three oral peniculi, protargol impregnation is needed), (5) colony size and number of zooids, (6) habitat and (7) number and position of contractile vacuoles.

Zoothamnopsis is a newly erected genus (Song 1997) to include those peritrichs which are morphologi-

cally similar to *Zoothamnium* but have reticulate silverline system with both latitudinal and longitudinal lines. Up to date, only two species have been included (Song 1997).

In May 2002, some peritrichs were isolated from an abalone-culturing pond near Qingdao, including an unknown morphotype with reticulate silverline system. After careful comparison, we convinced that it represents a new member in the genus *Zoothamnopsis*, which is described here. As a morphologically similar form, the buccal structure of *Zoothamnium maximum* Song, 1986, was re-checked and some additional descriptions are supplied.

MATERIALS AND METHODS

Zoothamnopsis sinica sp. n. was collected on 18 May, 2002. Ciliates were isolated from the surface of green alga *Ulva* sp., which attached to the stones at the bottom of an abalone-farming pond near Qingdao (Tsingtao), China. Individuals were observed *in vivo* using an oil immersion objective and differential interference contrast microscopy. The infraciliature was revealed with protargol impregnation method according to Wilbert (1975). Silver nitrate method was used to demonstrate the silverline system (Song and Wilbert 1995).

Drawings of impregnated specimens were made with the help of a camera lucida at 1250× magnification. Terminology is mainly according to Corliss (1979) and Warren (1986).

RESULTS

Description of *Zoothamnopsis sinica* sp. n. (Figs 1-8, 17-25; Table 1)

Class: Oligohymenophora de Puytorac *et al.* 1974
Order: Peritrichida Stein, 1859
Family: Vorticellidae Ehrenberg, 1838
Genus: *Zoothamnopsis* Song, 1997

Diagnosis for *Zoothamnopsis sinica* sp. n.: Marine *Zoothamnopsis* with colony dichotomously branched; zooids elongated vase-shaped, *in vivo* about 70-105 × 40-55 μm, with double-layered, thick peristomial lip; contractile vacuole apically located; macronucleus C-shaped and horizontally oriented; number of transverse lines from oral area to aboral ciliary wreath *ca* 82-98, from aboral ciliary wreath to scopula, 48-55.

Type specimens: One holo- and one paratype slides (registration number: 0205180101, 0205180102) with silver nitrate and protargol impregnated specimens are deposited at the Laboratory of Protozoology, Ocean University of China, China.

Ecological features: Ciliates were found in great abundance in a clean abalone-farming pond, with salinity about 30‰, water temperature 15°C.

Morphology: Cell size and shape consistent, *in vivo* about 70-105 × 40-55 μm, generally 80-90 × 45-50 μm, and slender vase-shaped. Body constricted slightly below the double-layered, thick peristomial lip; maximum width of cell mostly at oral border; large peristomial disc highly elevated (Figs 1, 3, 18). Pellicle very finely striated, which can be detected only using powerful objectives (× 400 or higher) (Fig. 19), yet completely smooth when observed at low magnification.

Cytoplasm colorless to slightly greyish, usually containing several large greenish food vacuoles (5-10 μm across) (Figs 1, 18), and numerous small greyish granules which are 1-2 μm in diameter. One large, apically located contractile vacuole (Fig. 1) rather inactive, and contracting at a rate of *ca* 3 min. Macronucleus thick and C-shaped, horizontally located (Figs 1, 3, 6); micronucleus not observed.

Small colony (< 30 zooids) regularly dichotomously branched, whereas irregularly branched in large colony, with up to 100 zooids (Figs 2, 17). Stalk up to 1500 μm long, diameter about 15 μm in main branch and 10 μm in distal part, surface smooth under low magnification, with very fine striations (Fig. 1). Myoneme system consisting of thick spasmoneme, which are 6-7 μm in width in main branch and 3 μm at distal ends, granules extremely fine (< 0.5 μm) on spasmoneme. Around scopula, myoneme extending anteriorly to central region of the cell as commonly seen in other peritrichs (Fig. 6).

Cells not differentiating to micro- and macrozooid, and insensitive to stimuli. Contracted zooid usually oval-shaped. Telotroch flattened, *ca* 40 × 60 μm in size (Figs 4, 18, arrow).

Infraciliature as shown in Figs 5 and 6, which are similar to that of other congeners. Haplokinety (H) and polykinety (Po) describing about 1.5 turns around peristomial disc before entering vestibulum, where they make a further turn (Figs 5, 6). Near distal end of haplo- and polykinety, always one kinety fragment recognizable (Figs 5, 6, 21, arrows).

Polykinety forming three peniculi in lower half of vestibulum, each consisting of three kineties. Peniculus 1 (P1) and 2 (P2) much longer than peniculus 3 (P3). At anterior end of P2, the outer kinety apparently separated from the other two (Fig. 5, double arrowheads); P1 and P3 terminating at about same level whereas P2 ending between and above these two; characteristically, two close-set outer kineties in P3 mostly separated from the
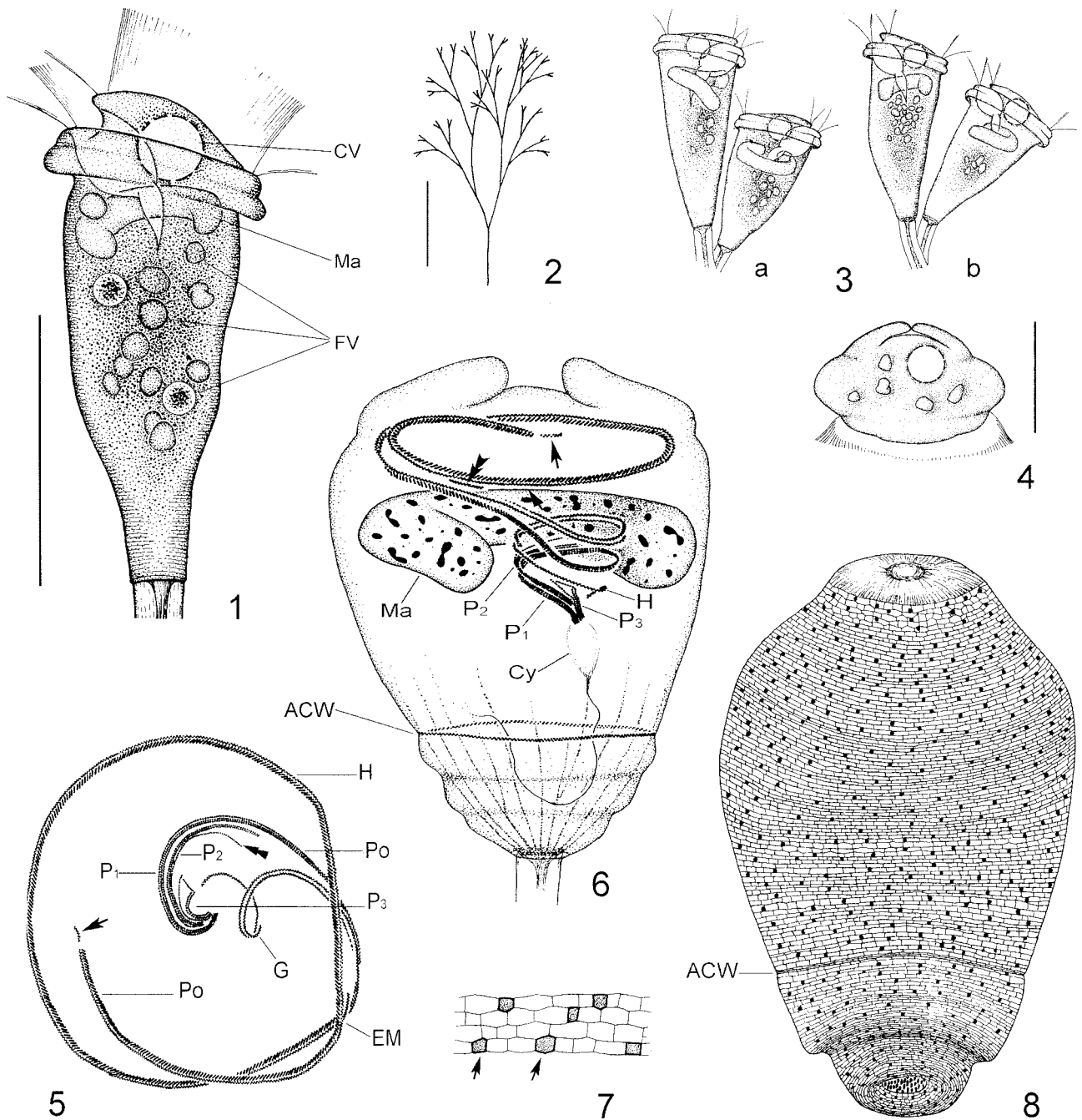
Figs 1-8. Morphology of *Zoothamnopsis sinica* sp. n.from life (1-4), after silver nitrate (5-6) and protargol (7-8) impregnations. **1 -** general view of a typical zooid; **2 -** colony form; **3 -** zooids at low magnification, showing varieties of body shape and macronucleus; **4 -** a telotroch; **5 -** apical view of the oral apparatus, noting the arrangement of three peniculi and the distal fragment (arrow). Double-arrowheads indicate the separated kinety of peniculus 2; **6 -** general infraciliature, double-arrowheads mark the epistomial membrane, arrow denotes the distal fragment; **7 -** details of silverline system, arrows mark the pellicle pores; **8 -** general silverline system. ACW - aboral ciliary wreath, CV - contractile vacuole, Cy - cytopharynx, EM - epistomial membrane, FV - food vacuole, G - germinal kinety, H - haplokinety, Ma - macronucleus, P_{1-3} - peniculus 1-3, Po - polykinety. Scale bars 50 μm (1); 300 μm (2); 40 μm (4).
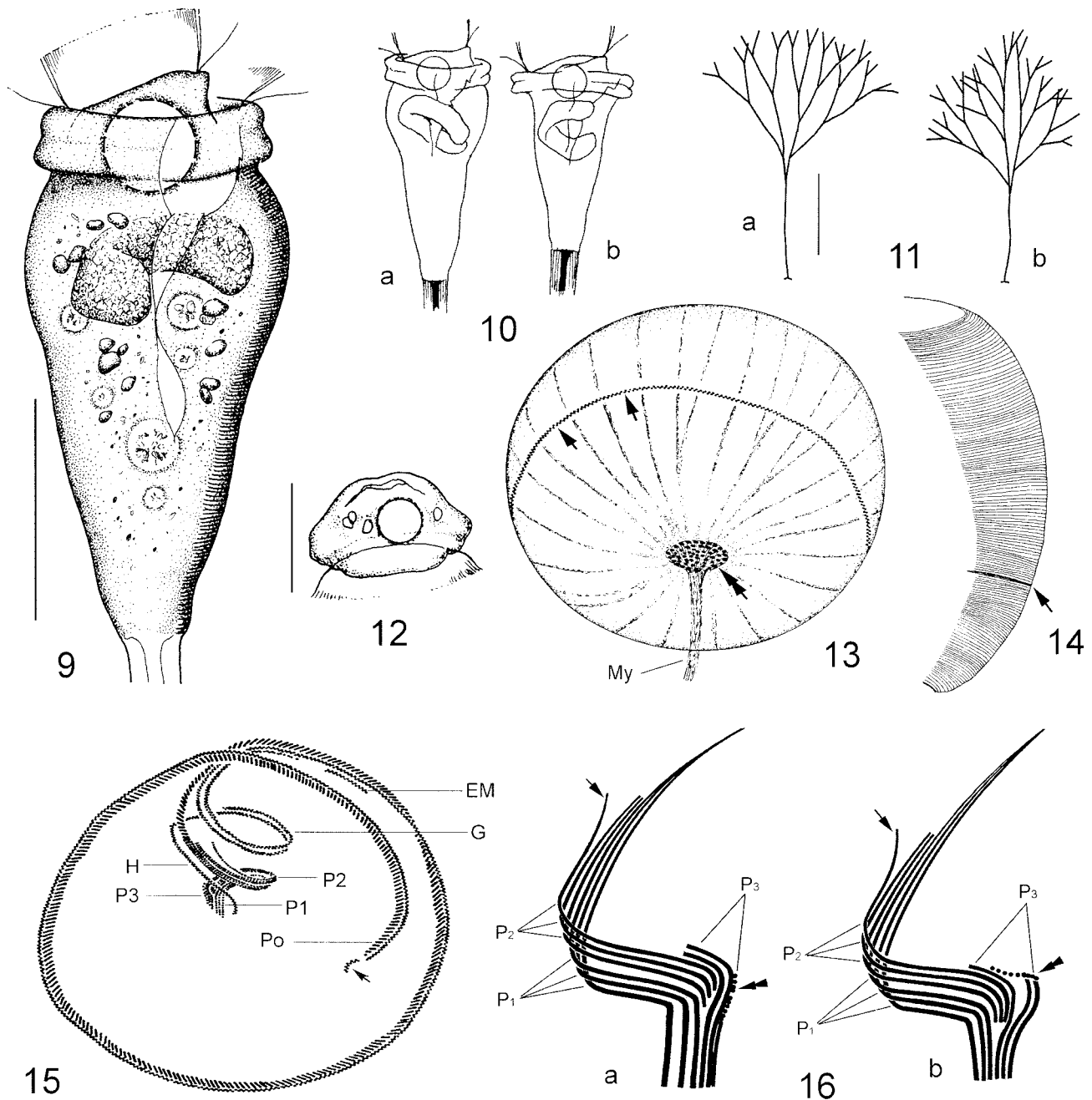
Figs 9-16. Morphology of *Zoothamnium maximum* from life (9-12), after protargol (13, 15-16) and silver nitrate (14) impregnations (9-12, after Song 1986; 13-16, original). **9** - general view of a typical zooid; **10** - zooids of different shape; **11** - two colony forms; **12** - a telotroch; **13** - lateral view, showing the myoneme system. Double-arrows indicate the scopula, arrows mark the aboral ciliary wreath; **14** - silverline system, arrow marks aboral ciliary wreath; **15** - apical view of the oral apparatus, arrow marks the distal fragment; **16** - comparison of detailed arrangement of three peniculi between *Z. maximum* (a) and *Zoothamnopsis sinica* (b), showing the different pattern of peniculus 3 (double-arrowheads). EM - epistomial membrane, G - germinal kinety, H - haplokinety, My - myoneme, P1-3 - peniculus 1-3, Po - polykinety. Scale bars 50 µm (9); 40 µm (12); 300 µm (11).
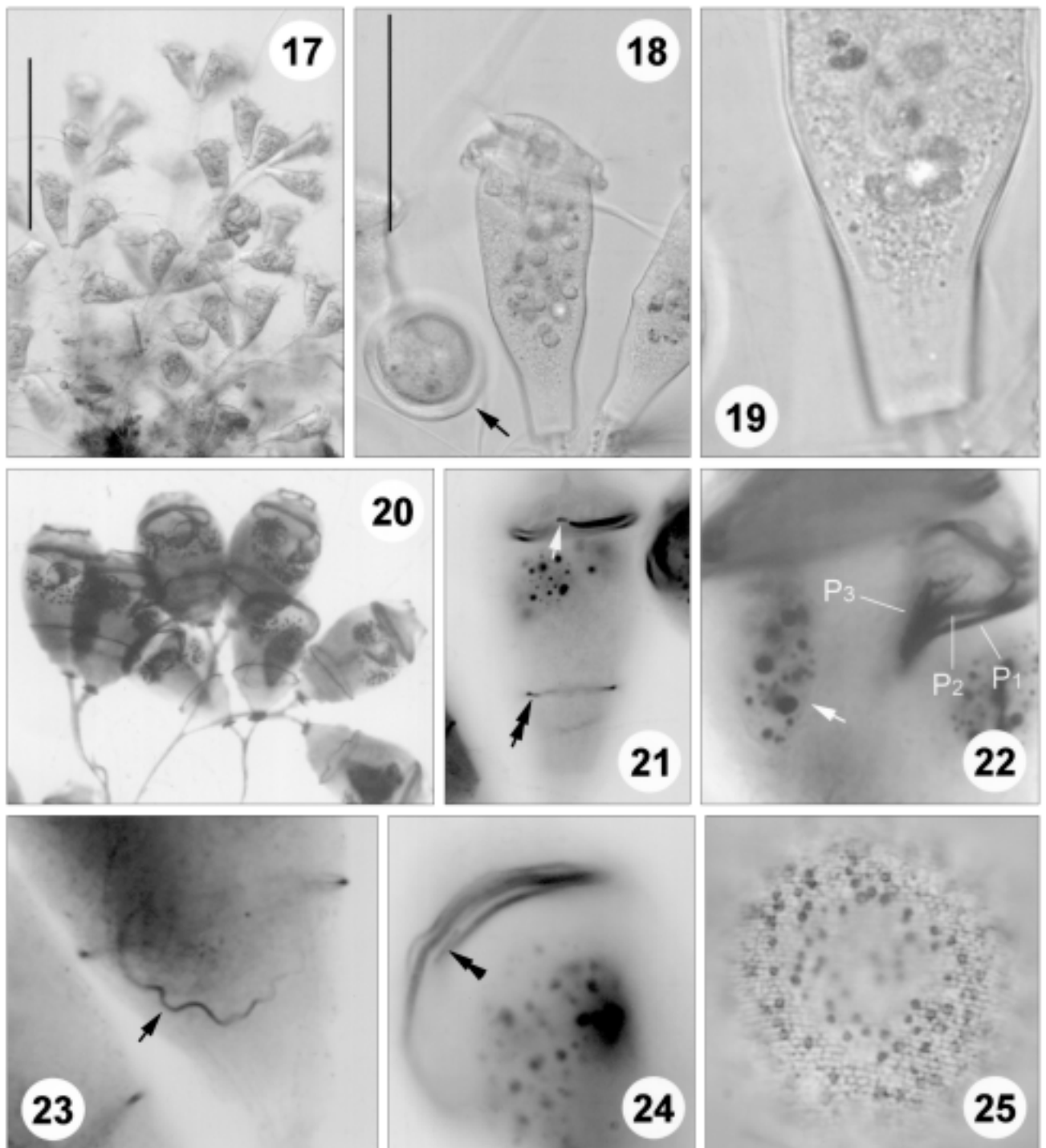
Figs 17-25. Photomicrographs of *Zoothamnopsis sinica* sp. n.from life (17-19), after protargol (Figs 20-24) and silver nitrate (25) impregnations; **17** - colony at low magnification; **18** - zooids at 400 × magnification, arrow marks the telotroch in formation; **19** - lateral part of a zooid at 1250 × magnification, showing the pellicle striations; **20** - to show the branching form; **21** - to show the distal fragment (arrow) and the aboral ciliary wreath (double-arrows); **22** - oral apparatus, indicating three peniculi (P_{1-3}) and macronucleus (arrow); **23** - the posterior end of the cytopharynx (arrow); **24** - to show the epistomial membrane (double-arrowheads); **25** - silverline system. Scale bars 200 µm (17); 50 µm (18).

Table 1. Morphometrical characterizations of *Zoothamnopsis sinica* sp. n. (upper line) and *Zoothamnium maximum* (Song, 1986) (lower line). Measurements in μm. Min - minimum, Max - maximum, Mean - arithmetic mean, SD - standard deviation, SE - standard error of the mean, Vr - coefficient of variation, n - sample number.

Character	Min	Max	Mean	SD	SE	Vr	n
Body length *in vivo*	70	105	91.4	10.10	2.81	11.1	13
	81	121	-	-	-	-	-
Body width *in vivo*	40	52	47.3	3.34	0.96	7.1	12
	47	64	-	-	-	-	-
Body length after protargol	43	68	54.6	5.44	1.01	10.0	29
	36	51	44.6	5.00	0.96	11.2	27
Body width after protargol	25	38	31.8	4.27	0.79	13.4	29
	26	42	34.7	5.03	5.20	2.9	27
Number of silverlines from oral area to aboral ciliary wreath	82	98	89.7	4.72	0.67	5.3	7
	82	95	-	-	-	-	4
Number of silverlines from aboral ciliary wreath to scopula	48	55	51.7	2.58	1.05	5.0	6
	45	58	-	-	-	-	4

third one and only converged with it at the end of vestibulum (Figs 5, 6, 16b, double-arrowheads, 22).

Haplokinety passing around vestibulum on opposite wall to peniculi. Cytopharynx highly developed, the distal end hook-shaped and extending below aboral ciliary wreath (Figs 6, 23). Germinal kinety (G) lying parallel to haplokinety within upper half of vestibulum (Fig. 5). Epistomial membrane (EM) short, located near upper level of vestibulum (Figs 5, 24). Aboral ciliary wreath (ACW) formed by double-rowed kineties, which encircle cell in posterior region (Figs 6, 21).

Silverline system, as shown in Figs 7, 8 and 25, genus typical. Transverse lines equably close-set in whole region, mesh rows *ca* 0.5 μm at interval. Pellicle pores distributed irregularly, densely located in some areas but sparsely in others (Figs 7, arrows; 8, 25). ACW represented by two or three parallel lines (Fig. 8). Number of transverse silverlines from peristome to ACW, 82-98; from ACW to scopula, 48-55.

## Redescription of *Zoothamnium maximum* Song, 1986 (Figs 9-16, 26-34; Table 1)

Zoothamnium maximum was originally found from some shrimp-farming waters in the Yellow Sea, China (Song 1986). As the report was made in Chinese and descriptions on some oral structures were not supplied in sufficient details, a complementary redescription is thus added based on re-checking of the slides and the documents reserved by the junior author.

Morphology: Body flexible and slightly variable, but generally elongate and slender vase-shaped (Figs 9, 10,

26), widest at anterior 1/3 of the body, and usually constricted below peristomial lip. Fully extended zooid *ca* 110 (80-120) x 50 (40-55) μm in size, mostly length to width about 2-2.2:1. Peristomial disc strongly elevated (Fig. 9). Peristomial lip conspicuously thick, double-layered (Fig. 9). Pellicle smooth at low magnification, fine striations detected only with more powered objectives (x 400 or higher). Cytoplasm colourless and transparent, several large light-reflecting granules (*ca* 3-5 μm in diameter) often present. Macronucleus relatively short, C-shaped and horizontally oriented. Single large contractile vacuole apically located (Fig. 9).

Stalk strong, about 12 μm thick with smooth surface. Colony typically dichotomously branched and reaching a total length of 1-1.5 mm with often more than 50 homomorphic zooids (Fig. 11). Stalk myoneme conspicuous, thecoplasmic granules indetectable. Telotroch flattened, *ca* 60 μm in diameter (Fig. 12).

Oral apparatus typical of genus. Haplokinety (H) and polykinety (Po) circling about one and half turns around peristomial disc and accomplishing a further turn after plunging into vestibulum (Fig. 15). All peniculi consisting of 3 kineties while peniculus 1 (P1) and P2 are much longer than P3. Three kineties in P1 about equally long, converged with P3 at posterior end (Fig. 16a). The outer kinety of P3 loosely ciliated, about 2/3 of the other two in length and closely located to the middle one (Fig. 16a, double arrowheads). P2 interposed between P1 and P3, the anterior end of the outer kinety apart from the other two (Fig. 16a, arrow; 29, double-arrowheads), and all of them terminating at different levels above P1 and P3
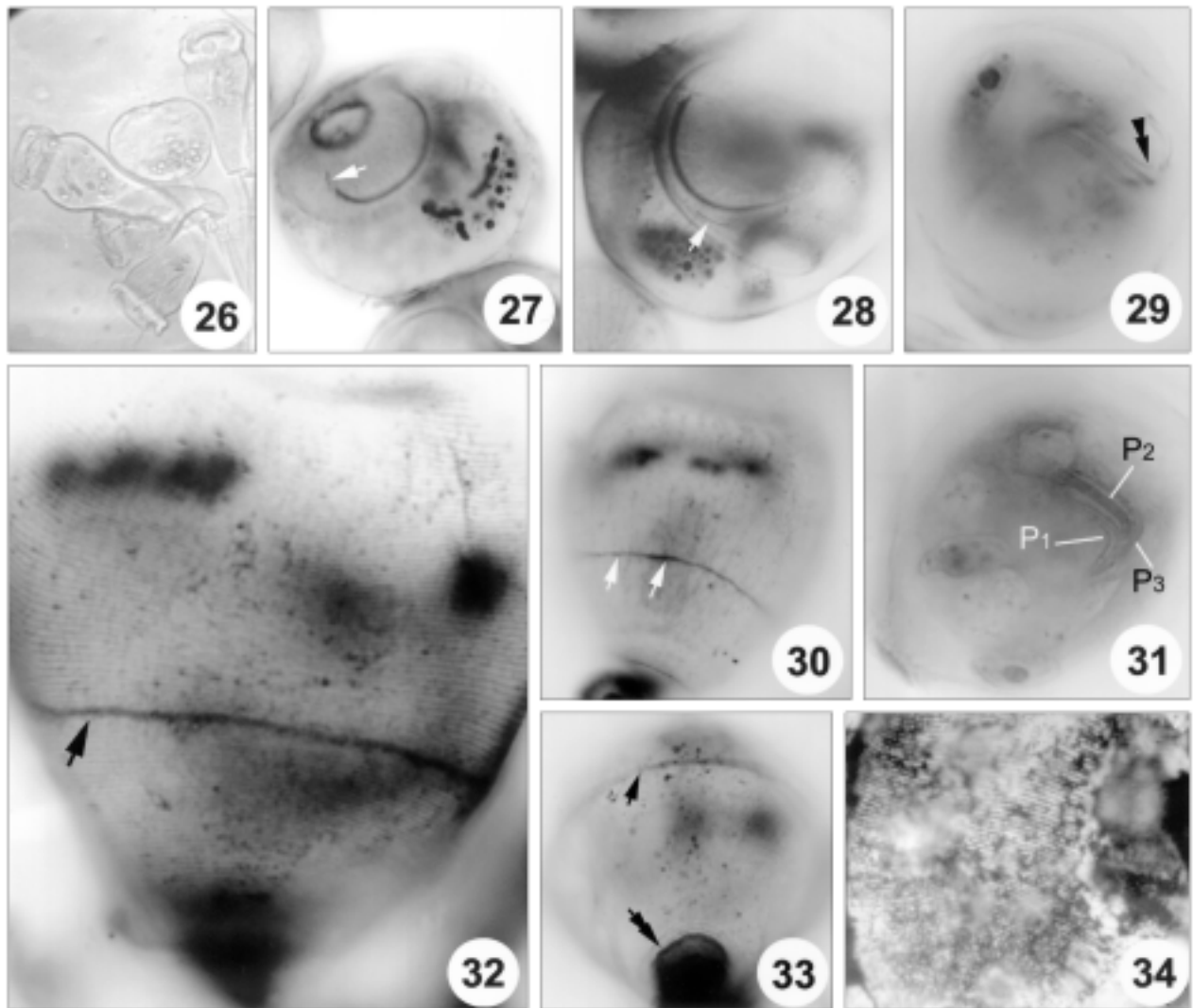
Figs 26-34. Photomicrographs of *Zoothamnium maximum* from life (26), after protargol (27-33) and silver nitrate (34) impregnations. **26** - zooids at low magnification; **27** - apical view, showing the distal fragment (arrow) of oral apparatus; **28** - apical view, arrow marks epistomial membrane; **29** - oral apparatus, denoting the outer kinety of peniculus 2 (double-arrowheads); **30** - side view, showing aboral ciliary wreath (arrows) and myoneme system; **31** - detailed arrangement of three peniculi (P_{1-3}); **32, 34** - general silverline system, arrow marks the aboral ciliary wreath; **33** - lateral view, showing the scopula (double-arrows) and the aboral ciliary wreath (arrow).

(Fig. 16a). Haplokinety passing around vestibulum on opposite wall to peniculi. Germinal kinety (G) lying parallel to haplokinety within upper half of vestibulum. Epistomial membrane (EM) relatively long, and located near opening of vestibulum (Figs 15, 28). Aboral ciliary wreath composed of zig-zag structure of kinetosomes, which encircles cell at about the level of posterior 1/3 of body length (Figs 13, 30, arrows).

Myoneme system similar to that of *Vorticella* spp., consisting of strong spasmoneme in stalk and thin myonemes (My) around scopula, which extend anteriorly to oral area (Figs 13, 30). Silverline system typical of *Zoothamnium*-pattern (Figs 14, 32-34), striations close-set and no conspicuous pellicular pores associated with silverlines. Number of transverse silverlines between peristomial lip and aboral ciliary wreath *ca* 82-95, between aboral ciliary wreath and scopula, 45-58.

COMPARISON AND DISCUSSION

The genus *Zoothamnopsis* was established by Song very recently (Song 1997) with two species included, *Z. mengi* Song, 1997 (Figs 35-36) and *Z. perlatum*
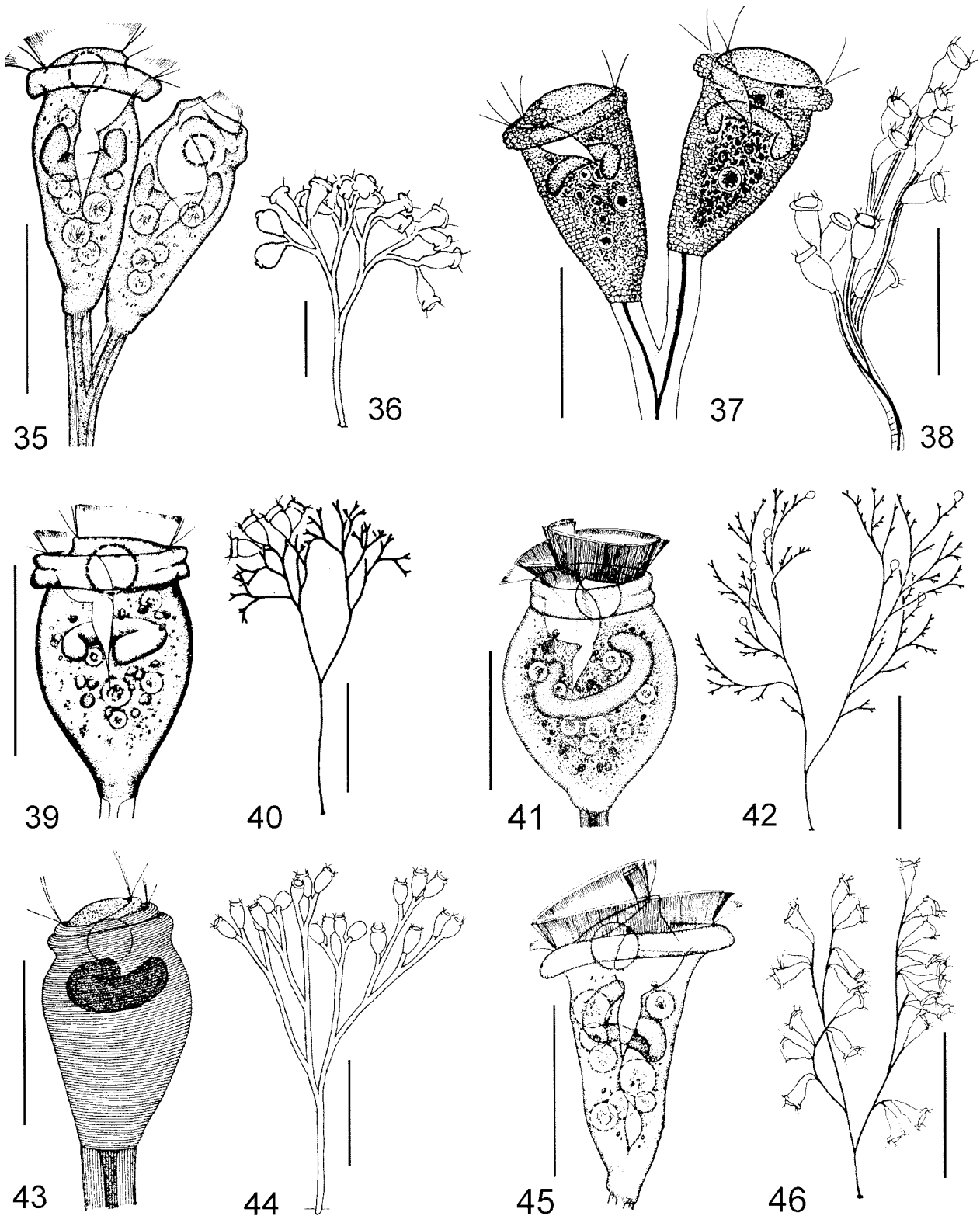
Figs 35-42. Comparison of some closely related morphotypes. **35-36** - *Zoothamnopsis mengi* (after Song 1997); **37-38** - *Zoothamnopsis perlatum* (after Stiller 1946); **39-40** - *Zoothamnium duplicatum* (after Song 1991a); **41-42 -** *Zoothamnium penaei* (after Song 1992b); **43-44 -** *Zoothamnium rigidum* (after Precht 1935); **45-46 -** *Zoothamnium paraentzii* (after Song 1991b). Scale bars 50 μm (35, 37, 39, 41, 43, 45); 100 μm (36); 200 μm (38, 40, 44, 46); 400 μm (42).

Table 2. Morphological comparison between *Zoothamnopsis sinica* sp. n. and other morphologically similar *Zoothamnopsis* and *Zoothamnium* species. Measurements in μm. ? - data not available.

Species	Body length *in vivo*	Body width *in vivo*	Number of transverse silverlines from scopula to aboral ciliary wreath	Number of transverse silverlines from aboral ciliary wreath to anterior end	Appearance of peristomial lip	Habitat	Number of zooids	Data source
Zoothamnopsis sinica sp. n.	70-105	45-52	48-55	82-98	double-layer	marine	ca 50	Original
Zoothamnopsis mengi	50-70	30-40	30-36	76-87	single-layer	marine	ca 20	Song 1997
Zoothamnopsis perlatum	60-100	-	-	-	single-layer	freshwater	10-12	Stiller 1946
Zoothamnium duplicatum	45-84 (69)	27-49 (44)	25-28	50-54	double-layer	marine	>100	Kahl 1933, Song 1991a
Zoothamnium maximum	81-121 (109)	47-64 (56)	45-58	82-95	double-layer	marine	-	Song 1986, Original
Zoothamnium paraentzii	50-80 (68)	27-43 (35)	ca 27	ca 60	single-layer	marine	20-30	Song 1991b
Zoothamnium penaei	54-95 (78)	38-62 (51)	-	-	double-layer	marine	>100	Song 1992b
Zoothamnium rigidum	70-95	-	-	-	double-layer	marine	ca 20	Precht 1935

(Stiller, 1946) Song, 1997 (Figs 37-38). *Z. sinica* sp. n. differs from *Z. mengi* by its larger size (70-105 × 40-55 *vs.* 50-70 × 20-30 μm), double-layered peristomial lip (*vs.* single-layered) and distinctly more transverse silverlines from the scopula to the aboral ciliary wreath (48-55 *vs.* 30-36) (Table 2). *Z. perlatum* has similar size to *Z. sinica*, but can be recognized by freshwater habitat (*vs.* marine) and less transverse striations (*ca* 40, from original illustration *vs.* over 130).

Considering the living appearances and the marine habitat, some *Zoothamnium* species with dichotomously-branched stalk and double-layered peristomial lip should be compared with the new organism, i.e. *Z. maximum* Song, 1986, *Z. duplicatum* Kahl, 1933, *Z. penaei* Song, 1992 and *Z. rigidum* Precht, 1935 (Table 2).

Morphologically, *Zoothamnium duplicatum* (Figs 39, 40) is possibly most related to *Zoothamnopsis sinica in vivo*, which can be separated, however, besides the different silverline system (*Vorticella*-type *vs. Pseudovorticella*-type), by the conspicuously thicker peristomial lip and less slender body shape (Kahl 1933, Song 1991a).

Different from the giant form, *Zoothamnium maximum*, the new species is relatively smaller (90 *vs.* 110 μm on average), possesses thinner peristomial lip and more elevated peristomial disc (Figs 1, 9, 18) (Table 2). In addition, they have completely different pattern of silverline system as well.

Zoothamnium penaei (Figs 41, 42) has a conspicuously oval body shape and differentiated zooids (macro- and microzooids?), thus can be clearly identified at the level of living observations.

Besides different silverline pattern (Precht 1935), *Zoothamnopsis sinica* can be distinguished from *Zoothamnium rigidum* (Figs 43, 44) by more elevated peristomial disc, thinker oral border and conspicuously slender body.

Zoothamnium paraentzii (Figs 45, 46), found from the body surface of marine shrimp *Penaeus sinensis* by Song (1991b), exhibits thin, single-layered oral border and less transverse silverlines from scopula to aboral ciliary wreath (*ca* 27 *vs.* 48-55), thus can be clearly separated form the current organism.

As summarized in Table 2, *Zoothamnium maximum* differs form other related congeners, *Z. duplicatum*, *Z. paraentzii* and *Z. panaei* in the following combination: large size and higher number of silverlines (Table 2).

REFERENCES

Corliss J. O. (1979) The Ciliated Protozoa: Characterization, Classification and Guide to the Literature. 2nd ed. Pergamon Press, New York

Ehrenberg C. G. (1838) Die Infusionsthierchen als Volkommene Organismen. Leipzig

Hu X., Song W. (2001) Description of *Zoothamnium chlamydis* sp. n. (Protozoa: Ciliophora: Peritrichida), an ectocommensal peritrichous ciliate from cultured scallop in North China. *Acta Protozool.* **40:** 215-220

Jankowski A. W. (1976) A revision of the order Sessilida (Peritricha). *Mater. Pub. Meet. Protozool.*, Kiev, 168-170 (in Russian)

Jankowski A. W. (1985) Life cycles and taxonomy of generic groups *Scyphidia*, *Heteropolaria*, *Zoothamnium* and *Cothurnia* (class Peritricha). *Trudy zool. Inst., Leningr.* **129:** 74-100 (in Russian)

Kahl A. (1933) Ciliata librae et ectocommensalia. In: Die Tierwelt der Nord- und Ostsee (Eds G. Grimpe and E. Wagler). Lief. 23, Leipzig, 147-183

Kahl A. (1935) Urtiere oder Protozoa I: Wimpertiere oder Ciliata (Infusoria) 4. Peritricha und Chonotricha. *Tierwelt Dtl.* **30:** 651-886

Küsters E. (1974) Ökologische und systematische Untersuchungen der Aufwuchsciliaten im Königshafen bei List/Sylt. *Arch. Hydrobiol.* **45 (Suppl.):** 121-211

Precht H. (1935) Epizoen der Kieler Bucht. *Nova Acta Leopol.* **3:** 405-474

Puytorac P. de, Batisse A., Bohatier J., Corliss J. O., Deroux G., Didier P., Dragesco J., Fryd-Versavel G., Grain J., Grolière C-A., Hovasse E., Iftode F., Laval M., Roque M., Savoie A., Tuffrau M. (1974) Proposition d'une classification du phylum Ciliophora Doflein, 1901 (Réunion de systematique, Clermont-Ferrand). *C. r. Hebd. Séanc. Acad. Sci., Paris* **278:** 2799-2802

Sommer G. (1951) Die peritrichen Ciliaten des großen Plöner Sees. *Arch. Hydrobiol.* **44:** 349-440

Song W. (1986) Descriptions of seven new species of peritrichs on *Penaeus orientalis* (Peritricha: Zoothamnidae: Epistylidae). *Acta Zootax. Sin.* **11:** 225-235 (in Chinese with English summary)

Song W. (1991a) Contribution to the commensal ciliates on *Penaeus orientalis*. II. (Ciliophora, Peritrichida). *J. Ocean Univ. Qingdao* **21:** 45-55 (in Chinese with English summary)

Song W. (1991b) A new commensal ciliate, *Zoothamnium paraentzii* (Ciliophora, Peritrichida). *Zool. Res.* **12:** 355-359 (in Chinese with English summary)

Song W. (1992a) Contribution to the commensal ciliates on *Penaeus orientalis*. III. (Ciliophora, Peritrichida). *J. Ocean Univ. Qingdao* **22:** 107-116 (in Chinese with English summary)

Song W. (1992b) A new marine ciliate, *Zoothamnium penaei* sp. nov. (Ciliophora, Peritrichida). *Oceanol. Limnol. Sin.* **23:** 90-94 (in Chinese with English summary)

Song W. (1997) A new genus and two new species of marine peritrichous ciliates (Protozoa, Ciliophora, Peritrichida) from Qingdao, China. *Ophelia* **47:** 203-214

Song W., Wilbert N. (1995) Benthische Ciliaten des Süßwassers. In: Praktikum der Protozoologie (Ed. R. Röttger). Gustav Fischer Verlag, New York, 156-168

Song W., AL-Rasheid K. A. S., Hu X. (2002) Notes on the poorly-known marine peritrichous ciliate, *Zoothamnium plumula* Kahl, 1933 (Protozoa: Ciliophora), an ectocommensal organism from cultured scallops in Qingdao, China. *Acta Protozool.* **41:** 163-168

Stein F. von (1859) Der Organismus der Infusionsthiere nach eigenen Forschungen in systematischer Reihenfolge bearbeitet. I. Leipzig

Stiller J. (1946) Beitrag zur Kenntnis der Peritrichenfauna der Schwefelthermen von Split. *Annls Hist. Nat. Mus. Natn. Hung.* **39:** 19-57

Stiller J. (1971) Szájkoszorús Csillósok-Peritricha. *Fauna Hung.* **105:** 1-245

Warren A. (1986) A revision of the genus *Vorticella* (Ciliophora: Peritrichida). *Bull. Br. Mus. nat. Hist. (Zool.)* **50:** 1-57

Wilbert N. (1975) Eine verbesserte Technik der Protargolimprägnation für Ciliaten. *Mikrokosmos* **64:** 171-179

ACTA
PROTOZOOLOGICA

Brachiola gambiae sp. n. the Microsporidian Parasite of *Anopheles gambiae* and *A. melas* in Liberia

Jaroslav WEISER[1] and Zdeněk ŽIŽKA[2]

[1]Insect Pathology, Institute of Entomology, Czech Academy of Sciences, České Budejovice; [2]Electron Microscopy, Institute of Microbiology, Czech Academy of Sciences, Prague, Czech Republic

Summary. *Brachiola gambiae* sp. n., former *Nosema* cf. *stegomyiae,* infected natural and insectary colonies of *Anopheles gambiae* and *A. melas* in Liberia and reduced susceptivity of the mosquito to development of malaria parasites and their transmission to man. It infects most tissues of adult male and female mosquitoes, destroying the midgut, Malpighian tubules, the fat body, muscles, hypoderm and connective tissues. It is usually transmitted with feces released by mosquitoes during feeding on cotton swabs with honey water. In sporogony the oval binucleate spores, 2.5-3 × 1.5-2 µm, have an anisofilar polar filament coiled in 9 coils in one row. Five anterior coils are of larger diameter than the posterior three to four. Macrospores 3-4 × 2 µm form a low percentage of mature spores (1:30). Tubulo-vesicular secretions are present.

Key Words: *Anopheles gambiae, A. melas*, *Brachiola gambiae* sp. n.*,* life cycle, *Nosema stegomyiae,* spore morphology.

INTRODUCTION

The recent identification of *Brachiola vesicularum* Cali, Takvorian, Lewin, Rendel, Sian, Wittner, Tanowitz, Koehne et Weiss, 1998 as a new genus and species of microsporidia infecting man associated with AIDS and the transfer (Lowman *et al*. 2000) of *Nosema algerae* Vávra and Undeen 1970 to the same genus brought up the question of the systematic position of other mosquito born microsporidia with direct infectivity. In 1959 Fox and Weiser published a case of a *Nosema* identified at that time as *Nosema stegomyiae,* isolated from rearing

of *Anopheles gambiae* in Liberia, preventing the development of malaria parasites in infected mosquitoes. The microsporidian caused destructive epizooties in mosquito rearing in the insectary. The pathogen with minute oval binucleate spores 2.5-3 × 1.5-2 µm (Fox and Weiser 1959) was a very aggressive pathogen attacking all tissues of adult mosquitoes. Present were also macrospores 3 × 5 µm. It was transmitted in food in mosquito colonies and released with the feces of all infected animals. The main source of infection in colonies was infected cotton feeding wads with sugar water or honey where infected animals defecated during feeding. This microsporidian infected beside *A. gambiae* also *A. melas.*

Former mentions of microsporidian infections of mosquitoes in rearing and nature were of *Plistophora*

Address for correspondence: Jaroslav Weiser, Herálecká 964, Praha 4, 140 00 Czech Republic; E-mail: weiser@biomed.cas.cz

stegomyiae by Marchoux *et al.* 1903, *N. stegomyiae* Lutz and Splendore 1908, *N. stegomyiae* Simond 1903 in *Aedes aegypti* and *N. anophelis* Kudo 1924 in *Anopheles quadrimaculatus.* The microsporidia involved had all oval spores 3.5-7 × 2-2.5 µm, therefore the microsporidia from Liberia were identified as belonging to this group. Relations of these infections were not clear, but the general pathology of such infections was rather similar and very typical. They often caused spectacular massive mosquito mortality in rearing and therefore all were considered as conspecific. In 1970 Vávra and Undeen described another microsporidian, *N. algerae* from a colony of *Anopheles stephensi,* and this organism, causing numerous epizooties in mosquito rearing, was studied further repeatedly in many cases but its relation to *N. stegomyiae* was not investigated. In all cases reported after 1970 the spore size was identical, 3.5-6 × 2.5-3 µm. The difference in size of mature spores (2.5 µm in *N. stegomyiae* Fox et Weiser, 1959 and 4.5-5 µm in *N. algerae* Vávra et Undeen, 1970) were overlooked due to the fact that both species have elongate sporoblasts about of the same size (4.5-5 µm) and these were in fresh material and section preparations difficult to distinguish from mature spores. Later it was shown that *N. algerae* survives under temperatures close to 37°C in tissue culture and to some extent also in vertebrate hosts. Recently *Brachiola vesicularum* infecting man was established as a type for a genus of microsporidia surviving under higher temperatures, with specific surface secretions produced during late schizogony. *N. algerae,* with the same type of secretions, was transferred to the newly formed genus *Brachiola.* Both species have also some similar ultrastructural details in the organization of the polar filament (terminal part thinner). *B. vesicularum* is not known to appear in rearing of mosquitoes. It is a pathogen of immunodeficient man. The *N. stegomyiae* of Fox and Weiser (1959) isolated from an infected mosquito colony caused a similar pathology as *B. algerae,* but its spores were of the size of *B. vesicularum.* Therefore the old material from Liberia was used for comparison and new evaluation.

MATERIALS AND METHODS

The type series for *Nosema* cf. *stegomyiae* Fox and Weiser, 1959 was prepared from 70% alcohol fixed infected adults of *Anopheles gambiae* from rearing at the Liberian Institute, Harbel, Liberia. There were no smears available. Adult mosquitoes were refixed in Bouin´s,

embedded in paraffin and cut in sections 4-6 µm thick. Part of this material stained with Heidenhain´s iron hematoxylin and mounted in Canada balsam in 1957 was used for reprocessing for TEM. Slides were opened, balsam was removed and sections were transferred into alcohol and water. The sections were closed in 2% agar, refixed in 2% glutaraldehyde in cacodylate buffer, postfixed in 1% osmium tetroxide, washed in buffer and dehydrated in alcohol. The material was embedded in Epon and ultrathin sections were contrasted with uranyl acetate and lead citrate and inspected in a Philips EM 300 TEM.

RESULTS

Optical microscopy and pathology

According to R. Fox (personal comm.), at the Harbel insectary the adult mosquitoes, males and females were infected. There was no evidence of larval infection. Infected females did not produce progeny. Most infections of adults started only after feeding. Spores were released in infected feces and adult mosquitoes in rearing were infected with contaminated sugar solution offered in wads to males and used also by females. Besides fecal pellets also saliva contained spore material released from bursting cells in the pharyngeal pump of the mosquitoes. After observations by R. Fox (personal comm.) during dissections of living animals, the pharyngeal pump and the foregut were the primary location of the infection in every mosquito before spread of infection to all other organs.

After entry of some vegetative stages in the host tissue (Fig. 1) sporogonial stages filled the centre of the lobe with stages of the same degree of development (Figs 3, 5), destroyed the midgut, the Malpighian tubules and invaded the hypoderm and fat body. They infected the connective tissues of the ovary and muscles (Fig. 2).

In most regions of the fat body adjacent to the body cavity there are broad oval brown bodies, in their final size 6 × 8 µm (Figs 2, 4). The brown mass is clear, not stained with haematoxylin, without any granulation and in the centre of the body is one single spore of the microsporidian (Figs 4, 6). This brown mass (melanin) - ensheeted spores are solitary, do not form coherent masses and have no connection with any period of the invasive process of the microsporidian in tissues. They are mainly in the hypoderm and adjacent layers of the fat body.

The center of the midgut inside the peritrophic membrane is filled with remains of red blood cells and groups of spores. These spores have their wall impregnated with brown coagulate. This explains some early obser-
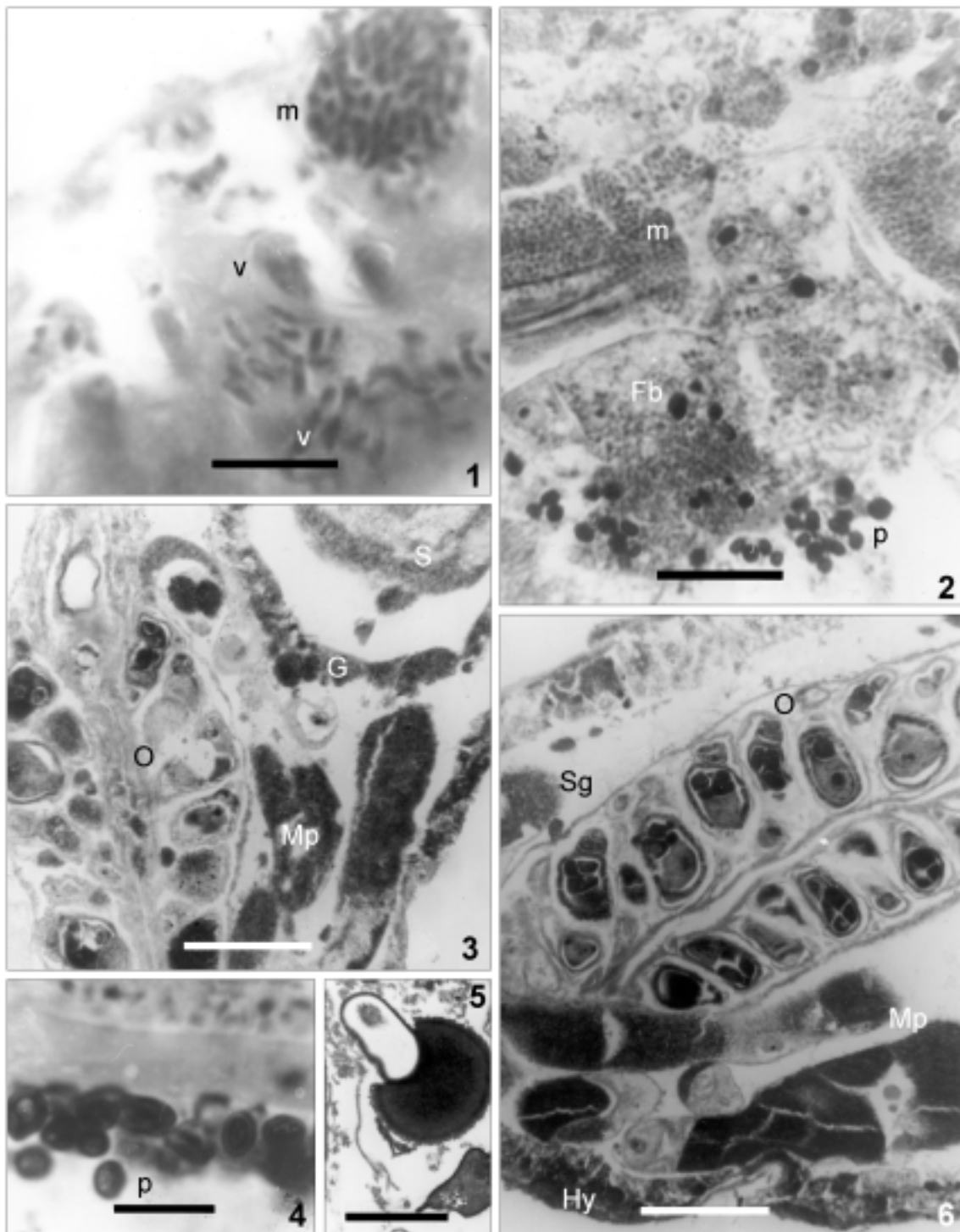
Figs 1-6. 1 - *Brachiola gambiae* sp. n. (Heidenhain); **2** - infected muscle of *Anopheles gambia,* ensheathed spores with melanin; **3** - body of a female mosquito infected with *B. gambiae* with eggs degenerating. In the gut content are released spores in part closed in a brown sheath of melanin; **4** - spores ensheathed with melanin and muscle filled with spores; **5** - spore with melanin cover; **6** - heavy infection of female mosquito Malpighian tubules, salivary glands and hypoderm while ovary is not infected. Fb - fat body, G - dark spores fill cells of the midgut epithel, Hy - hypoderm, m - spores in muscle, Mp - Malpighian tubules, O - ovary, p - ensheathed spores with melanin, S - spores, Sg - salivary glands, v - schizonts in the fat body. Scale bars 3 µm (5); 10 µm (4); 15 µm (1) - 25 µm (2, 3, 6).
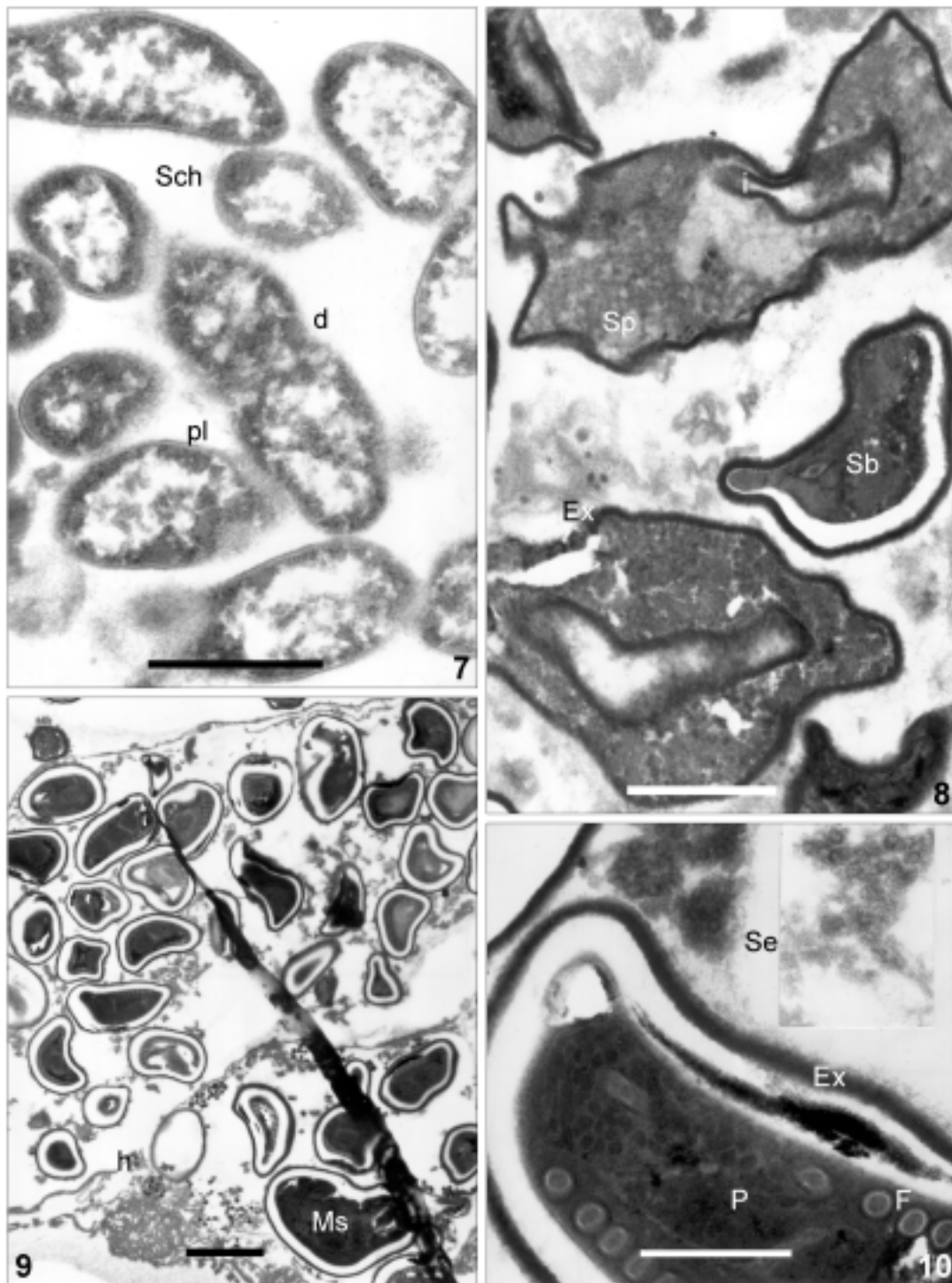
Figs 7-10. 7 - *Brachiola gambiae* sp. n. schizonts with destroyed structures of nuclei and smooth plasmalemma. Schizonts of the same stage, formed by synchronous binary fission. The grouping is not closed in any sac or pansporoblast. 8 - crenate sporonts with deep invaginations of their wall, plasmalemma is dissolved. The smooth cell wall is thick and formed of a layer of fine electron-dense granulations. Sporoblast with forming polar filament. 9 - group of mature spores in the remains of the membrane of the host cell. Spore wall not rigid, twisted, on the side a macrospore. 10 - vesiculo-tubular structures produced during sporogony, damaged by other fixation, not connected with the exospore of the spore. In its interior cross sections of the polar filament and the polaroplast. d - dividing stage, E - electron-dense granulations, Ex - exospore wall, F - polar filament, h - host cell, i - invaginations of wall, MS - macrospore, P - polaroplast, pl - smooth plasmalemma, Sb - sporoblasts, Sch - schizonts, Se - vesiculo-tubular structures, Sp - crenate sporonts, Scale bars 500 nm (8, 10); 1 μm (7); 2 μm (9).
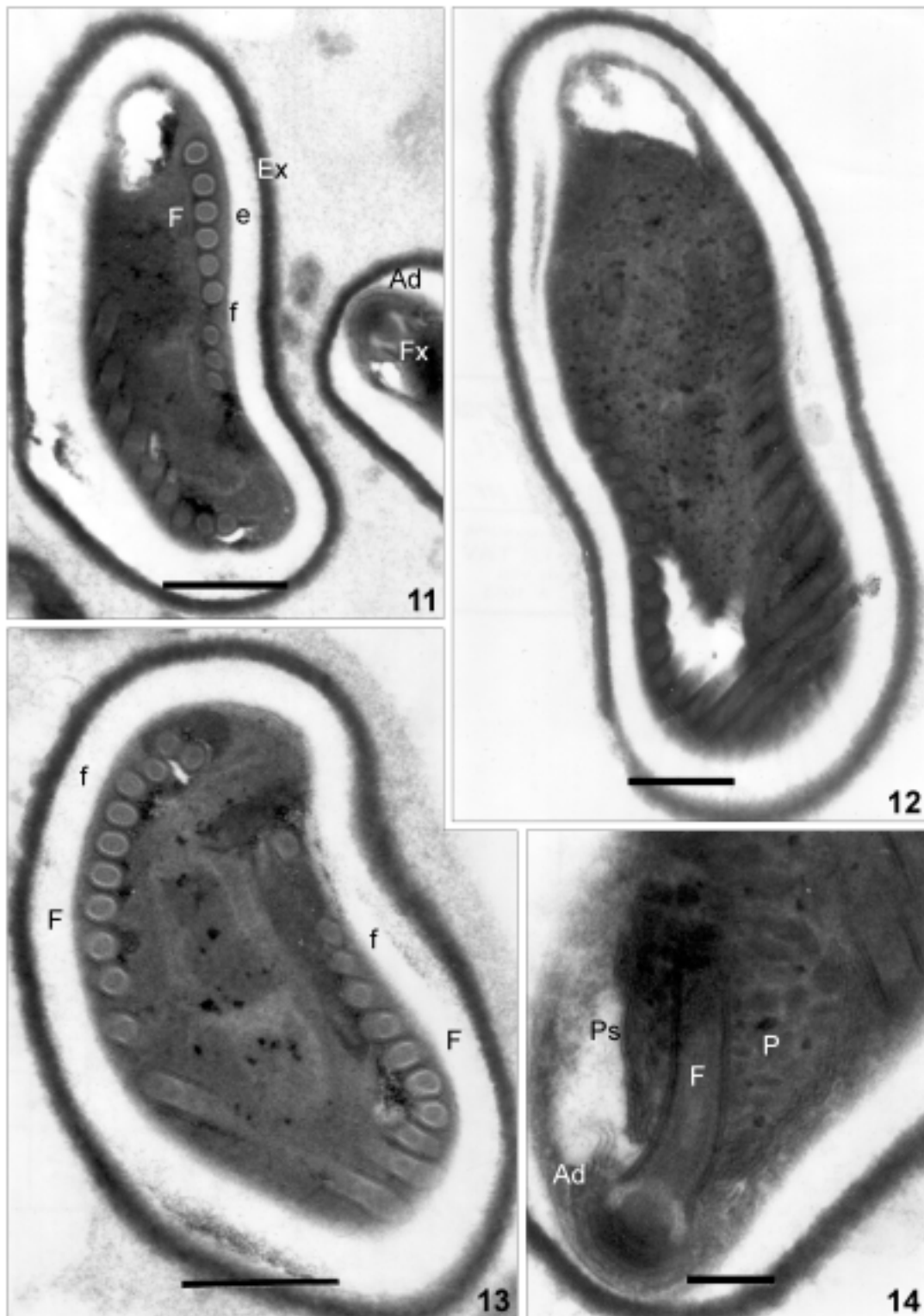
Figs 11-14. 11 - *Brachiola gambiae* sp. n. mature spore with finely granular exospore and lucent endospore, six larger coils of polar filament and three with minor diameter. Other spore with anchoring disc and the electron lucent fixation of the polar filament. **12** - macrospore with 13 coils of polar filament, without apparent anisofilarity. **13** - normal spore with 9 large and 3 reduced coils and two nuclei. **14** - apical spore end with anchoring disc, fixation of the polar filament and polaroplast closed in the polar sac. Ad - anchoring disc, e - endospore wall, Ex - exospore wall, f - polar filament of minor diameter, F - polar filament, P - polaroplast, Ps - polar sac. Scale bars 200 nm (13, 14); 500 nm (11, 12).

vations of Marchoux *et al.* (1903) and Simond (1903). Spores in the area between infected epithelial cells and the peritrophic membrane were not stained. The spread of the microsporidian in the host is mediated by hemocytes containing spores. In the mass of spores in different tissues there are two types of spores: such with intensive staining with Hematoxylin and others, which are less stained. On sections there is no perfect evidence of empty spores. Vegetative stages (Fig. 1) are visible only as empty areas in the infected tissue, usually on the border of a large group. In narrow muscle bands (Fig. 4) the spores are arranged in rows, in dense tissues such as midgut muscles or Malpighian tubules (Figs 3, 6) the spores are in dense groups, in the fat body (Fig. 2) they are distributed in the cytoplasm around fat droplets. In sections of the ovary the infection appears late and infects mainly the connective tissue (Fig. 6) and nutrient cells of the ovary. Eggs without nutrition degenerated (Fig. 3). In other cases developing eggs were not infected (Fig. 6). Fresh spore material and smears were not available and the exact determination of sizes and shapes of spores (Figs 1, 2) was difficult (missing exact contours in dried smears). Therefore, supported by identical symptoms of the mosquito attack in rearing, the organism was indicated as identical with *Nosema stegomyiae* Marchoux, Salimbeni et Simond, 1903. The diagnosis was supported by dense groupings of mature spores in infected tissues and the brown impregnation of spores in the gut content. Some details in descriptions of Marchoux *et al.* (1903) and Simond (1903) indicate a possibility of a further species involved (plasmodial stages, reniform spores), but could be connected with the different host.

Ultrastructure

In the re-fixed and stained ultrathin sections we find stages of the end of schizogony, early and late sporonts and mature spores. Late schizonts are in groups of twenty and more (Fig. 7) seen as oval bodies, 2.5-3 × 0.8 µm, some constricted in the centre. The nucleus (diplokaryon?) is evident due to fixation of paraffin blocks only as an irregular empty space without nuclear membrane in the centre of the cell with content in irregular clumps. The schizont is closed in a fine continuous smooth coat of electron dense material (Fig. 7). The outer surface of this coat is covered by a thin layer of fine electron dense granulation, without irregular secretory processes. Evidently the schizonts are formed by synchronous nuclear division and binary fission. In the interspace are fine electron dense concretions without direct connection with any stage (Fig. 10). The group is not closed in any sac or pansporoblast.

The next step, thick walled sporonts with smooth walls (Fig. 8) are rather rare in the studied material. Where present they are in groups of the same age. Usually they measure 2.5 × 3 µm. Their wall is of fine granular electron-dense material, 37-40 nm thick, without a smooth layer on their outer or inner surface. There is no evidence of any system of gaps or blisters in this wall. There is no electron lucent layer between the wall and the cytoplasm. The cytoplasm is a dense granulated mass without distinct diplokaryotic nucleus, its eventual location visible only as confluent grouping of empty areas in the centre. Internal structures were destroyed during the fixation with Bouin's in 1957. Eventual surface deposits on the sporonts were dissolved. Tiny membranous wicks and minute surface granulations are coiled in the interspace (Fig. 10). Evaginations of the plasmalemma were absent, but there are deep invaginations (Fig. 8) connected with formation of crenate sporonts with first signs of formation of the polar filament.

Spores are oval to pyriform, with deformations and compressions from fixation. Fixed for TEM they measure 2.2-2.5 × 1.4-1.6 µm. They appear in dense groups, all of the same stage of development (Fig. 9). The electron-dense exospore (Figs 11, 13) is 70 nm thick, the electron-lucent interspace, the endospore, is 170 nm thick (Figs 11, 13). The anterior pole is attenuated, 50 nm. The plasmalemma is very thin and indistinct. In the centre are two electron dense nuclei. The polar filament is fixed in the anterior hemispheric knoblike anchoring disc 280-300 × 120 µm (Figs 11, 14). The polar sac encloses the polaroplast with irregular remains of its lamellar structure. In it is fixed the polar filament with its manubrium part with a broadened end 150-180 nm in diameter, with a distinct electron lucent ring. The filament has a system of 20 electron-lucent slightly twisted longitudinal columns. The coiled part of the filament is anisofilar, has 6 broader (diam. 100 nm) and 3 narrow (diam. 70 nm) turns (Fig. 11). Besides spores with 9 (6+3) turns there are some with up to 12 turns (8+4) (Fig. 13). The fixing umbrella is adhering to the plasmalemma in a collar 150 nm broad.

At the periphery of a group of normal spores are some larger (macro-) spores (Figs 9, 12), usually 1in 30.

They are larger in size, 4.5-5 × 2 μm, with all structures equal to normal spores, but with up to 13 turns of the polar filament.

DISCUSSION

It is interesting that all published cases of infections of mosquito colonies after 1970 were ascribed to *Nosema algerae* with typical oval spores 3-4.5 × 2-2.5 μm. Possibly in some cases the real size of spores was not measured due to the typical spectacular massive invasion of mosquito rearing and differences in spore size were estimated as natural variability.

The *Brachiola* definition is based on thermophily of the members of the genus, proliferation and sporulation at temperatures close to 37°C. Schizogony with diplokaryotic schizonts dividing by simple fission without multinucleate plasmodia. Stages are not closed in any membrane. Late schizonts with a layer of secretion on their plasmalemma producing rows of blisters and ridges and free vesiculo-tubular electron dense secretions. They are connected with different proliferations on the surface of late schizonts. Starting with early sporogony, binucleate sporonts are covered with a thick layer of fine granular electron-dense material replacing the plasmalemma and forming later the exospore. Groups of vesiculo-tubular secretions are fixed to the exospore or remain as appendages fixed to the spore. Sporogony is disporoblastic, sporonts produce two diplokaryotic spores with fine granular exospore. Spores with short polar filament with up to 10 coils, of which the final three (*B. vesicularum*) or one *(B. algerae)* are narrower. In *B. algerae* the principal host is an insect (mosquito, caterpillar), in *B. vesicularum* the host is the immunodeficient human patient.

Some parts of this definition need further verification. The separation of the genus *Brachiola* is characterized mainly based on its survival in warm-blooded animals at 37°C. This characteristic seems to be in *B. (N.) algerae* achieved artificially. In Lowman *et al*. (2000) evidently spores in figures 31-34 are not normal and may not be able to infect a normal warm-blooded host. But after conjunctival instillation (Vávra personal comm. 2002) *B. algerae* appears in liver and other organs without degeneration of spores. In the survival of *B. vesicularum* there is no experience with development of the pathogen in normal human hosts and its entry of the pathogen into the host and its circulation. With this experience the requirement of development of *Brachiola* in warm-

blooded hosts for definition of the genus is rather weak and may depend very much of qualities of strains and resistance of hosts. If we consider myositis of left leg muscle of the patient without considering the way of entry and tissue affinity under support of AIDS, we should not base the definition of the genus on such details.

A comparison of ultrastructures of *N. stegomyiae* Fox et Weiser, 1959 with *B. vesicularum* brings interesting similarities. The development of both microsporidia is very similar. Schizogony (proliferate forms) have a thin smooth plasmalemma and the formation of sporonts is signalized by thickening of the outer wall composed of electron-dense granular material. On the surface of this wall there is in our material no sign of any adhering vesiculo-tubular secretion (eventually destroyed due to previous fixation for paraffin). There are groups of vesiculo-tubular material present in groupings of mature spores (Fig. 10).

In crenellated late sporonts there are deep invaginations of the wall in *N. stegomyiae* (Fig. 8). Almost identical is the ultrastructure of mature spores of *B. vesicularum* and *N. stegomyiae*: the structure of the spore wall and the size and shape of binucleate spores, the type of polar filament and its anisofilar formation with three narrow cross sections and 6 ordinary sections.

There is no experience with survival and development of *N. stegomyiae* under higher temperature but conditions of rearing of mosquitoes in tropical Africa offered temperatures close to 30°C. R. Fox (personal comm.), considered as possible a transmission of the microsporidian from cage to cage with the chicken used for feeding adults, with contamination of their skin with infective feces. The microsporidian with spores 2.5-3 × 2 μm has not been recognized again during the last 50 years. Nevertheless, evident differences of spore size in the Nigerian case and in *B. algerae* and the striking ultrastructural similarity of the (1957) material with members of the genus *Brachiola* invites to correct the old identification and to propose for the pathogen of *Anopheles gambiae* and *A. melas* in Liberia, interactive with transmission of malaria parasites in mosquitoes described above, the new name, *Brachiola gambiae* sp. n.

REFERENCES

Cali A., Takvorian P. M., Lewin S., Rendel M., Sian C. S., Wittner M., Tanowitz H. B., Koehne E., Weiss L. M. (1998) *Brachiola*

vesicularum n. g., n. sp., a new microsporidium associated with AIDS and myositis. *J. Eukaryot. Microbiol.* **45:** 240-251

Fox R. M., Weiser J. (1959) A microsporidian parasite of *Anopheles gambiae* in Liberia. *J. Parasitol.* **45:** 21-30

Kudo R. (1924) A biologic and taxonomic study of the Microsporidia. *Ill. Biol. Monographs.* **9:** 1-268

Lowman P. M., Takvorian P. M., Cali A. (2000) The effect of elevated temperatures and various time-temperature combinations on the development of *Brachiola (Nosema) algerae* n. comb. in mammalian cell culture. *J. Eukaryot. Microbiol.* **47:** 221-234

Lutz A., Splendore A. (1908) Ueber Pebrine und verwandte Mikrosporidien, II. Z*entrbl. Bakt. Abt. I.* **45:** 311-315

Marchoux E., Salimbeni A., Simond P. L. (1903) La fievre jaune. Rapport de la mission francaise. *Ann. Inst. Pasteur* **17:** 665-731

Simond P. L. (1903) Note sur une Sporozoaire du genre *Nosema*, parasite du *Stegomyia fasciata. Compt. rend. Soc. Biol.* **55:** 1335-1337

Vávra J., Undeen A. H. (1970) *Nosema algerae* n. sp. a pathogen in a laboratory colony of *Anopheles stephensi* Linston. *J. Protozool.* **17:** 240-249

ACTA
PROTOZOOLOGICA

The Life Cycle of *Leidyana ampulla* sp. n. (Apicomplexa: Eugregarinorida: Leidyanidae) in the Grasshopper *Ronderosia bergi* (Stål) (Orthoptera: Acrididae: Melanoplinae)

Carlos E. LANGE[1] and María Marta CIGLIANO[2]

[1]Scientific Investigations Commission (CIC) of Buenos Aires province, Center for Parasitological Studies and Vectors (CEPAVE), La Plata National University (UNLP) and National Research Council (CONICET); [2]Department of Entomology, Museum of Natural Sciences, La Plata National University (UNLP), La Plata, Argentina

Summary. *Leidyana ampulla*, a new species of septate eugregarine, is described from the Argentine grasshopper *Ronderosia bergi*. Prevalence was high (76 %, n = 50) in San Pedro, Misiones province in northeastern Argentina, but the parasite was not detected in the center of the country (Bagual and Buena Esperanza in San Luis province, and Pehuajó in Buenos Aires province) where *R. bergi* is also normally an abundant species. Trophozoites, which had a simple, globular epimerite and were solitary, occurred attached to the intestinal epithelium. During transition from trophozoite to gamont the epimerite was not shedded but retracted into the protomerite. Gamonts were solitary, had a characteristic bottle-like appearance, and a total length that ranged from 280 to 584 µm (mean: 526.2 ± 13.3). Syzygy was biassociative and caudofrontral, the associates resembled each other in shape but not size. Spherical gametocysts measured 104 to 360 µm (mean: 247.7 ± 49.3). Gametocyst dehiscence was by a variable number of sporoducts (up to 12). Oocysts were dolioform, measuring 5.7 ± 0.06 by 2.8 ± 0.08 µm.

Key words: Argentina, grasshopper, gregarine, *Leidyana*, parasite, Protozoa.

INTRODUCTION

The melanopline grasshopper *Ronderosia bergi* (Stål) is widely distributed in southern South America, occupying eastern North and central Argentina, Uruguay, most of Paraguay, the southeastern tip of Bolivia, and southeastern Brazil (COPR 1982, Cigliano 1997). Dam-

age to crops and forage by *R. bergi* has been reported in some areas (Ronderos 1959, COPR 1982). In spite of the common occurrence and economic importance of *R. bergi*, virtually nothing is known about the parasites and pathogens that are associated to it. In recent years, while conducting surveys in search for natural enemies of grasshoppers in Argentina, we noticed an undescribed septate eugregarine (Eugregarinorida: Septatorina) parasitizing *R. bergi*. The present study describes the new gregarine, *Leidyana ampulla* sp. n., based on life cycle observations, and provides information on its natural occurrence.

Address for corespondence: Carlos E. Lange, CEPAVE, calle 2 nr. 584, (1900) La Plata, Argentina. Fax: 54 221 423 2327 E-mail: Lange@mail.retina.ar

MATERIALS AND METHODS

Older nymphs (fourth and fifth instars) and adults of *R. bergi* were collected with sweep nets in fields at the vicinity of the localities of San Pedro (northern Misiones province), Pehuajó (western Buenos Aires province), and Bagual and Buena Esperanza (southern San Luis province), areas where *R. bergi* is normally common. The samples were immediately transferred to the Center for Parasitological Studies and Vectors (CEPAVE) where the grasshoppers were either frozen at -32°C upon arrival for later examination or were maintained in groups in wire-screened cages in rearing rooms under controlled conditions (30°C, L:D = 14:10, 40 % RH) as described by Henry (1985) but without the addition of antibiotics in the diet. Grasshoppers in cages were kept for several weeks and individuals were frequently examined in order to conduct the observations. Frozen samples were employed for estimating the natural prevalence, infection intensity, and location of the gregarine within the host. All grasshoppers collected in Pehuajó (n = 108) and Bagual (n = 103) were frozen. Grasshoppers from San Pedro and Buena Esperanza were either frozen (n = 50 for San Pedro; n = 100 for Buena Esperanza) or kept in cages (n = 44 for San Pedro; n = 30 for Buena Esperanza) in two different rooms.

The grasshoppers, thawed or alive, were examined by longitudinal, ventral dissection under a stereo zoom microscope. Before dissecting living individuals, a droplet of haemolymph was obtained by pulling a leg off. Haemolymph samples were readily examined as fresh preparations under a phase-contrast microscope (400×, 1000×). Fresh mounts of host intestinal tissue and luminal contents were prepared either with or without a small drop of one-quarter-strength Ringer´s solution (Poinar and Thomas 1984), and observed and photographed under phase-contrast microscopy. Some entire alimentary canals were removed, fixed in alcoholic Bouin´s fluid, embedded in paraffin, sectioned at 3-5 µm, and stained with Heidenhain´s haematoxylin (Becnel 1997). Gregarine gametocysts were recovered with a capillary tube appressed to incised midgut or hindgut tissues or with a delicate brush from faeces, and transferred to Petri dishes containing moistened filter paper, where they were held at room temperature for maturation and dehiscence. Oocysts were obtained from chains dehisced from gametocysts and suspended in double distilled water when desired. Emergence of sporozoites was induced by placing oocysts in fresh mounts of host digestive tract extracts as described by Hoshide *et al.* (1994). The developmental stages, gametocysts, and oocysts from fresh mounts were measured using an ocular micrometer. Terminology for the stages of the gregarine follows Levine (1971).

For scanning electron microscopy, oocysts were fixed in 2.5% (v/v) glutaraldehyde buffered with 0.1 M cacodylate buffer (pH 7.4), dried in a critical point dryer or treated with hexamethydisilazane (Nation 1983, Lange 1993), coated with gold-palladium, and photographed with a JEOL-JSM-T100 electron microscope.

RESULTS

The gregarine was detected in 76 % of the frozen grasshoppers from San Pedro, and was present in increasing intensity as time went by in grasshoppers kept in cages from the same locality. Samples from Bagual, Buena Esperanza, and Pehuajó never revealed the presence of the parasite. Detection of the gregarine in frozen samples was by observation of some solitary gamonts in the gut and gastric caecae. Trophozoites, gamonts in association, and gametocysts were not observed in grasshoppers from frozen samples. On the contrary, the presence of the gregarine in *R. bergi* from San Pedro held in cages for prolonged periods of time was abundant, as attached trophozoites (Fig. 1) and solitary gamonts (Fig. 3) in midgut and gastric caecae, and as gametocysts (Figs 5, 6) in midgut, hindgut and faeces. The gregarine was never observed in haemolymph samples.

Very young, unsegmented or segmenting trophozoites were not seen. The earliest trophozoites observed were slender, solitary bodies that were typically divided into epimerite, protomerite, and deutomerite, and were attached to the intestinal epithelium (Fig. 1). Only once a trophozoite was seen free (i.e. unattached to the host intestinal epithelium), and its epimerite was simple and globular (Fig. 2). Its total length was 103 µm.

Gamonts (Figs 3, 4), the most common developmental stages observed, were normally whitish, and visible through the wall of the midgut and gastric caecae under the dissecting microscope. Gamonts ranged in length from 280 to 584 µm (Table 1) and had a slender, bottle-like appearance. They were solitary and showed progressive locomotion by gliding (Fig. 3). The epimerite of trophozoites appeared to retract into the protomerite during the transition trophozoite/gamont because a scar where the epimerite would have been eventually shedded

Table 1. Range and mean (± SE) measurements in µm of gamonts of *Leidyana ampulla* sp. n. (n = 30). (TL) total length, (LP) length of protomerite, (LD) length of deutomerite, (WP) width of protomerite, (WD) width of deutomerite.

Character	Range	Mean
TL	280-584	526.2 ± 13.3
LP	96-192	129.8 ± 5.3
LD	180-464	396.4 ± 12.4
WP	72-160	133.3 ± 4.8
WD	104-296	223.1 ± 8.5
TL:LD	1 : 1.2-1.7	1 : 1.3
WD:WP	1 : 1.3-2	1 : 1.7
TL:LP	1 : 2.4-5.1	1 : 4.2
LD:WD	1 : 1.2-2.3	1 : 1.8
WP:LP	1 : 0.6-1.4	1 : 1.1
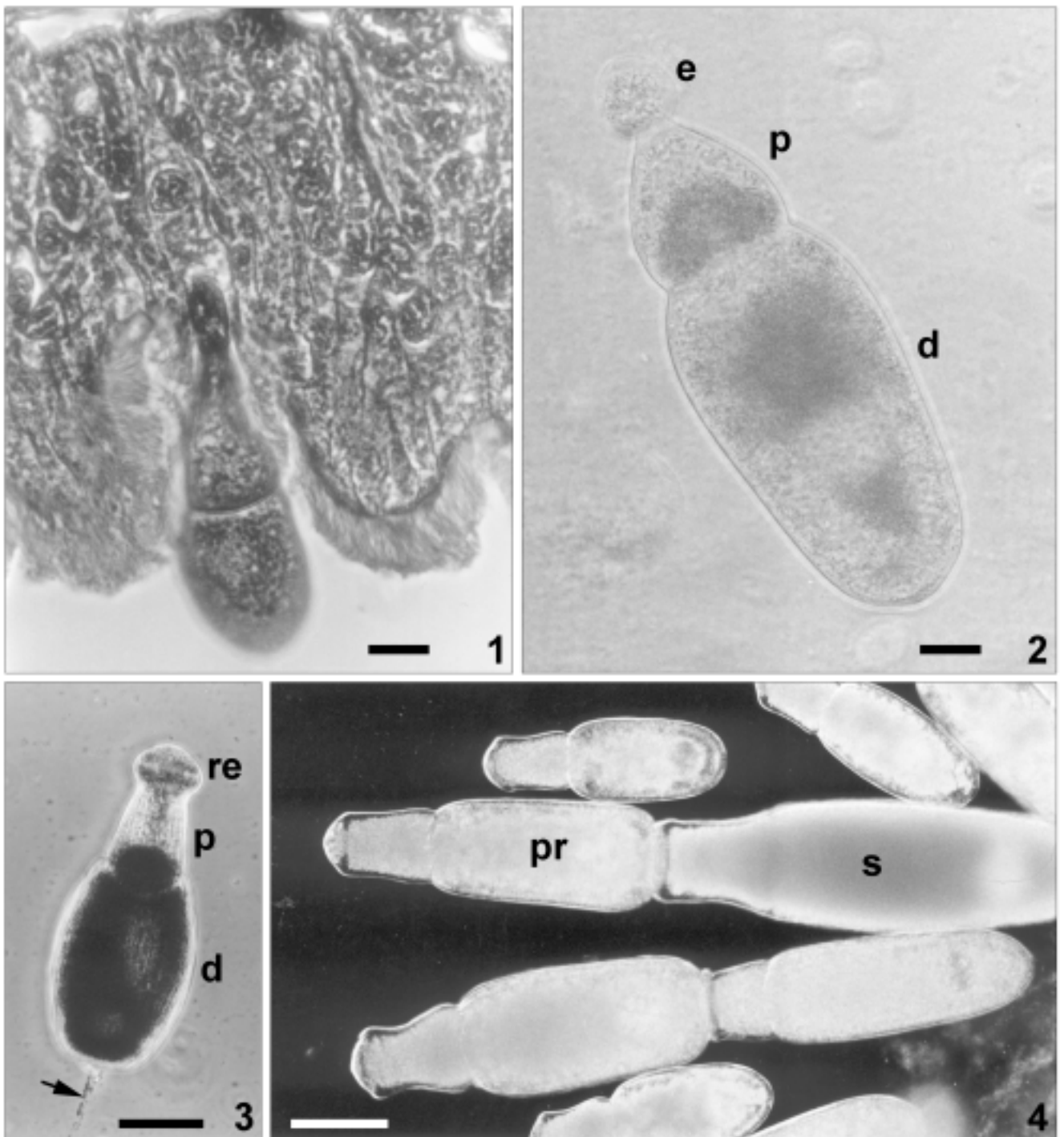
Figs 1-4. Trophozoites and gamonts of *Leidyana ampulla* sp. n . **1** - young trophozoite attached to midgut epithelium; **2** - unattached trophozoite; **3** - solitary, bottle-like shaped gamont leaving a trail of unknown material (arrow) while gliding forward. Also note the absence of a scar in the protomerite where the epimerite was located, and the bulb shape of the anterior end of protomerite where the epimerite was retracted; **4** - solitary gamonts and gamonts in biassociative, caudofrontal syzygy. e - epimerite, d - deutomerite, p - protomerite, pr - primite, re - retracted epimerite, s - satellite. Scale bars 10 μm (1, 2); 100 μm (3, 4).
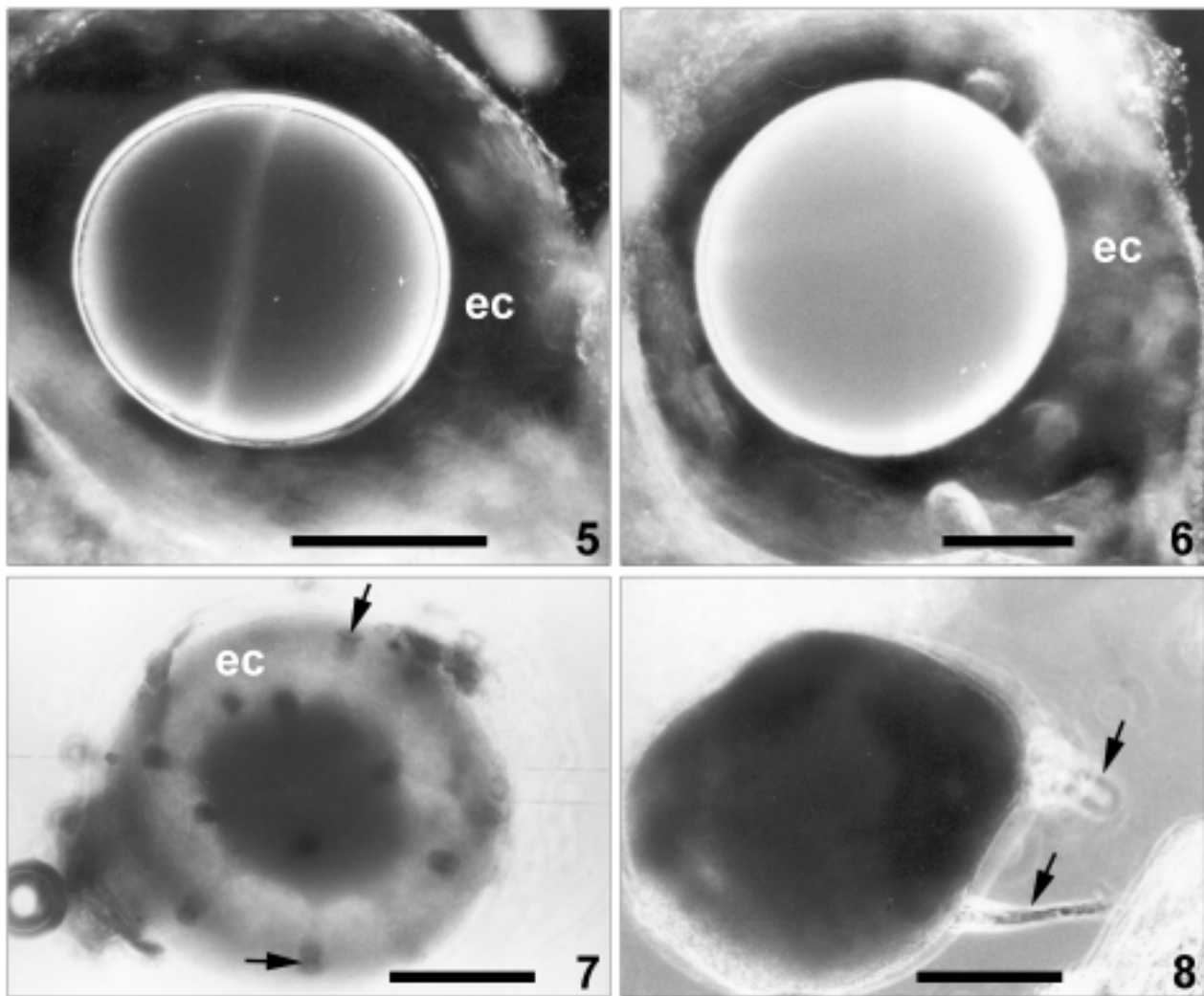
Figs 5-8. Gametocysts of *Leidyana ampulla* sp. n. **5** - young gametocyst in which members of the syzygyal association are still in separate condition; **6** - immature gametocysts; **7** - mature gametocyst showing basal discs of sporoducts (arrows); **8** - disrupted gametocyst showing two everted sporoducts (arrows). ec - ectocyte. Scale bars 100 μm (5-8).

was never seen in protomerites of gamonts, and these also showed an evident thickening at the protomerite´s free end (Fig. 3). Only once gamonts in biassociative, caudofrontal syzygy were seen (Fig. 4). Primites and satellites resembled each other in shape but not size. Rotational movements, which in gregarines normally mark the onset of encystment (Lange and Wittenstein 2002), were not seen.

Gametocysts (Figs 5-8) were spherical, yellowish or whitish, and variable in size, measuring from 104 to 360 μm in diameter (mean: 247.7 ± 49.3; n = 50). A hyaline coat, the ectocyst, of an unusually large thickness of up to 100 μm was normally evident (Figs 5-

7). The two members of a syzygy were usually still discernable as separate entities in gametocysts found in the midgut or hindgut (Fig. 5). In gametocysts observed in faeces, fusion of members was normally already accomplished (Fig. 6). Mature gametocysts in Petri dishes with moistened filter paper showed the basal discs of the sporoducts, easily seen due to their orange coloration (Fig. 7). The number of basal discs per gametocysts was difficult to determine but appeared to be variable. The maximum number observed was 12. Eversion of sporoducts resulted after further retention of gametocysts under humid conditions (Fig. 8). Sporoducts were basally wide but its length could not be determined.
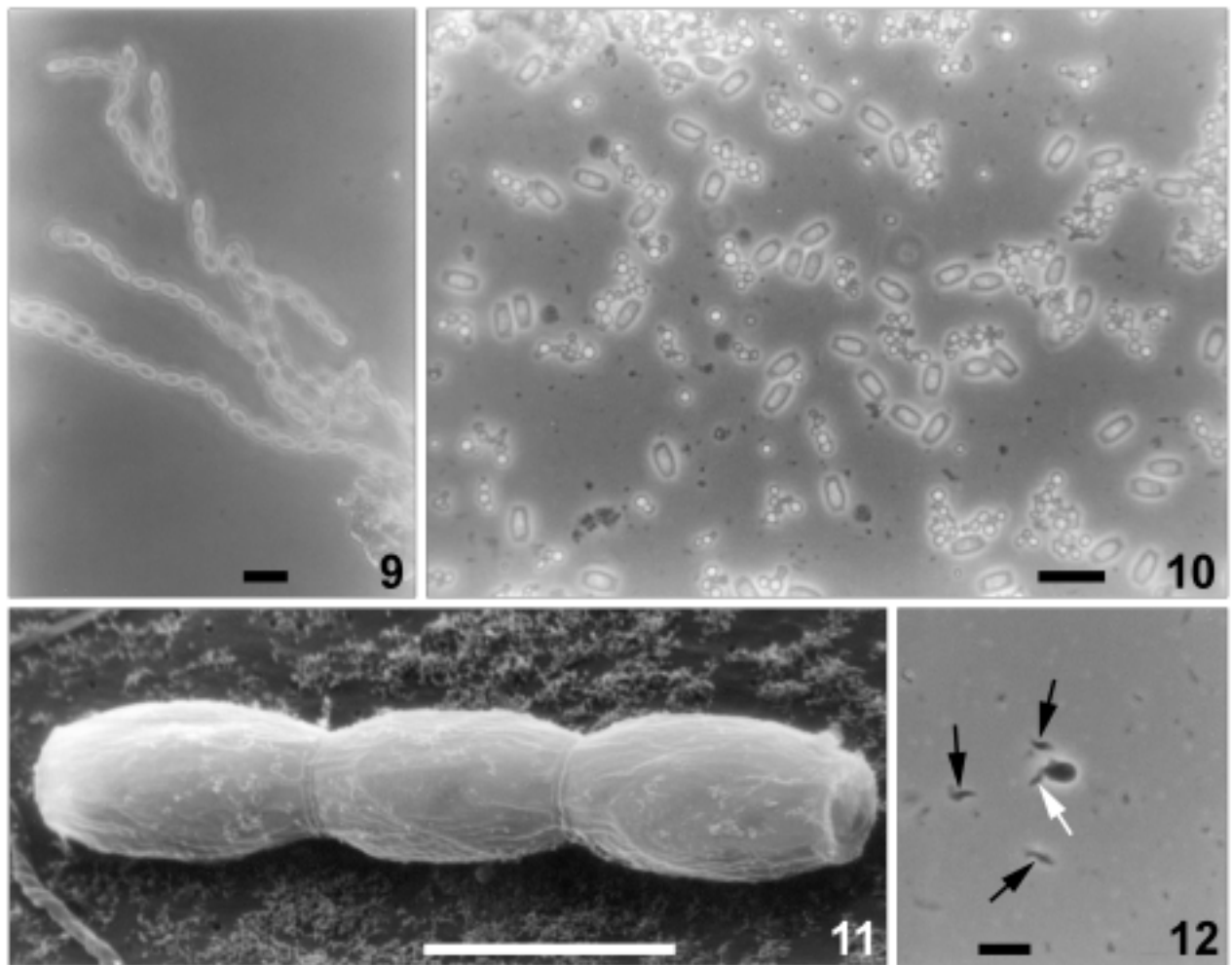
Figs 9-12. Oocysts and sporozoites of *Leidyana ampulla* sp. n. **9** - disrupted chains of oocysts just dehisced from gametocysts; **10** - isolated oocysts in suspension; **11** - short section of oocyst chain (three oocysts); **12** - a sporozoite emerging from an oocyst (white arrow) and three emerged sporozoites (black arrows). Scale bars 5 µm (11); 10 µm (9, 10, 12).

Oocysts (Figs 9-12) were liberated as delicate and easily disrupted chains through the sporoducts of the gametocysts. While oocysts were still in chains they were somehow attached one after the other by their ends (Fig. 11). Oocysts were dolioform and measured 5.7 ± 0.06 by 2.8 ± 0.08 µm (n = 50). Fusiform, mobile sporozoites emerged from oocysts following addition of host digestive extracts (Fig. 12).

Diagnosis

Type host: *Ronderosia bergi* (Stål) 1878 (Orthoptera: Acrididae: Melanoplinae).

Type locality: Surroundings of San Pedro, Misiones province, northeastern Argentina.

Infection site: Epithelium and lumen of gut and gastric caecae.

Trophozoite: Attached to intestinal epithelium, and very rarely free in lumen. Solitary. Slender appearance, with simple, globular epimerite.

Gamont: Bottle-like shape, epimerite retracted into protomerite, considerable variation in size [280-548 (mean: 526.2 ± 13.3) by 104-296 (mean: 223.1 ± 8.5) µm], solitary, caudofrontal biassociation just prior to syzygy. Primite and satellite of similar shape but not size.

Gametocyst: Spherical, whitish or yellowish, and variable in size (104-360 µm in diameter, mean: 247 ± 49.3). With up to 12 basal discs of sporoducts.

Oocyst: Uniform in shape (dolioform) and size (5.7 ± 0.06 by 2.8 ± 0.08 µm).

Deposition of specimens: Type material [gamonts in AFA (alcohol-formalin-acetic acid, Richardson and Janovy 1990) and gametocysts in feces] will be designated and deposited in the collections at the "Center for Parasitological Studies and Vectors (CEPAVE)", La Plata National University, Argentina.

DISCUSSION

By having trophozoites with a simple, globular epimerite, solitary gamonts, gametocyst dehiscence by sporoducts, and dolioform oocysts, the gregarine from *R. bergi* can be clearly assigned to genus *Leidyana*, which was originally established by Watson (1915), and is the single genus in family Leidyanidae (Clopton 2000). Genus *Leidyana* is very similar in many respects to the much larger genus (in terms of known species) *Gregarina* Dufour (family Gregarinidae) but in the former the association of gamonts is delayed until the onset of syzygy while in the latter gamont association is precocious. Although genus *Leidyana* is acknowledged to be cosmopolitan in distribution (Clopton and Lucarotti 1997), the species found in *R. bergi* is the first one to be recorded in Argentina. Most of the *Leidyana* species known from orthopteroid insects have been recorded as parasites of crickets (Gryllidae) from the old world and North America (Dufour 1837; Watson 1915; Narain 1961; Corbel 1968; Geus 1969; Hoshide 1973, 1978; Haldar and Sarkar 1979; Hooger and Amoji 1986; Sarkar 1988). There is an additional record from a Malagasy cockroach (Blattaria) in North American laboratory colonies (Clopton 1995). Only one other species, *Leidyana subramanii* Pushkala and Muralirangan, has been described from a grasshopper (Acrididae: Eyprepocnemidae), *Eyprepocnemis alacris alacris* (Serville), in Tamil Nadu, India (Pushkala and Muralirangan 1998). Aside from differences based on geographical and host grounds (far apart localities, and different host species belonging to a different subfamily), which would probably suffice as justification for a separate specific status in the present case, the gregarine from *R. bergi* can also be distinguished from *L. subramanii* by its smaller oocysts (5.7 by 2.8 µm *vs.* 6.6 by 3.5 µm in *L. subramanii*), its epimerite retractile into the protomerite, and the bottle-like appearance of the gamonts. We propose the creation of a new species, *Leidyana ampulla*, for the gregarine in *R. bergi*. The specific name is taken from the Latin *ampulla* ("bottle"), and refers to the characteristic bottle-like shape of gamonts.

REFERENCES

Becnel J. J. (1997) Complementary techniques: preparations of entomopathogens and diseased specimens for more detailed study using microscopy. In: Manual of Techniques in Insect Pathology, (Ed. L. A. Lacey). Academic Press, San Diego

Cigliano M. M. (1997) *Ronderosia*, a new genus of South American Melanoplinae (Orthoptera: Acrididae). *J. Orthoptera Res.* **6**: 1-19

Clopton R. E. (1995) *Leidyana migrator* n. sp. (Apicomplexa: Eugregarinida: Leidyanidae) from the Madagascar hissing cockroach, *Gromphadorhina portentosa* (Insecta: Blattodea). *Invertebr. Biol.* **114**: 271-278

Clopton R. E. (2000) Order Eugregarinorida. In: The Illustrated Guide to the Protozoa, (Eds. J. J. Lee, G. F. Leedale, P. Bradbury). Society of Protozoologists, Lawrence, **1**: 205-288

Clopton R. E., Lucarotti C. J. (1997) *Leidyana canadensis* n. sp. (Apicomplexa: Eugregarinida) from larval eastern hemlock looper, *Lambdina fiscellaria fiscellaria* (Lepidoptera: Geometridae). *J. Euk. Microbiol.* **44**: 383-387

COPR (1982) The Locust and Grasshopper Agricultural Manual. Centre for Overseas Pest Research (COPR), London

Corbel J. C. (1968) La spécificité parasitaire des Grégarines d'Orthopteres. *Ann. Parasitol. Hum. Comp.* **43**: 25-32

Dufour L. (1837) Recherches sur quelques entozoaires et larves parasites des insectes Orthopteres et Hyménopteres. *Ann. Sci. Nat.* **7**: 5-20

Geus A. (1969) Sporentierchen, Sporozoa: die Gregarinida der land- und sußwasserbewohnenden Arthropoden Mitteleuropas. In: Die Tierwelt Deutschlands und der angrenzenden Meeresteile (Ed. F. Dahl). Gustav Fischer, Jena. **57**: 1-697

Haldar D. P., Sarkar N. K. (1979) Cephaline gregarine *Leidyana linguata* n. sp. parasite of a gryllid *Pteronemobius concolor* Walker from India. *Acta Protozool.* **18**: 435-440

Henry J. E. (1985) *Melanoplus* spp. In: Handbook of Insect Rearing, (Eds. P. Singh, R.F. Moore). Elsevier, Amsterdam, **1**: 451-464

Hooger V. V., Amoji S. D. (1986) *Leidyana bimaculata* sp. n. a new cepahline gregarine parasite of a cricket *Gryllus bimaculatus* De Geer. *Acta Protozool.* **25**: 465-470

Hoshide K. (1973) Notes on gregarines in Japan 5. A new eugregarine *Leidyana suzumushi* n. sp. from *Homoeogryllus japonicus* de Haan. *Bull. Fac. Ed. Yamaguchi Univ.* **23**: 69-75

Hoshide K. (1978) Notes on gregarines in Japan 9: Three new eugregarines and nine other gregarines from Orthoptera and Dictyoptera. *Bull. Fac. Ed. Yamaguchi Univ.* **28**: 91-126

Hoshide K., Nakamura H., Todd K. S. (1994) *In vitro* excystation of *Gregarina blattarum* oocysts. *Acta Protozool.* **33**: 67-70

Lange C. E. (1993) Aplicación del método de Nation para la preparación de microsporidios (Protozoa: Microspora) en estudios de microscopía electrónica de barrido. *Neotrópica* **39**: 35-39 (in Spanish, English summary)

Lange C. E. Wittenstein E. (2002) The life cycle of *Gregarina ronderosi* n. sp. (Apicomplexa: Gregarinidae) in the Argentine grasshopper *Dichroplus elongatus* (Orthoptera: Acrididae). *J. Invertebr. Pathol.* **79**: 27-36

Levine N. D. (1971) Uniform terminology for the protozoan subphylum Apicomplexa. *J. Protozool.* **18**: 352-355

Narain N. (1961) Studies on two cephaline gregarines from the intestine of Indian insects, *Gryllodes sigillatus* and *Liogryllus bimaculatus*. *Parasitology* **51**: 117-122

Nation J. L. (1983) A new method using hexamethyldisilazane for preparation of soft insect tissues for scanning electron microscopy. *Stain Tech.* **58:** 347-351

Poinar G. O., Thomas G.M. (1984) Laboratory Guide to Insect Pathogens and Parasites. Plenum Press, New York

Pushkala K., Muralirangan M. C. (1998) Life history and description of *Leidyana subramanii* sp. n. (Apicomplexa: Eugregarinida). A new caphaline gregarine parasite of a grasshopper (Insecta: Orthoptera) in Tamil Nadu, India. *Acta Protozool.* **37:** 247-258

Richardson S., Janovy J. (1990) *Actinocephalus carrilynnae* n. sp. (Apicomplexa: Eugregarinida) from the blue damselfly, *Enallagma civile* (Hagen). *J. Protozool.* **37:** 567-570

Ronderos R. A. (1959) Identificación de las especies de tucuras mas comunes de la provincia de Buenos Aires. *Agro* **1:** 1-31

Sarkar N. K. (1988) *Leidyana guttiventrisa* sp. n. A new cephaline gregarine (Apicomplexa: Eugregarinida) parasite of a gryllid of West Bengal, India. *Acta Protozool.* **27:** 67-73

Watson M. E. (1915) Some new gregarines from arthropods. *J. Parasitol.* **2:** 25-36

ACTA
PROTOZOOLOGICA

BOOK REVIEW

Protistology **by Klaus Hausmann, Norbert Hülsmann and Renate Radek with contributions by Hans Machemer, Maria Mulisch and Günter Steinbrück, 3rd edition, E. Schweizerbart'sche Verlagsbuchhandlung (Nägele u. Obermiller) Stuttgart, Germany; ISBN 3-510-65208-8 hardcover € 64.-/ U.S. $ 78.-, and ISBN 3-510-65209-6 € 49.-/ U.S. $ 59.- student edition as stated in the promotional leaflet.**

Klaus Hausmann, Norbert Hülsmann and Renate Radek have written a contemporary protistology textbook. This is the completely revised third edition of the book by Hausmann and his co-authors. The success of the recent edition of the *Protistology,* like the previous editions, derives from its insight into the complexity and beauty of protists.

The book provides an excellent compilation of current branches of knowledge, with contributions from all the main scientists in protist research, giving us to a deeper understanding of protists. The authors have divided their book into three major parts. The first part gives the reader an introduction and overview of definitions, the history of nomenclature and a historical overview of protistological research, concluding with the unique cellular organization of protists. The second part discusses the context and foundation for understanding evolution and taxonomy, which includes the evolution of unicellular eukaryotes, the development of classification systems and concludes with the proposal of the Protists' system. The third part concerns six selected topics of general protistology, namely: comparative morphology and physiology, nuclei and sexual reproduction, morphogenesis, molecular biology, behavior and ecology. The book as a whole ends with a helpful glossary of terms used almost exclusively in protistology, mentioning leading protozoological journals and periodicals, a bibliography comprising about 500 classical references concerning topics dealt with in the book, and an alphabetically arranged subject index.

At the very beginning, the authors pose the question: what are protists or protozoans? And they are not very convinced they can give an answer in the rest of the book, that covers an assemblage of the factual information on protists. In my opinion, the book gives the convincing answer that protists are almost always unicellular eukaryotic organisms, having a lot in common with other higher eukaryotes, but because of their "fantastic diversity", (quoting the authors) are hard to classify in a clear and equal terms.

Promising molecular biology techniques applied recently have given results that lead at the moment to complication of the taxonomical relations based on morphological features /characters. It seems a plausible expectation that in due time we shall gain a new understanding and insight into these highly differentiated living creatures, defined for the moment as protists.

On the positive side, this edition deals with the emergence and use of techniques currently driving the development of molecular biology, a subject insufficiently examined in previous editions. Examples of extensive biochemical and genetical analysis have added to our pool of knowledge. This is recognized by the authors and should make this book interesting to read, even for postgraduates. Students will benefit greatly from this clearly presented and illustrated text and from the analysis of the historical development of the subject from its very beginnings. I would chiefly recommend this book to students who are interested in unicellular organisms.

An additional strength of the book is undoubtedly in its listing (and illustrations) of many examples of selected topics such as morphology, motility, nutrition, reproduction, molecular biology, behavior and ecology of protists, arranged in a very readable way.

The success of the most recent edition of *Protistology,* as in previous editions, is derived from a clear layout of text and photographs and drawings that serve to illustrate the book. I got the feeling that the authors are certainly fascinated with protists. A good piece of work and the result is a great read.

Finally, I shall agree with the authors "that protists are amazing, lovely and wonderful creatures which can give pleasure and delight…" not only "…just by observing them under a microscope…" but by reading about them in *Protistology* as well.

Jerzy Sikora,
Nencki Institute of Experimental Biology,
Warsaw, Poland

INSTRUCTIONS FOR AUTHORS

Acta Protozoologica is a quarterly journal that publishes current and comprehensive, experimental, and theoretical contributions across the breadth of protistology, and cell biology of lower Eukaryote including: behaviour, biochemistry and molecular biology, development, ecology, genetics, parasitology, physiology, photobiology, systematics and phylogeny, and ultrastructure. It publishes original research reports, critical reviews of current research written by invited experts in the field, short communications, book reviews, and letters to the Editor. Faunistic notices of local character, minor descriptions, or descriptions of taxa not based on new, (original) data, and purely clinical reports, fall outside the remit of *Acta Protozoologica*.

Contributions should be written in grammatically correct English. Either British or American spelling is permitted, but one must be used consistently within a manuscript. Authors are advised to follow styles outlined in The CBE Manual for Authors, Editors, and Publishers (6th Ed., Cambridge University Press). Poorly written manuscripts will be returned to authors without further consideration.

Research, performed by "authors whose papers have been accepted to be published in *Acta Protozoologica* using mammals, shall have been conducted in accordance with accepted ethical practice, and shall have been approved by the pertinent institutional and/or governmental oversight group(s)"; this is Journal policy, authors must certify in writing that their research conforms to this policy.

Nomenclature of genera and species names must agree with the International Code of Zoological Nomenclature (ICZN), International Trust for Zoological Nomenclature, London, 1999; or the International Code of Botanical Nomenclature, adopted by XIV International Botanical Congress, Berlin, 1987. Biochemical nomenclature should agree with "Biochemical Nomenclature and Related Documents" (A Compendium, 2nd edition, 1992), International Union of Biochemistry and Molecular Biology, published by Portland Press, London and Chapel Hill, UK.

Except for cases where tradition dictates, SI units are to be used. New nucleic acid or amino acid sequences will be published only if they are also deposited with an appropriate data bank (e.g. EMBL, GeneBank, DDBJ).

All manuscripts that conform to the Instructions for Authors will be fully peer-reviewed by members of Editorial Board and expert reviewers. The Author will be requested to return a revised version of the reviewed manuscript within four (4) months of receiving the reviews. If a revised manuscript is received later, it will be considered to be a new submission. There are no page charges, but Authors must cover the reproduction cost of colour illustrations.

The Author(s) of a manuscript, accepted for publication, must transfer copyrights to the publisher. Copyrights include mechanical, electronic, and visual reproduction and distribution. Use of previously published figures, tables, or brief quotations requires the appropriate copyright holder's permission, at the time of manuscript submission; acknowledgement of the contribution must also be included in the manuscript. Submission of a manuscript to *Acta Protozoologica* implies that the contents are original, have not been published previously, and are not under consideration or accepted for publication elsewhere.

SUBMISSION

Authors should submit manuscript to: Dr Jerzy Sikora, Nencki Institute of Experimental Biology, ul. Pasteura 3, 02-093 Warszawa, Poland, Fax: (4822) 8225342; E-mail: jurek@nencki.gov.pl or j.sikora@nencki.gov.pl.

At the time of submission, authors are encouraged to provide names, E-mails, and postal addresses of four persons who might act as reviewers. Extensive information on *Acta Protozoologica* is available at the website: http://www.nencki.gov.pl/ap.htm; however, please do not hesitate to contact the Editor.

Hard copy submission: Please submit three (3) high quality sets of text and illustrations (figures, line drawing, and photograph). When photographs are submitted, arranged these in the form of plate. A copy of the text on a disk or CD should also be enclosed, in PC formats, preferably Word for Windows version 6.0 or higher (IBM, IBM compatible, or MacIntosh). If they do not adhere to the standards of the journal the manuscript will be returned to the corresponding author without further consideration.

E-mail submission: Electronic submission of manuscripts by e-mail is acceptable in PDF format only. Illustrations must be prepared according to journal requirement and saved in PDF format. The accepted manuscript should be submitted as a hard copy with illustrations (two copies, one with lettering + one copy without lettering) in accordance with the standards of the journal.

ORGANIZATION OF MANUSCRIPTS

Text: Manuscripts must be typewritten, double-spaced, with numbered pages (12 pt, Times Roman). The manuscript should be organized into the following sections: Title, Summary, Key words, Abbreviations, Introduction, Materials and Methods, Results, Discussion, Acknowledgements, References, Tables, and Figure legends. Figure legends must contain explanations of all symbols and abbreviations used. The Title Page should include the title of the manuscript, first name(s) in full and surname(s) of author(s), the institutional address(es) where the work was carried out, and page heading of up to 40 characters (including spaces). The postal address for correspondence, Fax and E-mail should also be given. Footnotes should be avoided.

Citations in the text should be ordered by name and date but not by number, e.g. (Foissner and Korganova 2000). In the case of more than two authors, the name of the first author and *et al.* should be used, e.g. (Botes *et al.* 2001). Different articles by the same author(s) published in the same year must be marked by the letters a, b, c, etc. (Kpatcha *et al.* 1996a, b). Multiple citations presented in the text must be arranged by date, e.g. (Small 1967, Didier and Detcheva 1974, Jones 1974). If one author is cited more than once, semicolons should separate the other citations, e.g. (Lousier and Parkinson 1984; Foissner 1987, 1991, 1994; Darbyshire *et al.* 1989).

Please observe the following instructions when preparing the electronic copy: (1) label the disk with your name; (2) ensure that the written text is identical to the electronic copy; (3) arrange the text as a single file; do not split it into smaller files; (4) arrange illustrations as separate files; do not use Word files; *.TIF, *.PSD, or *.CDR graphic formats are accepted; (5) when necessary, use only italic, bold, subscript, and superscript formats; do not use other electronic formatting facilities such as multiple font styles, ruler changes, or graphics inserted into the text; (6) do not right-justify the text or use of the hyphen function at the end of lines; (7) avoid the use of footnotes; (8) distinguish the numbers 0 and 1 from the letters O and l; (9) avoid repetition of illustrations and data in the text and tables.

References: References must be listed alphabetically. Examples for bibliographic arrangement:
Journals: Flint J. A., Dobson P. J., Robinson B. S. (2003) Genetic analysis of forty isolates of *Acanthamoeba* group III by multilocus isoenzyme electrophoresis. *Acta Protozool.* **42:** 317-324
Books: Swofford D. L. (1998) PAUP* Phylogenetic Analysis Using Parsimony (*and Other Methods). Ver. 4.0b3. Sinauer Associates, Sunderland, MA
Articles from books: Neto E. D., Steindel M., Passos L. K. F. (1993) The use of RAPD's for the study of the genetic diversity of *Schistosoma mansoni* and *Trypanosoma cruzi*. In: DNA Fingerprinting: State of Science, (Eds. S. D. J. Pena, R. Chakraborty, J. T. Epplen, A. J. Jeffreys). Birkhäuser-Verlag, Basel, 339-345

Illustrations and tables: After acceptance of the paper, drawings and photographs (two copies one with lettering + one copy without) must be submitted. Each table and figure must be on a separate page. Figure legends must be placed, in order, at the end of the manuscript, before the figures. Figure legends must contain explanations of all symbols and abbreviations used. All line drawings and photographs must be labelled, with the first Author's name written on the back. The figures should be numbered in the text using Arabic numerals (e.g. Fig. 1).

Illustrations must fit within either a single column width (86 mm) or the full-page width (177 mm); the maximum length of figures is 231 mm, including the legend. Figures grouped as plates must be mounted on a firm board, trimmed at right angles, accurately mounted, and have edges touching. The engraver will then cut a fine line of separation between figures.

Line drawings should be suitable for reproduction, with well-defined lines and a white background. Avoid fine stippling or shading. Prints are accepted only in *.TIF, *.PSD, and *.CDR graphic formats (Grayscale and Colour - 600 dpi, Art line - 1200 dpi) on CD. Do not use Microsoft Word for figure formatting.

Photographs should be sharp, glossy finish, bromide prints. Magnification should be indicated by a scale bar where appropriate. Pictures of gels should have a lane width of no more than 5 mm, and should preferably fit into a single column.

PROOF SHEETS AND OFFPRINTS

After a manuscript has been accepted, Authors will receive proofs for correction and will be asked to return these to the Editor within 48-hours. Authors will be expected to check the proofs and are fully responsible for any undetected errors. Only spelling errors and small mistakes will be corrected. Twenty-five reprints (25) will be furnished free of charge. Additional reprints can be requested when returning the proofs, but there will be a charge for these; orders after this point will not be accepted.

ACTA PROTOZOOLOGICA

ORIGINAL ARTICLES